YUNIBESITI YA BOKONE-BOPHIRIMA
NORTH-WEST UNIVERSITY
NOORDWES-UNIVERSITEIT

Evaluation of isolated dorsal root ganglion cells as a model to study neural calcium overload

EE Jordaan Hons. B.Sc.

Dissertation submitted for the degree Magister Scientiae in Physiology at the North-West University

SUPERVISOR: Prof. K Dyason
CO-SUPERVISOR: Mrs. CMT Fourie

Potchefstroom
South Africa
2004

Acknowledgements

All the glory to our Heavenly Father for the potential, strength and mercy He blessed me with to complete this dissertation.

I would also like to express my sincere gratitude to the following persons who contributed to this final product:

- Prof. Karin Dyason, my supervisor, for the thorough and patient manner of guidance amidst huge workloads.
- Mrs. Carla Fourie, my co-supervisor, for her valuable insights, excellent advice and hands-on involvement. Also for the long, exhausting hours she went through in isolating the cells.
- Everyone at the Subject Group Physiology, for their friendly support and helpful advice. Especially Prof. Nico Malan, for creating the opportunity for me to continue on with my studies under circumstances that were not ideal at times.
- Prof. Faans Steyn for his valuable statistical inputs.
- Prof. Fons Verdonck for his concern about the project.
- My parents for the opportunities they gave me, their love, support and encouragement through the years. Also my mother-in-law for her support and interest.
- My wife, Emmerentia, for her selfless love, support, encouragement and patient sacrifices.

Table of Contents

Afrikaanse titel: **Evaluering van geïsoleerde dorsale wortel ganglion selle as 'n model vir die bestudering van neurale kalsium oorbelading**

Opsomming

Agtergrond en motivering: Dit is bekend dat neurale Ca^{2+} oorbelading verskeie nadelige gevolge het wat aanleiding gee tot seldood veroorsaak deur isgemie, hipoglisemie en verskeie neurodegeneratiewe siektes soos Alzheimer- en Parkinson se siekte en VIGS-verwante dementia. *In vitro* modelle waarmee die meganismes betrokke by Ca^{2+} oorbelading bestudeer word sluit breinskywe, neuronale kulture asook akuut geïsoleerde neurone in. Hierdie neurone word meestal geïsoleer vanuit die hippokampus en kortikale breinareas. Ondersoeke met nuwe Ca^{2+} oorbeladingsmodelle mag lig werp op aspekte van Ca^{2+} oorbelading wat tot op hede nie goed verstaan word nie.

Metodologie: In hierdie studie is verskeie teoretiese Ca^{2+} oorbeladingsverwante ingrepe gekombineer met die doel om seldood in akuut geïsoleerde dorsale wortel ganglia van die rot te induseer. Ten einde meer lig te werp op die meganisme/s betrokke by seldood na blootstelling aan hierdie ingreep, is die effekte van verskeie veranderings aan die ingreep se samestelling geassesseer. Hierdie ondersoek is verder gevoer deur verskeie erkende asook potensieel beskermende verbindings by die ingreep te voeg. Seldood is bepaal deur toediening van tripan blou na 'n 18 uur blootstellingsperiode aan die ingreep. Lewende sowel as dooie selle is onder 'n ligmikroskoop getel.

Resultate en gevolgtrekkings: Die doel van die studie was om die moontlike toepassing van dorsale wortel ganglia as 'n model vir neurale Ca^{2+} oorbelading buite die brein te evalueer. Aangesien Ca^{2+} nodig was om seldood te induseer, is die gevolgtrekking gemaak dat seldood hoofsaaklik veroorsaak word deur Ca^{2+} oorbelading. Buiten ekstrasellulêre Ca^{2+} was KCl-geïnduseerde depolarisasie ook nodig vir die induksie van seldood, terwyl die antagoniste nie beduidende beskerming teen die seldood tot gevolg gehad nie. Gebaseer op die resultate kon die meganisme

van Ca^{2+} oorbelading egter nie sonder twyfel uitgeklaar word nie, maar die spanningsafhanklike Ca^{2+} kanale is waarskynlik hierby betrokke.

Sleutelwoorde: Ca^{2+} oorbelading; glutamaat eksitotoksisiteit; model; dorsale wortel ganglia; lewensvatbaarheid; tripan blou; spanningsafhanklike Ca^{2+} kanale; NMDAR kanale

Summary

Background and motivation: The event of neural Ca^{2+} overload is known to have several deleterious effects resulting in cell death caused by ischaemia, hypoglycaemia, hypoxia and several neurodegenerative diseases such as Alzheimer's disease, Parkinson's disease and AIDS-related dementia. *In vitro* models for the investigation of the mechanisms involved in Ca^{2+} overload include brain slice preparations, neuronal cultures as well as acutely isolated neurons, mostly from the hippocampus and cortical brain areas. Additional models for investigating Ca^{2+} overload may bring about new knowledge to areas of the phenomenon that are still unresolved.

Methodology: In this study, several theoretical Ca^{2+} overload-related interventions were combined aimed at inducing cell death in acutely isolated rat dorsal root ganglia. To elucidate the mechanism/s involved in the cell death observed following exposure to this intervention, the effects of several alterations to the intervention's composition were assessed. This examination was extended by the addition of several recognized and potential protective compounds to the intervention. Cell death was indicated by the trypan blue exclusion assay and recorded after 18 hours exposure to the interventions by counting live and dead neurons under a light microscope.

Results and conclusions: The goal was to evaluate the possible application of dorsal root ganglia as a model for neural Ca^{2+} overload outside the brain. Since Ca^{2+} was required for cell death to be induced, it is concluded that the observed cell death was indeed primarily due to Ca^{2+} overload. Besides extracellular Ca^{2+}, KCl-induced depolarization was also required for cell death to be induced, while the antagonists did not demonstrate significant protection against cell death. Based on the results, the mechanism of Ca^{2+} overload could not be defined beyond doubt, but the voltage-activated Ca^{2+} channels are likely to be involved.

Key words: Ca^{2+} overload; glutamate excitotoxicity; model; dorsal root ganglia; viability; trypan blue; voltage-activated Ca^{2+} channels; NMDAR channels

LIST OF FIGURES AND TABLES

FIGURES

Chapter 2 **Page**

Chapter 3

TABLES

Chapter 3

Appendix A

LIST OF ABBREVIATIONS

Abbreviations	
AA	Arachadonic acid
ACPD	Aminocyclopentane-1,3-dicarboxylic acid
AdNT	Adenine nucleotide translocator
AIDS	Acquired immunodeficiency syndrome
AKAP	A-kinase anchoring protein
AMPA/R	S-α-amino-3-hidroxy-5-methyl-4-isoxazolepropionic acid / receptor
Apaf	Apoptotic protease activation factor
APV	Aminophosphonovaleric acid
ATP	Adenosine triphosphate
Ba^{2+}	Barium ion
Ca^{2+}	Calcium ion
CaMKII	Ca^{2+}/calmodulin-dependent protein kinase
cAMP	Cyclic adenosine monophosphate
CBP	Calcium binding protein
cDNA	Cyclic deoxyribonucleic acid
Cl^-	Chloride ion
CNS	Central nervous system
CREB	cAMP-response element binding protein
CyP-D	Cyclophilin-D
DAG	Diacylglycerol
DHPG	(S)-3,5-dihydroxyphenylglycine
DNA	Deoxyribonucleic acid
DRG/s	Dorsal root ganglion/ganglia
ED_{50}	Effective dose 50% of population
EGTA	Ethylene glycol-bis(beta-aminoethyl ether)-tetraacetic acid
ER	Endoplasmic reticulum
EthD-1	Ethidium homodimer
fEPSP	Fast excitatory post-synaptic potential
GluR/s	Glutamate receptor/s
GTP	Guanosine triphosphate
HIV	Human immunodeficiency virus
HVA	High voltage-activated
IC_{50}	Inhibition concentration 50% concentration
iGluR/s	Ionotropic glutamate receptor/s
IP3	Inositol triphosphate
K^+	Potassium ion
KA/R	Kainate / receptor
kD	KiloDalton
Kd	Dissociation constant
kg	Kilogram
Ki	Dissociation constant, measure of affinity
LAOBP	Leucin/arginine/ornithine-binding protein
LDH	Lactate dehydrogenase

LPA	Lysophosphatidic acid
LTP	Long-term potentiation
LVA	Low voltage-activated
M	Molar
MAO-B	Monoamine oxidase – B
MAP kinase	Mitogen-activated protein kinase
Mg^{2+}	Magnesium ion
mGluR/s	Metabotropic glutamate receptor/s
mM	Millimolar
MPTP	1-Methyl-4-phenyl-1,2, 3,6-tetrahydropyridine
mRNA	Messenger ribonucleic acid
MTT	3-(4,5-dimethylthiazol-2-yl)-2,5-diphenyltetrazolium bromide
mV	Millivolt
Na^{+}	Sodium ion
NAD	Nicotinamide adenine dinucleotide
NADPH	Nicotinamide adenine dinucleotide phosphate-H
NBM	Nucleas of Meynert
nM	Nanomolar
nm	Nanometer
NMDA/R	N-methyl-D-aspartate / receptor
nNOS	Neural nitric oxide synthase
NO	Nitric oxide
NOS	Nitric oxide synthase
PA	Phosphatidic acid
PCP	Phencyclidine
PKC	Protein kinase C
PL	Phospholipase
PLA	Phospholipase A
PLC	Phospholipase C
PLD	Phospholipase D
pS	Picoseconds
PSD-95	Post-synaptic density protein-95
PT	Permeability transition
PTP	Permeability transition pore
PUFA	Polyunsaturated fatty acids
RMS	Root mean square
ROS	Reactive oxygen species
SERCA	Sarco/endoplasmic reticulum Ca^{2+}-ATPase
SNARE	Soluble NSF-attachment protein receptor
VACC/s	Voltage-activated calcium channel/s
Zn^{2+}	Zinc ion
μM	Micromolar

1

INTRODUCTION

CHAPTER 1
INTRODUCTION

The cellular event culminating in the excessive increase in intracellular Ca^{2+} concentration, known as Ca^{2+} overload, widely occurs during events ultimately leading to cell death. Ca^{2+} overload has been observed in different excitable cells, where it is thought to play a role in various pathological states such as ischaemia, hypoxia and hypoglycaemia, leading to cell death. Glutamate, an abundant excitatory neurotransmitter with a wide range of neural functions, has attracted attention in recent years in connection with its supposed causative role in excitotoxicity, a phenomenon thought to give rise to neural Ca^{2+} overload. The toxic event is probably triggered by excessive activation of glutamate receptor channels followed by excessive influx of Ca^{2+} through these channels. Neural Ca^{2+} overload has also been implicated as the neurodegenerative mechanism associated with states such as Alzheimer's disease, Parkinson's disease, Huntington's disease and AIDS-related dementia (Riedel et al., 2003). Scientists are in pursuit of elucidating the mechanistic variety leading to Ca^{2+} overload in different tissues and due to different types of cellular events.

Glutamate receptors that are commonly expressed on the neuronal cytoplasmic membrane, can be divided into two main classes: the metabolic glutamate receptors (mGluRs) and the ionotropic glutamate receptors (iGluRs). Of special interest to this study, and belonging to the iGluR group, are the N-methyl-D-aspartate (NMDA) receptor channels (Riedel et al., 2003). The Ca^{2+}-permeable NMDA receptor (NMDAR) channel has special properties which make it the ideal pathway for facilitating complicated cellular functions such as long-term potentiation and developmental plasticity. Both of these functions are responsible for and involved in learning and memory formation. These channels, however, are allegedly involved in the induction of glutamate excitotoxicity-related Ca^{2+} overload (Kornhuber and Weller, 1997).

The VACCs might also play a major role in the excessive influx of Ca^{2+}, since they are densely expressed in neurones and are responsible for great quantities of Ca^{2+} influx upon activation (Kobayashi and Mori, 1998).

In vitro models for investigating glutamate excitotoxicity and Ca^{2+} overload are very useful, not only for elucidation of the yet unresolved underlying subcellular mechanisms, but also for basic research in the development of protective measures. Most models for Ca^{2+} overload involve preparations from brain tissue - frequently from the hippocampus, since this area is notoriously vulnerable to excitotoxic events and has a dense NMDAR channel expression (Moriyoshi et al., 1991). Slice preparations from this area is a popular approach (Frankiewics et al., 2000), but neuronal cultures (Marks et al., 2000; Taguchi et al., 2003) and freshly isolated neurones from the hippocampus and other areas (e.g. cortical neurones (Li et al., 2001)) are also commonly used. Ca^{2+} overload is induced in these models by exposing the neurons to a combination of interventions like a high glutamate (Li et al., 2001) or another GluR agonist (Jing et al., 2004) concentration, or an excessive extracellular Ca^{2+} concentration (Li et al., 2001). In addition, cells are frequently depolarized (Kiedrowski, 1998) and/or incubated in an environment devoid of adequate oxygen (Small et al., 1997), glucose (Kume et al., 2002) or Mg^{2+} (Kiedrowski, 1998). Inadequate oxygen and glucose in the cell's environment probably depolarizes the cell due to a resulting energy deficit. This depolarization activates the VACCs and abolishes the voltage-dependent Mg^{2+} block inside the NMDAR channel pore and thus also activate this receptor, resulting in Ca^{2+} entering the cell. Lack of Mg^{2+} in the cell's environment has a similar effect upon NMDAR channels, since this ion's blocking effect is negated under these circumstances (Ashcroft, 2000).

In this study, the use of freshly isolated dorsal root ganglia (DRGs) as a model for investigating Ca^{2+} overload has been evaluated. DRGs are found on either side of the spinal segment in the vertebral column. These ganglia are involved in supporting the transmission of sensory information between the peripheral and central nervous system (Martini, 1998). Pain conduction by DRGs is a subject attracting a lot of scientific attention and recently, the glutamate neurotransmitter system and NMDAR channels

have been identified as relevant for pain conduction in these neurons (Urch et al., 2001). In this particular study attempts were made to induce cell death using several interventions that should theoretically result in Ca^{2+} overload through activation of NMDAR and voltage-activated Ca^{2+} channels. Once cell death was induced, the evaluation was extended by administration of several recognized and potential therapeutic compounds. Cell viability was assessed under a light microscope, using trypan blue to discriminate between live and dead cells. If DRGs can be used as a model for Ca^{2+} overload, further investigations regarding the character of the lethal mechanisms and evaluations regarding protective measures could be extended.

1) HYPOTHESIS

The *in vitro* dorsal root ganglia model is an appropriate tool for investigating Ca^{2+} overload and protection against it.

2) AIMS

- To evaluate the use of freshly isolated DRGs as a model for studying Ca^{2+} overload by developing an experimental protocol for observing Ca^{2+} overload and cell death in these cells.

- To assess the validity and applicability of the model by evaluating the effectivity of several well-known or potential protective compounds in preventing cell death.

3) MOTIVATION

Several aspects should be considered as contributive towards the scientific relevance of this project:

- The unresolved phenomenon of glutamate toxicity and Ca^{2+} overload can be further elucidated when experimental models are developed.

- The particular relevance of DRGs as such a model could make an important contribution in studying Ca^{2+} overload outside the brain.

- DRGs are also of interest because of the role it plays in pain conduction.

- The behaviour of well-known protective compounds were investigated in this environment.

- The isolation of DRGs is a standardised practice in our laboratory.

4) STRUCTURE OF DISSERTATION

Following the introductory chapter of this dissertation, the literature study gives a wide background of the main components necessary to understand the relevance of Ca^{2+} overload and the importance of evaluating new models. It also gives background to understand the motivation behind the development and evaluation of the model of concern. Chapter 3 contains the principle issues, results and conclusions of this study in the format of a journal article, which is to be submitted for publication in the *Journal of Neuroscience Methods*. The article, which presents the most important aspects of this project, is followed by Chapter 4, which summarizes the work done during the project, whereupon the main conclusions are emphasized and recommendations are made. The

original experimental data is presented in Appendix A. Each chapter is supplied with a list of references.

Prescriptions in the *Manual for postgraduate study* (Van der Walt, 2004) of the North-West University were applied for the general format of the dissertation, except for Chapter 3, where the prescriptions of the *Guide for Authors* of the *Journal of Neuroscience Methods* (Elsevier Author Gateway, 2004) received preference. As allowed by the *Manual for postgraduate study* of the North-West University referrals in the text and lists of referrals at the end of each chapter were done according to the manner used in the *Journal of Neuroscience Methods* and as prescribed by the *Guide for Authors*. This complete guide is included in Appendix B.

6) REFERENCES

Ashcroft FM. Ion channels and disease. Academic Press: London, 2000: 302.

Elsevier Author Gateway. Journal of Neuroscience Methods – Guide for authors. 2004; [Web:] http://www.authors.elsevier.com/JournalDetail.html?PubID=506079 &Precis=DESC [Date of access: 6 Jun. 2004].

Frankiewics T, Pilc A, Parsons CG. Differential effects of NMDA-receptor antagonists on long-term potentiation and hypoxic/hypoglycaemic excitotoxicity in hippocampal slices. Neuropharmacology, 2000; 39: 631-642.

Jing G, Grammatopoulos T, Ferguson P, Schelman W, Weyhenmeyer J. Inhibitory effects of angiotensin on NMDA-induced cytotoxicity in primary neuronal cultures. Brain Res. Bull., 2004; 62: 397-403.

Kiedrowski L. The difference between mechanisms of kainate and glutamate excitotoxicity *in vitro*: Osmotic lesion versus mitochondrial depolarization. Restor. Neurol. Neurosci., 1998; 12: 71-79.

Kobayashi T, Mori Y. Ca^{2+} channel antagonists and neuroprotection from cerebral ischemia. Eur. J. Pharmacol., 1998 363: 1-15.

Kornhuber J and Weller M. Psychotogenicity and N-methyl-D-aspartate Receptor Antagonism: Implications for Neuroprotective Pharmacotherapy. Biol. Psychiatry, 1997; 41: 135-144.

Kume T, Nishikawa H, Taguchi R, Hashino A, Katsuki H, Kaneko S, Minami M, Satoh M, Akaike A. Antagonism of NMDA receptors by σ-receptor ligands attenuates chemical ischemia-induced neuronal death *in vitro*. Eur. J. Pharmacol., 2002; 455: 91-100.

Li J, Kato K, Ikeda J, Morita I, Murota S-I. A narrow window for rescuing cells by the inhibition of calcium influx and the importance of influx route in rat cortical neuronal cell death induced by glutamate. Neurosci. Lett., 2001; 304: 29-32.

Marks JD, Bindokas VP, Zhang X-M. Maturation of vulnerability to excitotoxicity: intracellular mechanisms in cultured postnatal hippocampal neurons. Brain Res. Dev. Brain Res., 2000; 124: 101-116.

Martini FH. Fundamentals of anatomy & physiology, fourth ed. Prentice Hall: New Jersey, 1998: 417.

Moriyoshi K, Masu M, Ishii T, Shigemoto R, Mizuno N, Nakanashi S. Molecular cloning and characterization of the rat NMDA receptor. Nature, 1991; 354: 31-37.

Riedel G, Platt B, Micheau J. Glutamate receptor function in learning and memory. Behav. Brain Res., 2003; 140: 1-47.

Small DL, Monette R, Buchan AM, Morley P. Identification of calcium channels involved in neuronal injury in rat hippocampal slices subjected to oxygen and glucose deprivation. Brain Res., 1997; 753: 209-218.

Taguchi R, Nishikawa H, Kume T, Terauchi T, Kaneko S, Katsuki H, Yonaga M, Sugimoto H, Akaike A. Serofendic acid prevents acute glutamate neurotoxicity in cultured cortical neurons. Eur. J. Pharmacol., 2003; 477: 195-203.

Urch CE, Rahman W, Dickenson AH. Electrophysiological studies on the role of the NMDA receptor in nociception in the developing rat spinal cord. Brain Res. Dev. Brain Res., 2001; 126: 81-89.

Van der Walt E. Manual for postgraduate study. 2004; [Web:] http://www.puk.ac.za /beleidsdokumente/handleiding-nagraads-apr2004.pdf [Date of access: 5 Nov. 2004].

2

LITERATURE STUDY

CHAPTER 2
LITERATURE STUDY

1) Ca^{2+} CHANNELS

Ion channels serve as one of the body's primary integration and regulation mechanisms for control and excitability on cellular level. This function is mediated through selective movement of ions over membranes via ion channels. The ion movement is driven by an electrochemical gradient, with intracellular concentrations for Na^+, Ca^{2+} and Cl^- generally being lower compared to the extracellular concentration, while the opposite is generally the case for K^+ (Triggle, 1999).

Ca^{2+} channels are expressed widely in both excitable and non-excitable cells. The Ca^{2+} channel family is quite diverse in terms of functional role and structural subtypes. Ca^{2+} that enters the cell through these channels serves as second messengers and initiates and modulates intracellular functions such as contraction, secretion, protein phosphorilation, gene expression, neurotransmitter release and action potential patterns (Hille, 2001).

1.1) Classification of Ca^{2+} channels

Because of its diversity in structure and function, the classification of Ca^{2+}-selective ion channels is complicated. Criteria used for classification of ion channels in general, are in the first place selectivity, and furthermore, affinity for endogenous or exogenous ligands, voltage dependence, subunit constitution as well as location of expression (Meir et al., 1999; Triggle, 1999). These criteria were considered in the classification of Ca^{2+} channels as proposed in Figure 1:

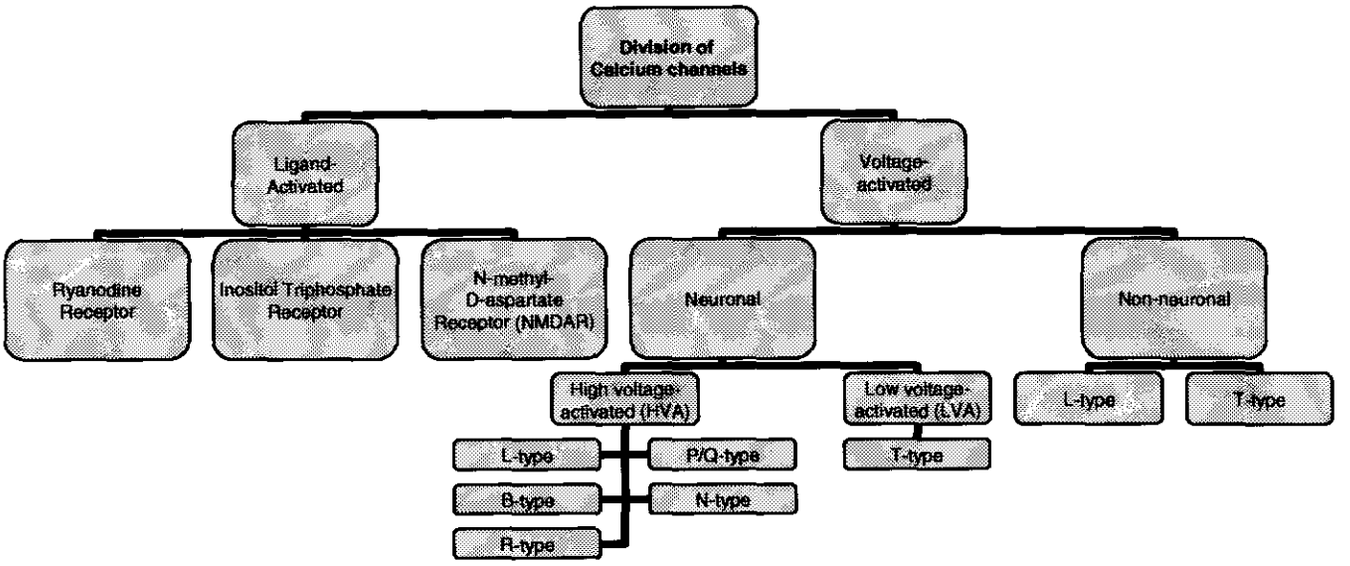

Figure 1. Classification of Ca^{2+} channels. This diagram summarizes the classification system implemented for Ca^{2+} channels. (From Reuter, 1996; Lehmann-Horn and Jurkat-Rott, 1999; Meir et al., 1999)

The classification in Figure 1 is commonly used in the literature (Reuter, 1996; Lehmann-Horn and Jurkat-Rott, 1999; Meir et al., 1999) and can be regarded as the conventional system, but confusion sometimes arises when other classification systems are used or when new Ca^{2+} channel subtypes are discovered. Classification with α-subunit identity as sole criterium is another system frequently used . Each subunit is assigned a different alfabetic number (e.g. $\alpha_{A, B, C, D, E}$ etc.) from those first discovered to the most recent. This classification can create confusion as the channel called α_B might be confused with the B-type high-voltage activated Ca^{2+} channel. Also, when new α-subunits are discovered, the possibility that a particular channel will be classified as α_L can create confusion with the L-type channel from the conventional classification system. To override this problem, some groups use non-alphabetic numbering (Anderson and Greenberg, 2001)

1.2) Voltage-activated Ca^{2+} channels (VACCs) in neurons

Despite VACCs' selectivity for Ca^{2+}, other divalent ions and even monovalent ions can pass through these channels at low Ca^{2+} concentrations. Any extracellular Ca^{2+} concentration measuring in the millimolar range, results in an almost exclusive inward Ca^{2+} current (Lehmann-Horn and Jurkat-Rott, 1999; Chung and Kuyucak, 2002).

The normal extracellular Ca^{2+} concentration is 10^4 to 10^5 times greater than the intracellular concentration. The driving force behind the exclusively inward current is, therefore, a combination of the electrochemical gradient and the channel's open state probability (Hille, 2001).

1.2.1) Molecular structure

Each VACC channel is composed of an α-subunit and a maximum of four additional subunits, namely the α_2, δ, β, and γ-subunits (Caterall, 1991; Brust et al., 1993; Anderson and Greenberg, 2001), which are shown in Figure 2. Only the mRNA of the α-, α_2-, δ-, and β-subunits have been isolated from neurons (Caterall, 1991), since the γ-subunit is probably expressed exclusively in skeletal muscle (Reuter, 1996; Meir et al., 1999).

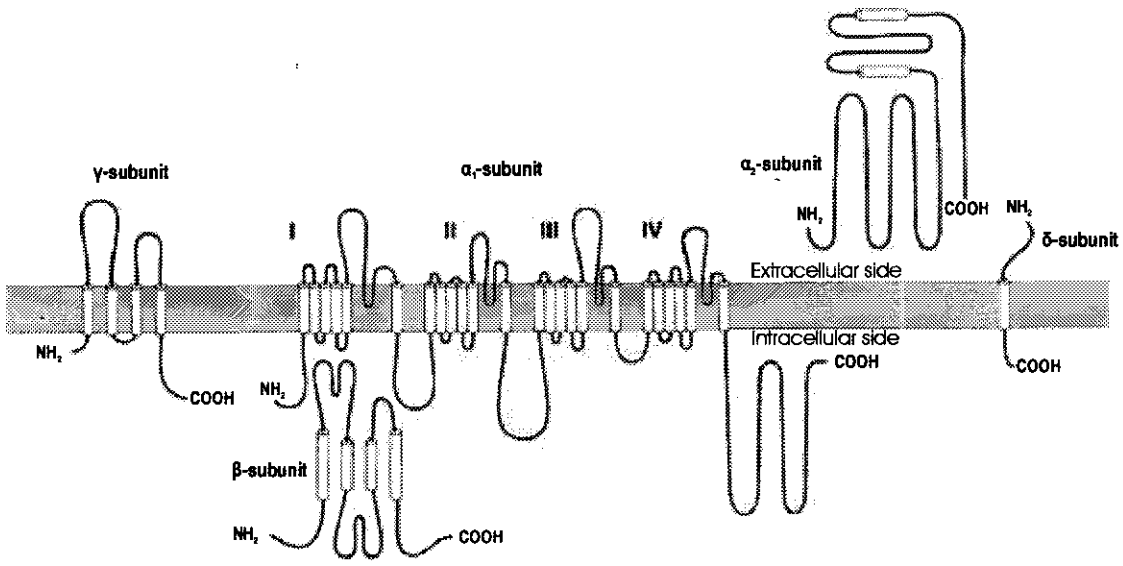

Figure 2 Model representing the molecular structure of the VACCs. The α, δ, and γ-subunits are transmembrane proteins, while the α_2-subunit is expressed extracellularly and the β-subunit cytoplasmically. Domains I-IV of the α-subunit folds in such a way that a central pore is formed (Edited from Lehmann-Horn and Jurkat-Rott, 1999)

1.2.1.1) The α-subunit

The α-subunit, of which the structure and function is well conserved between the different subtypes, is expressed in all VACCs (Lehmann-Horn and Jurkat-Rott, 1999; Anderson and Greenberg, 2001). This essential subunit (175 kD) forms the functional pore structure. Within its structure, parts are also included that act as voltage sensors, channel gates and receptors for the binding of most Ca^{2+} channel ligands. The additional subunits modulate the function of the α-subunit influencing the voltage-dependency, rate of activation and inactivation, ion conductance and density of channel expression. (Caterall, 1991; Brust et al., 1993; Hosey et al., 1996).

Besides seven different α-subunits that are expressed by their separate representative genes, variety in Ca^{2+} currents is further expanded by the expression of different splice variants by each of these genes (Brust et al., 1993; Reuter, 1996; Meir et al., 1999). The

eventual localization, kinetic properties and subunit composition are determined to a great extent by at least ten different splice variants (Lehmann-Horn and Jurkat-Rott, 1999).

The α-subunit consists of four homologous domains, each with six helix-shaped transmembrane segments (S1-S6). These structures are connected by intra or extracellular loops, also known as binding elements. It is generally accepted that the four domains form a tetrameric structure with the pore area in the middle (Lehmann-Horn and Jurkat-Rott, 1999; Meir et al., 1999; Anderson and Greenberg, 2001).

The structure and function of the channel pore have been thoroughly elucidated. The pore is lined by the S4-S5 binding element, called the P-area. The P-area contains strategically placed negative amino acids, which act as a selectivity filter with strong cation affinity. This filter is of importance for the normal functioning of the channel. Replacing the lysine and alanine residues of the Na^+ channel with glutamate, in an area similar to the Ca^{2+} channel's P-area, results in a channel with typical Ca^{2+} channel selectivity and permeability attributes (Lehmann-Horn and Jurkat-Rott, 1999). The crucial residues in the selectivity filter are, therefore, the glutamate residues, four of which occur at critical positions in the P-area. The interaction of Ca^{2+} ions with these residues and surrounding water molecules and the resulting conformational and electrostatic changes in the pore are the determining factors in the movement of ions through the channel pore (Corry et al., 2000; Chung and Kuyucak, 2002). These glutamate residues are highly conserved throughout the different Ca^{2+} channel α-subunits (Corry et al., 2000; Chung and Kuyucak, 2002).

The flow pattern of Ca^{2+} through the channel suggests that there are two Ca^{2+} binding receptors in the pore (Hille, 2001). The dissociation constant for Ca^{2+} binding to these receptors is approximately 700 nM (Lehmann-Horn and Jurkat-Rott, 1999). When the electrochemical gradient for Ca^{2+} is high enough, Ca^{2+} is bound with great electrostatic force to the first receptor. A second Ca^{2+} ion is also attracted and binds to the second receptor, which creates the ideal circumstances for the firstly bound ion to overcome the

small electric barrier and exit the pore on the intracellular side of the channel (Ashcroft, 2000; Corry et al., 2000; Chung and Kuyucak, 2002). The same mechanism applies for Na^+ movement through the Ca^{2+} channel, with the difference that three Na^+ ions are bound simultaneously in the channel pore. This explains the greater Na^+ current compared to a Ca^{2+} current, through the Ca^{2+} channel when divalent cations are absent (Corry et al., 2000; Chung and Kuyucak, 2002).

1.2.1.2) The β-subunit

The hydrophilic β-subunit (54 kD) consists of six α-helices connected by binding elements (Caterall, 1991; Lehmann-Horn and Jurkat-Rott, 1999). Four separate genes encode for the β_1, β_2, β_3 and β_4-subunits. Various splice variants are known, with more than eight different variants identified in the brain (Brust et al., 1993; Meir et al., 1999). A single intracellular β-subunit binds to the α-subunit binding element between domains I and II, called the Alpha-interaction domain (Anderson and Greenberg, 2001). In some cases the β-subunit binds to the intracellular C-terminal of the α-subunit (Lehmann-Horn and Jurkat-Rott, 1999).

The function of the β-subunits is related to the identity of the associated α-subunit. In some cases the β-subunit determines the subtype identity of the channel, as is the case with P and Q-currents, where association of β_{2A} gives rise to the P-type and β_{1B} and β_3 to the Q-type current (Caterall, 1991; Lehmann-Horn and Jurkat-Rott, 1999; Anderson and Greenberg, 2001). Another important function is the β-subunit serving as a phosphorilation domain, where expression of Ca^{2+} channels can be up or down regulated (Reuter, 1996).

1.2.1.3) The γ-subunit

The γ-subunit (30 kD) has been identified in skeletal muscle. It comprises four α-helix transmembrane segments which non-covalently bind to other subunits (Caterall, 1991).

The transmembrane segments are, as with the other subunits, connected by binding elements. The N and C-terminals are located intracellularly.

It is presumed that the γ-subunit expressed in skeletal muscle shifts the inactivation curve to a more hyperpolarized membrane potential. When these subunits are artificially expressed in heart muscle, the current amplitude and the activation rate increase (Lehmann-Horn and Jurkat-Rott, 1999).

1.2.1.4) The α_2/δ-subunit

These two subunits (together 170 kD) are discussed as a single subunit since they are expressed by a single gene (Caterall, 1991). Splice variants of this subunit have been identified in rat neurons (Meir et al., 1999).

The α_2-subunit is located extracellularly and is bound to the transmembrane δ-subunit with disulphide bonds (Caterall, 1991; Meir et al., 1999). The presence of the α_2/δ-subunit causes an increase in the number of α-subunits expressed, which explains the increase in whole-cell Ca^{2+} current amplitude following artificial α_2/δ expression. The co-expression of this subunit also accelerates the activation and inactivation rates and shifts the activation and inactivation curves to more negative potentials. In some neurons, though, the effects of these subunits are unknown (Caterall, 1991; Lehmann-Horn and Jurkat-Rott, 1999).

1.2.2) Kinetics of VACCs

The Hodgkin-Huxley model is accepted as a general template to interpret the kinetics of voltage-activated channels. The model, which was designed for Na^+ currents in giant squid axons, describes two gating particles, the so-called m-gate and the h-gate, both of which have to be open in order for ions to move through the channel pore.

The gate's position (open or closed) determines the state of the channel. At rest, 60% of the channels are available for activation with the m-gate closed and the h-gate open. The remaining 40% of channels are deactivated with both gates in the closed position. Depolarization activates the available channels – the h-gates open and ions pass through. The channel is inactivated when the h-gate closes, which is followed by deactivation when the m-gate closes. For a channel to be ready to respond to a stimulus, the resting but available state has to be regained. The states of inactivation and deactivation, therefore, explain the refractory period during which the cell does not respond to stimuli. From a state of deactivation, the h-gate opens, the state of inactivation is, therefore, relieved and the channel is available for activation (Hodgkin and Huxley, 1952).

1.2.2.1) Activation of the Ca^{2+} channel

The prime stimulus for Ca^{2+} channel activation is, as with many other voltage-activated channels, depolarization. Depolarization leads to positive feedback since the influx of Ca^{2+} ions depolarizes the membrane even further (Hille, 2001). The activation rate is generally much slower (τ_a ±25 ms) compared to that of Na^+ channels (τ_a < 0.4 ms). The subtypes selectively expressed in neurons, and specifically in dorsal root ganglia, show less difference in activation rates, averaging τ_a ±1.87 ms for Ca^{2+} channels at voltages between 0 mV and +10 mV and τ_a ± 1.49 ms for Na^+ channels at voltages of approximately -10 mV (Catterall et al., 2000). The different Ca^{2+} channel subtypes have different activation thresholds, which vary from ± -50 mV for the low voltage-activated (LVA) channels to ± -30 mV for the high voltage-activated (HVA) channels. This defining attribute is important for current separation during experimental investigations of these channels (Bean, 1989).

It is assumed that the opening of the channels is mediated by voltage sensors that, when activated, lead to conformational changes in the α-subunit structure. When the highly-conserved positively charged arginine or lysine residues, located on every third position of the α-subunit's S4 transmembrane segment, are replaced by other amino acids, voltage-dependent activation is lost to a great extent. This led to the formation of the so-

it reaches a concentration threshold, which then gives rise to conformational changes resulting in inactivation (Ashcroft, 2000).

This Ca^{2+}-dependent inactivation mechanism is not applicable to LVA channels seeing that they inactivate at membrane potentials where there is no great influx of Ca^{2+}. The LVA channel probably inactivates via mechanisms more related to those of other voltage-activated channels (Hille, 2001), like Na^{+} and K^{+} channels. For these channels, N-type inactivation is a fast process where the cytoplasmic side of the pore is blocked by an intracellular part of the channel protein, the III-IV binding element (ball-and-chain inactivation). C-type inactivation is a slower process which includes conformational changes on the extracellular side of the pore (Ashcroft, 2000). Artificial mutations to the relevant channel structures suggest that N-type inactivation probably does not play a major part in the case of VACC inactivation. The S1 transmembrane element of domain I of the α-subunit, though, does make some contribution towards the fast inactivation of Ca^{2+} channels (Zhang et al., 1994).

1.2.3) Electrophysiological properties

Based on electrophysiological criteria, distinction is made between HVA (L, N, P/Q, R-type) and LVA (T-type) neuronal channels (Lehmann-Horn and Jurkat-Rott, 1999). N, P/Q and R-type channels are expressed exclusively on neuronal membranes, while L and T-type channels are also expressed on non-neuronal membranes, for instance myocytes. Distinctions on electrophysiological level are dependent upon the cell type and the protocol used in the experimental setup. Although the HVA and LVA channels can be broadly distinguished on the basis of their activation potentials, few generalizations can be made about these groups' electrophysiological properties, since it differs between different cell types. A property that clearly shows in one cell might be less prominent or even absent in the next, which adds to the complexity of classification (Meir et al., 1999).

In spite of differences between cell types and experimental protocol, some generalizations can be made. The HVA channels have a relatively high activation

threshold of ± -30 mV. L and P-type currents are activated between -30 mV and -35 mV, N-type currents at ± -45 mV and R-type currents between -50 mV and -60 mV (Bean, 1989; Sidach and Mintz, 2002). The LVA channels have an activation threshold of ± -50 mV. As mentioned previously, HVA channels are inactivated slowly in comparison with LVA channels (Ashcroft, 2000; Hille, 2001). When the HVA channel's single channel conductance is measured in an artificial membrane with 100 mM Ba^{2+}, a current of 25 pS compared to the LVA's 8 pS is measured (Ashcroft, 2000).

The HVA channels can be studied in isolation by setting the experimental protocol's holding potential above the inactivation threshold of LVA channels, typically between -30 mV and -45 mV (Bean, 1989; Hille, 2001). Separation between the different HVA subtypes can be obtained by using several selective antagonists (Sidach and Mintz, 2002).

1.2.4) General properties of antagonist binding to VACCs

One of the universal properties of ion channels is the availability of a certain amount of stereoselective receptors for exogenous ligands, which upon ligand binding result in a modulation of channel functioning. The fact that ion channels exist in all tissue types and that it is responsible for integrated cellular communication implicates that it also has a major role to play in some pathologies (Triggle, 1999). A wide range of pathological states where defective VACCs are involved have been identified. These include states such as chronic pain, migraine, cerebellar ataxia, angina, epilepsy, hypertension, ischaemia and certain arrhythmias, which are associated with either intracellular hypo or hypercalcaemic states (Lehmann-Horn and Jurkat-Rott, 1999; Triggle, 1999; Ashcroft, 2000). Identification of defective ion channels in a variety of illnesses promogates the continuous search for modulating ligands.

The functioning of ion channel modulators is complicated due to the conformational changes in channel structure during the voltage-dependent cycle of activation, inactivation and deactivation. These changes probably include alterations in the tertiary structure of the particular receptors, which is usually present on the α-subunit, and,

therefore, changes properties and conditions of ligand binding. This so-called state-dependent binding is a common phenomenon (Triggle, 1999; Hille, 2001) and results in one ligand having a whole series of affinities for the same receptor with different qualitative and quantitative effects (Triggle, 1999).

1.2.5) Function of VACCs in neurons

Ca^{2+} entering the cytoplasm through the VACCs is functionally diverse, modulating channel gating and acting as a second messenger in the induction of enzyme activation, neurotransmitter release, gene expression and activation of various other cascades (Hille, 2001).

Ca^{2+} affects action potentials and firing patterns of cells by activating the abundant Ca^{2+}-dependent K^+ and Cl^- channel subtypes in neurons (Hille, 1992). Ca^{2+} is also involved in the activation of a variety of enzymes, for example the proteases, phospholipases, caspases and endonucleases. These enzymes have copious substrates, and are involved in regulating membrane stability and permeability, gene expression and in the activation of various other cascades (Nicotera et al., 1992; Philles and O'Regan, 2004), the discussion of which falls beyond the scope of this review.

The VACCs, and especially the L-type VACC, is involved in the activation of neuronal gene expression. Several intracellular signalling molecules, for example Ca^{2+}-sensitive adenylate cyclase, calcium/calmodulin activated kinases and Ras, are activated upon Ca^{2+} influx through the VACC channels. These signalling molecules are presumably activated by molecules that are physically coupled to the VACC, such as the protein kinase anchoring protein AKAP (A-kinase anchoring protein), the tyrosine kinase Src and calmodulin. Several cascades are activated by the signalling molecules and the cascade is eventually transduced into the nucleus, where transcription factors, of which cAMP-response element binding protein (CREB) has been studied thoroughly, is phosphorilated. Transcription of activity induced genes that promotes alterations in gene expression is mediated by the phosphorilated CREB (West et al., 2001).

It is a well known fact that Ca^{2+} entering the presynaptic neuronal membrane is the trigger for neurotransmitter release. Intracellular vesicular packages containing neurotransmitters are signalled to fuse with the presynaptic membrane and release its content by exocytosis. The N and P/Q VACC-subtypes are primarily expressed on the presynaptic membrane, and are thus responsible for the triggering of Ca^{2+} influx (Spaffold and Zamponi, 2003). The proteins involved in transferring the initial Ca^{2+}-entry into the eventual exocytosis are, although not fully elucidated, thought to be the so-called synaptotagmins and the SNARE (soluble NSF-attachment protein receptor) proteins (Augustine, 2001; Spaffold and Zamponi, 2003). The ability of the synaptotagmins to insert into lipid membranes upon binding with Ca^{2+} is thought to be closely linked to its exocytotic function. The sensitivity to increased Ca^{2+} concentrations of SNARE proteins, which do not bind Ca^{2+} directly, is conferred by association of SNARE to Ca^{2+} activated synaptotagmins (Augustine, 2001).

Since Ca^{2+} is chelated and sequestered immediately upon entering the cytoplasm, it is important that the proteins concerned with exocytosis are in close proximity to the entrance sites. Therefore the N and P/Q-type channels have a unique 225 amino acid area on the linker between domains II and III of the α_1-receptor that binds the exocytotic proteins (Spaffold and Zamponi, 2003). The distance between the proteins concerned and the intracellular pore side of the Ca^{2+} channels as well as the quantity of proteins and activated channels ultimately determines the necessary Ca^{2+} concentration in the vicinity of the proteins and, therefore, the rate at which the exocytosis will take place. This Ca^{2+} concentration varies considerably, for example, fast excitatory transmitters release activation has a Ca^{2+} concentration range between 5 and 200 μM (Augustine, 2001).

1.3) The N-methyl-D-aspartate receptor channels (NMDAR channels)

1.3.1) Classification of glutamate receptors in the brain

Glutamate is the main excitatory neurotransmitter in the central nervous system (CNS) (Jonas, 1993). Its primary function includes general synaptic transfer, changes in synaptic structure during development as well as modulation of transfer efficiency during plastic changes in the adult brain, as frequently happens during learning and memory formation (Masu et al., 1993; Riedel et al., 2003).

Glutamate's diverse functions are mediated by two receptor classes: the so-called metabotropic receptors (mGluRs) and the ionotropic receptors (iGluRs). The mGluRs influence cell metabolism through coupling to second messenger systems by means of guanosine triphosphate (GTP) binding proteins. The effects of transmission through these receptors are slow and of a modulatory nature. Currently, six (mGluR1-6) subtypes are known (Masu et al., 1993; Riedel et al., 2003).

iGluRs contain ion channels of which glutamate is the primary agonist. These receptors are responsible for fast transmission of signals. iGluRs are divided into three types, the S-α-amino-3-hidroxy-5-methyl-4-isoxazolepropionic acid (AMPA), kainate (KA) and N-methyl-D-aspartate (NMDA) receptors (Masu et al., 1993; Riedel et al., 2003). The various iGluRs are named in accordance to the interaction with specific ligands (Mori, 1995; Riedel et al., 2003).

NMDARs are mainly permeable to Ca^{2+}, but also to Na^{+} and K^{+}. In contrast to this, AMPA and KA receptors are primarily permeable to Na^{+} and K^{+} ions and secondarily to Ca^{2+}. Compared to AMPA and KA receptors' fast activation and inactivation kinetics, NMDARs show slow kinetics and higher single-channel conductance (Riedel et al., 2003).

1.3.2) NMDAR channel activation

NMDAR channels are activated by simultaneous binding of glutamate and glycin, combined with adequate depolarization. Since NMDAR channels are extremely sensitive to glycin, the basal extracellular concentration of this agonist is adequate to activate these channels. Yet, it is essential that the membrane is depolarized to relieve a voltage-dependent blockade of a Mg^{2+} ion within the channel pore (Ashcroft, 2000).

1.3.3) Molecular structure

The great diversity in the function of NMDAR channels is due to the differences in molecular structure determined by the subunit composition (Cull-Candy et al., 2001). This functional diversity is seen in different areas of the nervous system as well as different stages of development (Mori and Mishina, 1995).

1.3.3.1) Subunit structure and composition

Currently, three subunit classes have been identified for the NMDAR channel, namely NMDAR1 (NR1), NMDAR2 (NR2) and NMDAR3 (NR3). The rat NR1-subunit (called GluRε in mice), when homomerically expressed in *Xenopus* oocytes, forms channels with small conductance properties that are activated by glutamate and glycin (Mori and Mishina, 1995; Yamakura and Shimoji, 1999). When the NR1-subunit is homomerically expressed in mammalian systems no functional channels are formed (Yamakura and Shimoji, 1999). No subtypes of the NR1-subunit have been identified yet, but eight splice variants have been demonstrated using various methods. The NR1 gene has a total of 22 exons, of which 3 are able to undergo alternative splicing. Exon 5 encodes a splice cassette (N1) containing 22 amino acids. This exon can be inserted on the N-terminal of the subunit, which gives rise to the NR1-1b, 2b, 3b and 4b variants. There are two different exons involved in C-terminal deletions of the variants known as NR1-2a, 3a and

4a. Exon 21 encodes a splice cassette (C1) containing 37 amino acids, while exon 22 encodes a 38 amino acid splice cassette (C2). By determining the number of cloned cDNAs, it has been estimated that the C-terminal deletion splice variants are expressed at ±18%, relative to the N1-inserted variants' 15% and the 67% of NR1-1a, which is the subunit without any insertions or deletions (Mori and Mishina, 1995; Yamakura and Shimoji, 1999).

The NR2-subunit (mouse-version called GluRζ) consists of four subtypes (NR2A-D). When these subunits are heteromerically co-expressed with the NR1-subunit in *Xenopus* oocytes, fully functional channels with conductance comparable to native NMDAR channels are formed. According to this model, the NMDAR channel must contain at least one NR1 and one of the four NR2-subunit subtypes to be fully functional. When a model implementing random aggregation is used, the NMDAR channel consists of 5 subunits, of which at least two are NR1 and two NR2-subunits (Yamakura and Shimoji, 1999). All the subtypes except NR2A have several splice variants (Mori and Mishina, 1995; Yamakura and Shimoji, 1999).

There is a 40-50% overlap in amino acid identity between the different subunits of the NR2 family, with a ±18% overlap between the NR1 and NR2 families (Mori and Mishina, 1995; Yamakura and Shimoji, 1999). Each subunit peptide contains an extracellular N-terminal signal peptide and a cytoplasmic C-terminal. The C-terminal of the NR2 subfamily, especially that of NR2A and NR2B, is enlarged (Yamakura and Shimoji, 1999). The NR1-subunit contains 920 amino acids and weighs approximately 103 kD. The NR2A, NR2B, NR2C and NR2D-subunits contain 1445, 1456, 1220 and 1296 amino acid residues and weigh 163kD, 163kD, 134kD and 141kD respectively (Mori and Mishina, 1995).

The recently identified NR3 class of subunit proteins (NR3A-B) is expressed just before or during the first postnatal week. These subunits aggregate with the functional channel and inhibit NMDAR activity, thereby assisting in synaptic development (Cull-Candy et al., 2001).

1.3.3.2) Transmembrane topology

Each subunit contains four hydrophobic segments in the middle of the peptide, called M1, M2, M3 and M4 (Fig. 3). The most popular model concerning transmembrane topology is the three transmembrane segment model, similar to the model for AMPA and KA receptor channels. According to this model, the M2 segment forms a reentrant loop into the membrane, with both ends dipping back into the cytoplasm. The ascending limb of this reentrant loop corresponds to an α-helix which would typically align all the critical amino acid residues on the one side of the helix. The descending limb probably consists of an extended structure or random coil, where consecutive residues are all exposed to the lumen of the channel. The M2 segment is instrumental in the forming of the pore area (Yamakura and Shimoji, 1999).

The N-terminal of the NMDAR-subunit is connected to the M1 segment, which is presumed to reside between the M2 and M3 transmembrane segments. The binding element between M3 and M4 is extracellular (Yamakura and Shimoji, 1999). The three transmembrane segment model is supported by the findings of binding studies, confirming that the C-terminal is cytoplasmic and the M3-M4 transmembrane element is extracellular (Mori and Mishina, 1995; Yamakura and Shimoji, 1999).

The key residue in the pore area of the NMDAR-subunits is the asparagine 586 (called the N-site) on the M2 segment. This residue is on the same position as the key glutamine and arginine residues of the AMPAR subunits. When the asparagine is replaced by a glutamine, the Mg^{2+} block is largely elevated and the channel becomes less selective for Ca^{2+} (Masu et al., 1993; Mishina et al., 1993; Mori and Mishina, 1995) . A cluster of hydrophilic residues close to the crucial asparagine site of the NR1 and NR2 residues, as well as asparagine and serine residues on the first and second position to the C-terminal side of the key asparagine 586, are the main contributors to the narrow constriction (0.55 nm) of the NMDAR pore. A tryptophan residue on the NR2B-subunit, eight positions

upstream of the N-site, possibly also contributes to the channels narrow constriction (Yamakura and Shimoji, 1999).

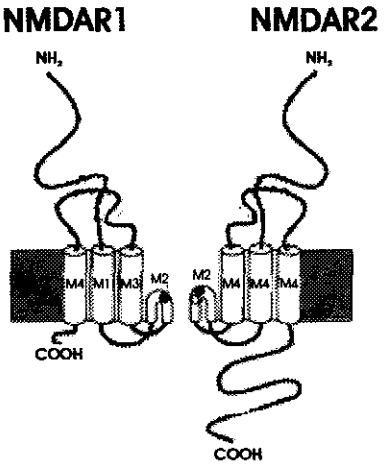

Figure 3. Model representing the molecular structure of the NMDAR channel. The N-terminal of the NMDAR-subunit is connected to the M1 segment, which is presumed to reside between the M2 and M3 transmembrane segments. The binding element between M3 and M4 is extracellular, and the M2 segment acts as selectivity filter inside the pore. (Edited from Mori and Mishina, 1995)

1.3.4) Kinetics of NMDAR channels

NMDAR channels display different gating behaviour compared to the other iGluRs in that they activate (± 10 ms) and inactivate (50-250 ms) slowly (Jonas, 1993). The slow inactivation results in the greater observed NMDAR current (Mori and Mishina, 1995). In contrast to the other two iGluR subtypes, the inactivation kinetics of NMDAR channels do not display any sensitivity towards the duration of glutamate administration (Jonas, 1993).

1.3.5) Binding of endogenous ligands to NMDAR channels

1.3.5.1) Glycin

Glycin, which is responsible for NMDAR channel activation, binds to a region with remarkable sequence similarity to a bacterial amino acid-binding protein called LAOBP (leucin/arginine/ornithine-binding protein). It partly consists of an area on the NR1-subunit preceding the M1 segment and particularly the phenylalanine-X-tyrosine motif around position 370, as well as phenylalanine 448 close to the N-terminal of the subunit. The second crucial part of the glycin binding motif is the loop region between segments M3 and M4, which, considering the three dimensional structure of the subunit, probably overlaps the before mentioned region (Mori and Mishina, 1995; Yamakura and Shimoji, 1999). These areas and also the NR1-subunit are not the sole determinants of the affinity of glycin binding, as demonstrated by the EC_{50} values of glycin binding of 2.1, 0.3, 0.2 and 0.1 μM for heteromeric channels containing NR2A, NR2B, NR2C and NR2C respectively (Yamakura and Shimoji, 1999).

1.3.5.2) Glutamate

Glutamate, together with glycin, acts as a co-antagonist of the NMDAR channel. The glutamate binding motif is situated on homologous areas to that of glycin, but only on the NR2-subunit, as has been demonstrated on the NR2A and NR2B-subunits. As with glycin, other factors play a role in the eventual binding affinity, as the EC_{50} values for the NR2A, NR2B, NR2C and NR2D-subunits are 1.7, 0.8, 0.7 and 0.4 μM respectively (Yamakura and Shimoji, 1999).

1.3.5.3) Mg^{2+}

As mentioned previously, replacement of the N-site asparagine drastically lowers the blocking effect of Mg^{2+}. It seems as if the NR2-subunits are the main contributors to the

Mg^{2+} block in heteromeric channels, since the NR1/NR2A and NR1/NR2B channels are much more sensitive to the blocking effect of Mg^{2+} than their NR1/NR2C and NR1/NR2D counterparts (Mishina et al., 1993; Yamakura and Shimoji, 1999). This higher affinity is primarily due to a difference in the voltage-dependency of Mg^{2+} binding to these channels. The asparagine, one position to the C-terminal side of the N-site asparagine, which is conserved throughout the NR2-subunit family, is also responsible for part of the Mg^{2+} blockade. The difference in Mg^{2+} blocking affinity between the different NR2-subunits must be due to other structures than those mentioned. A tryptophan residue, eight positions upstream of the N- site, was identified as involved in the Mg^{2+} block in NR2B-subunits. Furthermore, several parts in the M1 and M4 segments as well as the M2-M3 linker are also involved in Mg^{2+} blockade (Yamakura and Shimoji, 1999).

When the NMDAR channel's pore size (0.55nm) is compared to the diameter of the naturally occurring 6-fold hydration shell of Mg^{2+} of approximately 0.7nm, steric occlusion seems to be a reasonable explanation for the blockade. However, the partially hydrated Mg^{2+} ion should be fully permeable. Nevertheless, binding studies show that mutation of crucial residues for Mg^{2+} blockade do not have a sufficient effect on the pore diameter to justify this approach. It seems more likely that the combined energetics interaction between the narrowly constricted part of the pore and the Mg^{2+} ion is the telling factor (Yamakura and Shimoji, 1999).

The NMDAR channel is also blocked by intracellular Mg^{2+}. The sites responsible for this are not structurally similar and are separated by a high energy barrier from the sites responsible for the binding of extracellular Mg^{2+}. It seems as if the residues five to seven positions downstream of the N-site are mainly responsible, although the N-site asparagine has also been implicated (Yamakura and Shimoji, 1999).

1.3.5.4) Endogenous allosteric modulators

NMDAR channel function is constantly influenced by four modulators that occur prevalently in the CNS environment. Extracellular protons inhibit the NMDAR channel current with an IC_{50} near the physiological pH, which implicates that the channel is constantly inhibited (Yamakura and Shimoji, 1999; Hynd et al., 2004). This effect depends on the presence of the NR1-subunit containing the N1 insert. Heteromers containing the NR2C-subunit, though, are insensitive, regardless of the NR1-subunit (Yamakura and Shimoji, 1999). Other modulators, for example the polyamines, employ the pH sensitivity of the NMDAR channel to mediate its effect (Hynd et al., 2004).

The polyamines spermine and spermidine are abundant in the CNS (Yamakura and Shimoji, 1999), with concentrations varying in the micromolar range, depending on intricate regulatory pathways (Hynd et al., 2004). These amines have both stimulatory and inhibitory effects on the NMDAR channel. Its stimulatory effect is glycin-independent in conditions of saturating glycin concentrations. NMDAR channel current is enhanced, though, by a decrease in desensitization rate and an increase in open frequency. When glycin concentrations are such that complete saturation is not accomplished, so-called glycin-dependent stimulation by spermine and spermidine increases the NMDAR's sensitivity towards glycin binding, also resulting in increased channel activation. Spermine and spermidine's inhibitory effect is firstly mediated by lowering the receptor's affinity for glycin, thus partly negating the glycin-dependent stimulatory effect. A voltage-dependent inhibition of NMDAR channels is also observed. Another polyamine, ifenprodil, acts as a noncompetitive antagonist, antagonizing the effect of glycin on the receptor. All the polyamine effects are strongly dependent upon the subunit subtypes expressed in the NMDAR channels involved. Certain subunit combinations are insensitive towards the polyamine's effect, while heteromers containing the NR2B-subunit are stimulated by ifenprodil, instead of being inhibited (Yamakura and Shimoji, 1999).

NMDAR channels contain a sulfhydryl redox site on the NR1-subunit. Reducing agents have a stimulating influence on NMDAR channel current, while the opposite effect is mediated by oxidization. Zn^{2+} also inhibits the NMDAR channel current in a noncompetitive, voltage-independent manner at concentrations of 1-10 μM. Higher Zn^{2+} concentrations (10-100 μM) result in a more pronounced voltage-dependent inhibition. Both the redox and Zn^{2+} reactions are dependent on the subunit composition, as is the case for the effects of the other modulators (Yamakura and Shimoji, 1999; Hynd et al., 2004).

1.3.6) Differential expression of NMDAR-subunits

The differential expression of NMDAR-subunits in the nervous system was analyzed by *in situ* hybridization. In the adult brain, NR1 is ubiquitously expressed (Mishina et al., 1993; Mori and Mishina, 1995; Cull-Candy et al., 2001). The NR2A-subunits are also widely expressed throughout the brain (Yamakura and Shimoji, 1999), with higher levels in the cerebral cortex, the hippocampus and the cerebral granule cells (Mishina et al., 1993; Mori and Mishina, 1995). The NR2B-subunits are exclusively situated in the forebrain, with special high expressional levels in the cerebral cortex, hippocampus, septum, caudate putamen, olfactory bulb and thalamus (Mishina et al., 1993). The NR2C-subunits are almost exclusively found in the granule cell layer of the cerebellum, but are also weakly expressed in the olfactory bulb and the thalamus (Mishina et al., 1993; Yamakura and Shimoji, 1999). The least prevalent subunit in the adult brain is the NR2D-subunit, which is only weakly expressed in the diencephalons and the brainstem (Mishina et al., 1993).

The differential expression of NR2-subunits in the spinal cord is still controversial. Again, the NR1-subunit is expressed throughout the spinal cord. The NR2A and NR2B-subunits were identified in the mouse cervical cord, while the NR2C and NR2D-subunits were found in the lumbar cord of the rat (Yamakura and Shimoji, 1999).

The functional role of NMDAR channels differ as the nervous system makes the transfer from the embryonic phase to the post-birth phase. Especially the first two weeks after birth is accompanied by extensive changes in the NR2-subunit distribution. In the embryo brain, NR2B is widely expressed, while NR2D is densely expressed in the diencephalons and brainstem. Soon after birth, many of these subunits are substituted by NR2A and NR2C-subunits until the expressional pattern corresponds to that found in the adult brain (Mishina et al., 1993; Mori and Mishina, 1995). There is, though, a continuous trend for the aging brain NR2B-subunit to be gradually substituted by the NR2A-subunit (Cull-Candy et al., 2001).

1.3.7) Function of NMDAR channels in the brain

1.3.7.1) Long-term potentiation as a model for learning and memory formation

From the information processing paradigm comes the basic principle for effective information storage in a neuronal network, which states that the connections between the neurons must have the ability to undergo use-dependent functional changes (Hölscher, 2001). According to Bliss and Collingridge (1993) it was demonstrated more than a century ago by Cajal that changes in synaptic efficacy might bring about some form of information storage in the brain. Later theoreticists speculated that this synaptic change brings about a change in the neuronal circuitry that is expressed as specific spatiotemporal patterns of neural activity, which represents memory traces.

According to Hölscher (2001), Bliss and Lømo came forth with a model in 1973 that elucidated a possible form of memory storage based on the principles mentioned above – they called it long-term potentiation (LTP). Since then, it's been the most popular theoretical explanation for learning and memory formation on a cellular level, with many empirical studies confirming it, and some casting doubt. Nevertheless, with the lack of a better alternative explanation, this model is generally accepted (Bliss and Collingridge, 1993; Hölscher, 2001). It basically implies a sustained enhancement in synaptic efficacy

in a particular neural circuit, caused by high-frequency electrical stimulation (Bliss et al., 1990; Bliss and Collingridge, 1993), that can last for several hours *in vitro* and days *in vivo* (Bliss et al., 1999). It serves as an experimental model for studying the Hebb rule for synaptic change, which states that the synaptic activity is strengthened where the post and presynaptic neurons are stimulated simultaneously (Bliss and Collingridge, 1993; Bliss et al., 1999). LTP can be induced artificially by delivering tetanic stimuli to the particular pathway, or a lesser stimuli, provided it is within a certain frequency and amplitude range (Bliss and Collingridge, 1993).

LTP-like activity is observed in structures throughout the brain, but particularly in the hippocampus, a cortical structure that is responsible for conscious memory formation in humans, where LTP was first identified (Bliss and Collingridge, 1993; Bliss et al., 1999). The majority of current models for hippocampal functioning thus explains memory capturing by using LTP-like mechanistic models (Moser et al., 1998).

LTP is characterized by three defining attributes. Firstly, cooperativity or use-dependence, refering to a certain activity threshold that has to be surpassed in order for synaptic activity to be altered (Bliss and Collingridge, 1993; Hölscher, 2001). This threshold consists of an intricate interplay between stimulation intensity and pattern of stimulation (Bliss and Collingridge, 1993). The second basic attribute of LTP is called input specificity, which refers to the limitation of synaptic change to those synapses that were activated simultaneously in the particular neural circuit. The change does not spread to synapses in the vicinity. Lastly, association, meaning that LTP can be induced by independent, but convergent input. This input can be composed of two low frequency stimuli, which separately would not be able to induce LTP on the condition that the input is precisely synchronized (Bliss and Collingridge, 1993; Hölscher, 2001).

The association between experimentally induced and observed LTP with learning and memory was made by administering LTP-blocking compounds. When LTP is blocked, it's been shown several times that rats could not complete the maze memory test nearly as successfully compared to the control group. Furthermore, genetically manipulated

animal models with defects in LTP also showed decreased memory and learning test capability on several different occasions. Tang et al. (1999), for instance, developed a mouse model with increased expression of the NR2B-subunit in the NMDAR channel complex, substituting the NR2A-subunit. The NR2B-subunit enlarges the total NMDAR channel current, which, according to Tang et al. (1999), should lead to a greater degree of LTP. Tang's predictions were correct – LTP was enhanced in this mouse model and it effectively led to mice with greater performance in three different recognised assessments for learning and memory ability (Bliss et al., 1999; Tang et al., 1999).

According to the results of several ligand binding studies, a variety of amino acid receptor types play a role in the induction of LTP. Although NMDARs play a major role (Bliss et al., 1990; Bliss and Collingridge, 1993), it is not the only contributor, as indicated by the insufficiency of NMDA administration to induce LTP. Nevertheless, NMDAR's unique properties are ideally suited for its role as prime pathway towards LTP. Its simultaneous activation criteria of voltage-dependence via its Mg^{2+} block and glutamate binding goes a long way in explaining the phenomena of cooperativity, associativity and input-specificity. The threshold for cooperativity is mediated through the voltage-dependent Mg^{2+} block. In the same way, additional stimuli can contribute to the eventual overshoot of the threshold, thus explaining associativity. Any stimuli that adds to the final inputs' ability to depolarize to postsynaptic membrane, may thus contribute associatively to LTP. On the other hand, input specificity can be explained by the necessity of glutamate concentration to rise adequately for the receptor to activate, since the ambient glutamate concentration is inadequate (Bliss and Collingridge, 1993).

Ca^{2+} apparently serves as the trigger or signal for the induction of LTP, since EGTA administration blocks LTP (Bliss and Collingridge, 1993). Since NMDAR channels are a main carrier of Ca^{2+}, the arguments for NMDAR channels as a primary channel and that for Ca^{2+} being the signal inducer strengthen each other.

The synaptic change or changes that eventually give rise to the enhanced efficacy through increased stimulation of the postsynaptic neuron, is probably mediated through a

combination of several mechanisms. An increase in glutamate released per stimulus presynaptically, an increase in the number or change in characteristics of postsynaptic receptors, a decreased glial uptake of glutamate extrasynaptically or other morphological changes may all play a role. These changes, though, have to be implemented by some mechanism/s which is/are probably triggered by Ca^{2+} influx through NMDAR channels. The Ca^{2+} sensitive enzymes are naturally a prime target for investigations on this matter. In particular, Ca^{2+}/phospholipid-dependent protein kinase is a good candidate, after it was confirmed that inhibition of this enzyme inhibits LTP. This happens even after tetanic stimuli activity, which shows that the activity outlasts signal induction. Yet, this enzyme is necessary but probably not sufficient as a signal transducer. Other enzymes that also attracted attention were calmodulin and Ca^{2+}/calmodulin-dependent protein kinase (CaMKII). The synthesis of new proteins could also play a key role in LTP signal transduction. Inhibition of protein synthesis from existing mRNA blocked LTP, is an effect which supposedly is of major importance in the first few hours after the stimuli (Bliss and Collingridge, 1993).

Modifications in the number and properties of the relevant post-synaptic receptors and/or channels might also be mediated by protein kinase phosphorilation, since it was observed that PKC enhances NMDAR activity. Endogenous promoters of channel function, like phosphatidylinositol 4,5-biphosphate to inositol triphosphate (IP_3) and arachidonic acid for NMDAR channels, probably play a role as well in modulating postsynaptic membrane protein expression and function (Bliss and Collingridge, 1993).

The mechanism involved in enhanced neurotransmitter release after LTP might engage any one or more phases of the presynaptic neurotransmitter releasing process, from the initial Ca^{2+} entry to the exocytotic functions of vesicle mobilization, docking and fusion. Concensus exists, however, surrounding the necessity of a so-called retrograde messenger, which transmits a signal from the postsynaptic neuron to the presynaptic neuron to signal the change. Currently, because of its significant interaction with NMDAR channel function, it is thought that this role is at least partially fulfilled by arachidonic acid (Bliss et al., 1990; Bliss and Collingridge, 1993). Firstly, arachidonic

acid release is triggered by NMDAR activation. Furthermore, its administration has a diminishing effect on glial cell glutamate uptake and also a slow onset potentiating effect on hippocampal synapses. A further reason for arachidonic acid's proposed role as the retrograde messenger is the observation that LTP is inhibited by antagonism of this fatty acid (Bliss and Collingridge, 1993).

1.3.7.2) Developmental plasticity

Overwhelming evidence indicates the involvement of NMDAR channels in developmental plasticity. Chronic administration of the NMDAR antagonist, aminophosphonovaleric acid (APV), into the kitten visual cortex, blocks the developmentally determined ocular dominance shift. This phenomenon is usually associated with occlusion of one eye during development. Administration of the same antagonist reportedly prevents the regression of climbing fibre synapses in Purkinje cells. NMDAR antagonists also interfere with granule cell migration and have an effect on the neural map after birth (Mori and Mishina, 1995). The mechanistic pathway involved in this alteration of gene expression is comparable, although not identical, to that initiated by the VACCs, involving signalling pathways ultimately phosphorilating CREB. The proposed initial factor involved in linking the Ca^{2+} influx signal is the EphB tyrosine kinase receptor family, which is directly bound to the NMDAR channel on the intracellular side (West et al., 2001).

The ability of NMDAR channels to modulate neuronal gene expression is developmentally regulated. As the neuron matures, NMDAR channel activity does not induce sustainable phosphorilation of CREB, which is essential for Ca^{2+} modulated gene expression (West et al., 2001).

2) NEURAL Ca^{2+} OVERLOAD

Ca^{2+} overload is seen as a major common mechanism leading to cell death due to a variety of cellular impacts including hypoxia, hypoglycaemia and ischaemia, as well as a variety of neurodegenerative disorders such as Alzheimer's and Parkinson's disease. The excessive influx of extracellular Ca^{2+} into the intracellular space as well as the excessive release of Ca^{2+} from intracellular stores have been much studied, and various models explaining the mechanisms leading to the eventual cell death have been developed. The most popular model is the so-called glutamate excitotoxicity model, which states that the excessive influx of Ca^{2+} is mainly in response to an excessive glutamate concentration in the synaptic cleft. The excessive Ca^{2+} influx due to glutamate toxicity results in the activation of several reactional cascades, ultimately leading to cell death (Rothman and Olney, 1995).

Neuronal cell death is thought to be mediated by two mechanisms: necrosis and apoptosis. Necrosis is characterized by a more acute disruption of cellular metabolism, which includes complete ATP depletion, ion deregulation, activation of intracellular degradative enzymes, cellular and mitochondrial swelling (Phillis and O'Regan, 2004) and the eventual rupture of the cytoplasmic membrane (Gasic and Nicotera, 2003; Philles and O'Regan, 2004). Apoptosis is programmed cell death, highly active during the demise of unnecessary neurons during the developmental process (Boxer and Bigge, 1997; Gasic and Nicotera, 2003).

It is not simple, though, to distinguish between these two mechanisms during episodes of cell death, since the defining criteria are based on transient events (Boxer and Bigge, 1997). Furthermore, only parts of a certain pathway might be involved in the eventual observed process (Olney, 2003). Nevertheless, it is assumed that both mechanisms, to a varying degree, are involved in glutamate excitotoxic cell death (Gasic and Nicotera, 2003; Olney, 2003). Both mechanisms might be initiated by identical insults with a variance in outcome, probably dependent to a large degree on cellular composition and thus cell type. In some cells, for example, ATP production by other metabolic pathways (e.g. glycolysis) might still be adequate to supply in the cell's energy demands after failure of oxidative processes (Philles and O'Regan, 2004). It is proposed that apoptosis

is induced when the mitochondria's ability to produce ATP is only compromised and not completely abolished. When ATP hydrolysis is shut down completely, the apoptotic programme is not activated and necrosis probably contributes more significantly to the ultimate cell death. The exact nature of the insult to the individual cell is thus thought to play the decisive role regarding the pathway of death. Long-lasting, more excessive elevations in intracellular Ca^{2+} concentration probably lead to necrosis, while more subtle excessive Ca^{2+} loads for a lesser duration, induce apoptosis. The final lethal damage induced by an apoptotic insult is characterized by nuclear chromatin condensation and DNA fragmentation, followed by gradual autodigestion of the cell (Boxer and Bigge, 1997; Philles and O'Regan, 2004), in contrast to the characteristic disintegration of membranes observed during necrosis (Gasic and Nicotera, 2003).

Many proposals have been made regarding the *in vitro* and *in vivo* relation between glutamate toxicity and the resultant Ca^{2+} overload and cell death following ischaemia and ischaemia related states such as hypoxia and hypoglycaemia (Ferger and Krieglstein, 1996; Kornhuber and Weller, 1997; Kume et al., 2002). An immediate excessive rise in intracellular Ca^{2+} concentration, which is dependent upon the extracellular Ca^{2+} concentration (Li et al., 2001), immediately after an ischaemic insult, correlates with delayed neurodegeneration (Dubinsky et al., 1995; Li et al., 2001). The relationship is further strengthened by observations of significant increases in synaptic glutamate concentration following the induction of ischaemia (Kornhuber and Weller, 1997; Nishisawa, 2001; Kume et al., 2002). The Ca^{2+} overload cascade is probably triggered by persistant depolarization due to energy deficits during ischaemia (Kornhuber and Weller, 1997). The link between Alzheimer's disease and inefficient neuronal energy metabolism is a well known fact (Rothman and Olney, 1995; Miguel-Hidalgo et al., 2002). The much used 1-Methyl-4-phenyl-1,2, 3,6-tetrahydropyridine (MPTP) model for Parkinson's disease also relates to deficient ATP levels (Geldenhuys et al., 2003). In both latter cases, depolarization is probably induced by these energy deficits, which results in hyperactivation of the receptors involved and eventual Ca^{2+} overload.

Why are the neurons of the CNS so vulnerable towards these insults? In the first place, owing to the brain's unique function and its resulting high metabolic rate relative to other tissues, the brain consumes enormous amounts of oxygen and utilizes large quantities of ATP. Also, since neurons of the CNS are non-replicating, subtle long-lasting deleterious events might accumulate, decreasing the neuron's resistance towards future insults. Thirdly, neurons have relatively concentrated expressional patterns of receptors and ion channels that are implicated in Ca^{2+} overload. Potential triggers like glutamate and other excitatory neurotransmitters are also abundant in the neuronal environment (Cui et al., 2004).

Considerable variability exists between different neuronal types, though, as towards the vulnerability to different kinds of insults. This phenomenon can be attributed to differences in cellular composition, as demonstrated by the differential regional distribution of various relevant proteins such as ion channels, glutamate receptors and transporters, growth factors and other protective elements such as anti-oxidants, as well as differences in genetic response to a particular insult (Brustovetsky et al., 2004). These differences are pronounced and when the existence thereof is ignored, often result in surprisingly inconsistent experimental results. Neurons in close proximity might have completely irrelative reactions towards the same insult (Ke and Gibson, 2004). Regional differences in the expression of glutamate transporter proteins, for example, explain striatal neuronal death at excitotoxic glutamate concentrations that apparently do not affect the adjacent hippocampal neurons (Brustovetsky et al., 2004).

2.1) Neural Ca^{2+}-metabolism

Ca^{2+} homeostasis is regulated by an intricate balance in the function of Ca^{2+}-transporting membrane proteins, intracellular Ca^{2+}-stores, Ca^{2+} buffering and Ca^{2+} extrusion mechanisms. Since intracellular free Ca^{2+} is maintained at relatively low levels (approximately 100 nM), small local rises in this cation's concentration in the vicinity of strategically designed sites may trigger the activation of Ca^{2+}-dependent cascades, of which several might be induced simultaneously (Arundine and Tymianski, 2003; Pringle,

2004). Influx of Ca^{2+} from the extracellular space is mediated by the VACCs and the iGluRs, mainly the NMDAR. Two membrane proteins are primarily responsible for the removal of Ca^{2+} from the intracellular environment in order to reestablish resting Ca^{2+} levels, namely Ca^{2+}-ATPase and the Na^+/Ca^{2+} exchanger. Disruption of their function or exceeding their capacity by too much Ca^{2+} influx plays an important role in Ca^{2+} overload (Gasic and Nicotera, 2003). In contrast to the ATPase which is driven by metabolic energy, the Na^+/Ca^{2+} exchanger relies on the maintenance of the Na^+ electrochemical gradient. This gradient relies heavily on the function of the Na^+/K^+-ATPase, which thus transfers its ATP-dependence onto the Na^+/Ca^{2+} exchanger. The Na^+/K^+-ATPase uses approximately 50% of the total cell ATP production, hence metabolic stress will have an indirect but rather drastic influence on the Na^+/Ca^{2+} exchanger (Pringle, 2004). The endoplasmic reticulum (ER) acts as a Ca^{2+} sequestering agent. Ca^{2+} is taken up into the ER lumen by the sarco/endoplasmic reticululum Ca^{2+}-ATPase (SERCA) pump (Pringle, 2004), after which Ca^{2+} is bound in the lumen by various Ca^{2+}-binding proteins. Release of the stored Ca^{2+} is mediated by the ryanodine and IP_3 receptors. The ryanodine receptors are activated by a rapid rise in intracellular Ca^{2+} concentration, while the IP_3 receptors require simultaneous binding of IP_3 and Ca^{2+}. High glutamate exposure is thought to stimulate phospholipase (PL) to produce increased levels of PL_3 as well as a Ca^{2+} influx through the glutamate receptors, leading to activation of the IP_3 receptors (Budd, 1998).

Besides its role in ATP production, the mitochondria also act as a buffer of intracellular Ca^{2+}. Once a certain set-point in the intracellular Ca^{2+} concentration is exceeded, Ca^{2+} is transported into the mitochondria, thus maintaining the physiological Ca^{2+} concentration (Nicholls and Budd, 2000). The functional role of the mitochondrion's Ca^{2+} storage capacity is that various mitochondrial dehydrogenase enzymes that catalyze crucial steps in the cell's energy metabolism are Ca^{2+}-dependently activated (Budd, 1998). Influx of Ca^{2+} from the cytoplasm to the mitochondrial lumen is mediated through the so-called Ca^{2+} uniporter, driven by the Ca^{2+} electrochemical potential (Kuo and Zhu, 2000; Pringle, 2004). This gradient is sufficient to result in the mitochondria storing up to 0.1 M Ca^{2+} in the matrix, which is 10^5 to 10^6 times higher than the cytoplasmic concentration, although

the normal physiological mitochondrial Ca^{2+} concentration is less than 100 – 200 nM. The uniporter utilizes a phosphate anion to cotransport a H^+ cation over the membrane. This feature neutralizes the tendency of a greatly enhanced mitochondrial Ca^{2+} concentration to alkalinize the matrix. Ca^{2+} is transported out of the organelle primarily via Ca^{2+}/Na^+ transporters (Budd, 1998; Kuo and Zhu, 2000). These transporters probably make use of ATPase and transport the ion against the Ca^{2+} electrochemical gradient, which is probably exchanged with two or more Na^+ or H^+ ions, or otherwise cotransported outwardly with a phosphate ion. An important feature of mitochondrial Ca^{2+} metabolism with respect to Ca^{2+} overload is the fact that excessive mitochondrial Ca^{2+} influx abolishes ATP production by oxidative processes. This is probably due the sensitivity of ATP hydrolysis to a lowered mitochondrial membrane potential, which is induced during excessive Ca^{2+} influx (Budd, 1998).

Ca^{2+} chelating agents, mainly calciretinin, pervalbumin and especially calmodulin, have a major effect in lowering the total intracellular free Ca^{2+} concentration. These Ca^{2+} binding proteins (CBPs) also serve as ion distributors, controlling the increase in local free Ca^{2+} concentration at microdomains where it is functionally relevant, or the decrease in local Ca^{2+} concentration where it is not useful at that time (Pringle, 2004). The concentration of the different types of chelators varies considerably between different neuron types. Because of the chelators, the effective intracellular Ca^{2+} concentration is approximately between 20 and 300nM, which represents no more than 1% of the the total intracellular Ca^{2+} concentration which measures in the millimolar range. It must be noted, however, that this form of Ca^{2+} storage becomes saturated quickly, whereafter the other above mentioned stores take over responsibility for Ca^{2+} storage (Budd, 1998).

2.2) *In vitro* induction of Ca^{2+} overload

According to several studies, the state of ischaemia can be imitated in cell preparates by inducing the related states of hypoxia or hypoglycaemia. Hypoxia may be chemically induced by the addition of sodium cyanide (Ferger and Krieglstein, 1996) or sodium

azide to the cell medium (Kume et al., 2002), both of which inhibit the effectiveness of the oxidative phosphorilation process. Incubation environments where the usual 95% oxygen is replaced by 95% nitrogen are commonly used as well (Small et al., 1997; Frankiewics et al., 2000; Kubo et al., 2001). Apart from its isolated effects linked to Ca^{2+} overload, hypoglycaemic conditions also enhance the acute effect of excessive glutamate levels (Vergun et al., 2003; Ioudina et al., 2004). These conditions may be chemically induced by 2-deoxy-D-glucose, which inhibits the glycolytic process (Kume et al., 2002). Alternatively, incubation in a low or no glucose medium, where the glucose is replaced by the metabolically inactive d-mannitol, can be used (Small et al., 1997; Frankiewics et al., 2000). Many studies try to imitate *in vivo* circumstances more realistically by changing the cell preperate's environment closer to physiological conditions after the initial ischaemic insult, thereby imitating post-ischaemic reperfusion (Frankiewics et al., 2000; Kubo et al., 2001; Kume et al., 2002). Glutamate toxicity is induced by introducing glutamate concentrations, generally ranging between 50 μM and 10 mM, for various time periods (Li et al., 2001; Jing et al., 2004). This insult is frequently accompanied by artificially induced depolarization, normally by increasing the extracellular K^+ concentration (Kiedrowski, 1998; Baldassa et al., 2003).

According to Dubinsky et al., (1995), the characteristic variations in time frame needed to induce cell death can be divided between rapidly triggered and slowly triggered types. Rapidly triggered cell death is related to osmotic lysis, as seen after exposure to high concentration of Ca^{2+} permeable channel agonists, while the slowly triggered type is related to delayed Ca^{2+}-dependent mechanisms, induced by a more subtle agonist insult. This distinct reaction of cells to insults depends on the intrinsic strength of the cell, based on its recovery mechanisms, as well as the type of insult (Dubinsky et al. 1995), which is the duration of exposure and the concentration and character of the insult medium (Li et al., 2001).

The trend in cell death's relation to time might take a sigmoidal time course: the initial rise in glutamate concentration thus leads to an initial spurt of cell death, which probably is osmotically driven. This is followed by a period of no death, during which the

reactional cascade by which the Ca^{2+}-dependent mechanism induced cell death has to be completed, followed by ultimate degeneration of the rest of the vulnerable cells. More likely, several platos with increased cell death periods in between might be the time pattern, owing to various periods of increased cell death due to various end points of different responsible cascades. For this reason, many laboratories do their eventual assesment of cell death following an excitotoxic insult only after 18 to 24 hours (Dubinsky et al., 1995).

Another crucial time variable which attracted a lot of interest, is the critical duration of insult exposure after which cells are unable to recover. Electrophysiologically, a hypoxic/hypoglycaemic insult of 4 minutes suppressed fast excitatory post-synaptic potentials (fEPSPs), used as an indication of normal cellular function, to almost 0 mV. Upon restoration of normal conditions, there was an initial partial recovery of the fEPSPs, peaking after approximately 15 minutes, followed by a gradual irreversible decline (Frankiewics et al., 2000). Intracellular EGTA administration 5 minutes post-insult and removal of extracellar Ca^{2+} within less than 30 minutes were also reported to result in partial protection against neuronal death (Li et al., 2001).

Ca^{2+} overload might thus be induced by any one or a combination of these interventions. All these interventions, separated or combined, are applicable to the study of Ca^{2+}-related cellular death, although variations in mechanistic pathways do occur. The ultimate choice of intervention is determined by in depth consideration of the subject and objectives of each investigation.

2.3) Intracellular mechanisms responsible for neural cell death caused by Ca^{2+} overload

When, as happens during glutamate excitotoxicity, the Ca^{2+} load exceeds the cell's capacity to regulate Ca^{2+}, excessive activation of several Ca^{2+}-dependent cascades occur, leading to the activation of several necrosis and/or apoptosis-inducing cascades. These

cascades (as demonstrated in Fig. 4) probably include hyperactivation of several enzymes with damaging consequences for cell structure and function on various levels (Arundine and Tymianski, 2003).

As already mentioned (see section 2), the CNS is generally extraordinarily sensitive towards insults that compromise the cell's oxidative energy metabolism. Inadequate ATP levels depolarize the plasma membrane via malfunction of several ATP-dependent transport systems, in which the Na^+/K^+-ATPase plays the greatest quantitative role, also taking into account its reversing effect on the Na^+/Ca^{2+}-exchange mechanism. Multiple voltage-sensitive ion channels in the plasma membrane are activated by this depolarization (Pringle, 2004).

K^+ efflux and Na^+ influx generates a positive feedback cycle of depolarization and resultant ion channel activation. Water influx follows the inward osmotic force created by excessive intracellular Na^+ and Cl^- concentrations. This results in cellular swelling and membrane damage (Hynd et al., 2004; Rodriguez et al., 2004). VACCs are also activated by depolarization, leading to massive quantities of Ca^{2+} flowing into the cytoplasm. This Ca^{2+} load, which depolarizes the cell even more, activates several Ca^{2+}-dependent enzymes (Nencioni et al., 2004; Rajendra et al., 2004). It also overloads the mitochondrial matrix, which may lead to the activation of reactive oxygen species (ROS) and the release of apoptotic messenger proteins. Further disturbance in the already challenged mitochondrial electron transport cycle lessens the available ATP levels, which has more detrimental effects upon the cell (Philles and O'Regan, 2004). The increased intracellular Ca^{2+} level mediates the release of more glutamate from the presynaptic membrane, which leads to enhanced activation of the NMDAR channels, conducting greater quantities of Ca^{2+} (and Na^+) into the cell. The enhanced glutamate concentration also activates the glutamate dependent AMPAR and kainate receptor channels, resulting in a further increase in intracellular Na^+ and Cl^- levels (Kornhuber and Weller, 1997).

The excessive ROS activation and release of apoptotic messengers along with the Ca^{2+} dependent hyperactivated enzymes, damages the cell on the membrane, cytoskeleton,

mitochondria, nucleus and several other macromolecular levels (Nencioni et al., 2004; Rajendra et al., 2004). These insults might ultimately induce neuronal mortality. In the next section, several of the most important mediators of this cell death process will be discussed.

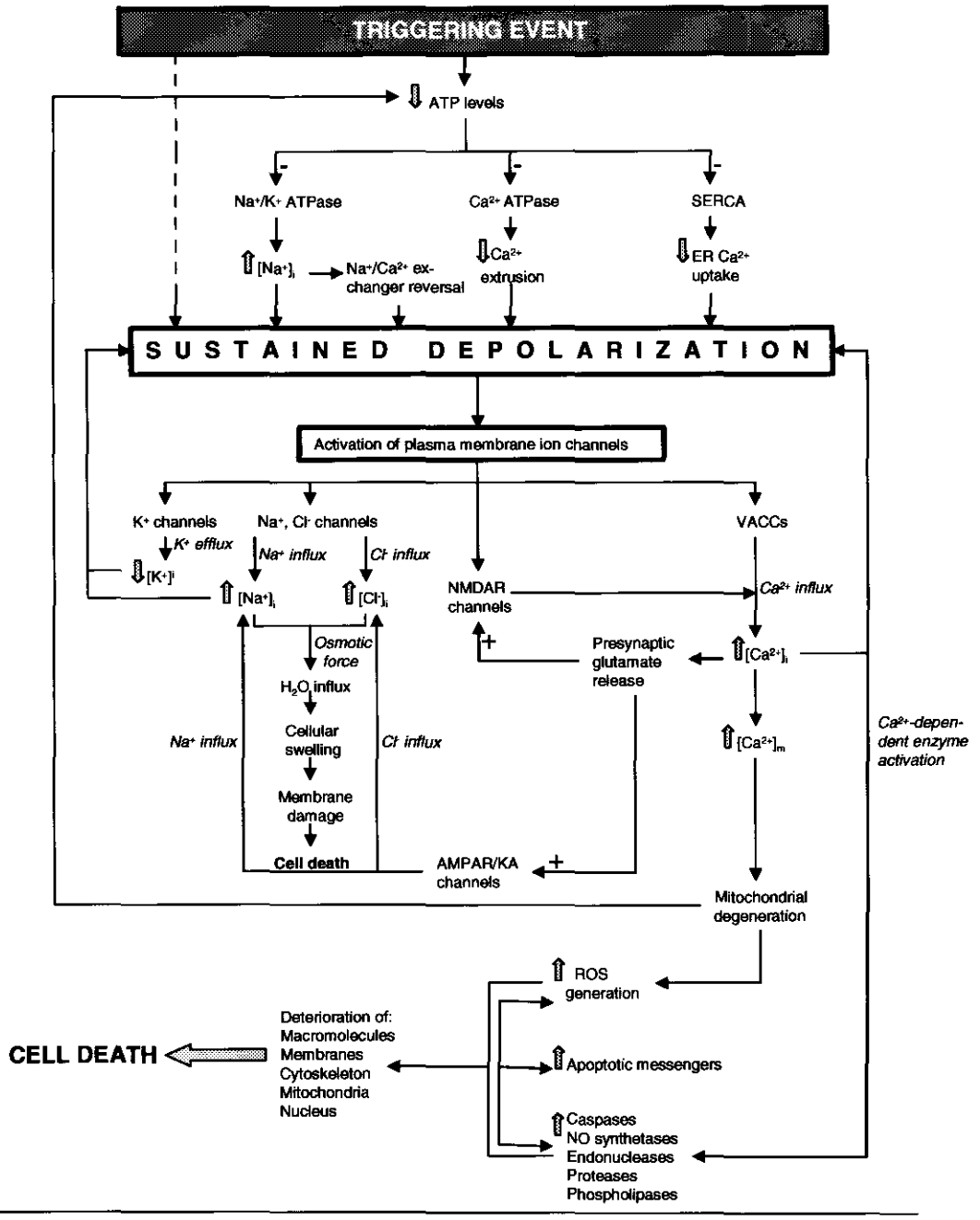

Figure 4. Proposed neurodegenerative pathway following an assault upon the cell's energy metabolism (compiled from Rodriguez et al., 2000; Hynd et al., 2004; Nencioni et al., 2004; Philles and O'Regan, 2004; Pringle, 2004; Rajendra et al., 2004)

Abbreviations: **SERCA** – *sarco/endoplasmic reticulum Ca2+ ATPase;* **ER** – *endoplasmic reticulum;* **[ion]$_i$** – *intracellular ion concentration;* **[ion]$_m$** – *mitochondrial ion concentration;* **VACCs** – *voltage-activated calcium channels;* **NMDAR** – *N-methyl-D-aspartate receptor;* **AMPAR** - *S-α-amino-3-hidroxy-5-methyl-4-isoxazolepropionic acid receptor;* **KA** - *kainate receptor;* **ROS** – *reactive oxygen species;* **NO** – *nitric oxide;* **+ sign** – *activation;* **- sign** - *inhibition*

2.3.1) Role of enzymes

Several types of enzymes are thought to be activated by a rise in intracellular Ca^{2+} concentration and are considered to be closely involved in Ca^{2+}-induced cell death.

The Ca^{2+}-activated proteases are located in cytoplasmic compartments. These enzymes, in association with the inhibitory protein calpastatin, associate upon activation with the cytoplasmic membrane. The preferred substrate for Ca^{2+}-activated proteases is probably one or more proteins responsible for the formation and stabilization of the cytoskeletal structure, since this structure is destroyed upon excessive protease activation. The cytoskeletal formation is mainly composed of three fibre types, differentiated by size, function and activity as well as composition. The microfilament, microtubule and intermediate filament organization are sometimes disrupted by an excessive increase in intracellular Ca^{2+} concentration. This leads to the formation of so-called "blebs", which are membrane processes with a thinning membrane appearance (Nicotera et al., 1992).

Actin and actin binding proteins require Ca^{2+} for interaction. An excessive Ca^{2+} concentration leads to dissociation of these compounds. Various enzymatic cascades are activated by the increased Ca^{2+} presence, which eventually leads to the disengagement of the structural microfibres. Excessive activation of Ca^{2+}-dependent proteases catalyze the hydrolytic splicing of several cytoskeletic proteins, leading to disruption of the cytoskeleton. Along the same route excessively activated Ca^{2+}-dependent phosphorilases may catalyze phosphorilating reactions of membrane proteins, causing the cytoskeleton to disintegrate (Nicotera et al., 1992).

The phospholipases catalyze the hydrolysis of mainly glycerophospholipids, which constitute 50-60% of the total neuronal membrane mass. This preferred substrate of the phospholipases is responsible for membrane stability, fluidity and permeability. Several

phospholipid subfamilies are involved in the induction of neuronal cell death following excitotoxicity (Philles and O'Regan, 2004).

The phospholipase A2 (PLA2) subfamily is involved in the regulation of neurotransmitter release, membrane remodelling and in the repair of apoptotic processes. Excessive activation of these enzymes leads to enhanced activation of non-NMDAR iGluRs by glutamate and a direct deleterious action upon the plasma and mitochondrial membranes. Lipid breakdown by PLA2 produces, among others, arachidonic acid (AA), which acts as a modulator of ion channels and regulates the activity of several enzymes, such as NADPH oxidase, diacylglycerol (DAG) kinase and Na^+/K^+-ATPase (Nicotera et al., 1992; Philles and O'Regan, 2004). The oxidation product of AA, eicosanoid, has several degenerative cellular consequences and acts as a ROS. Besides this oxidative product, excessive AA has several direct detrimental consequences. It blocks glutamate reuptake from the synaptic cleft, directly enhances NMDAR channel current and acts as a detergent, destabilizing plasma membrane integrity and fluidity (Philles and O'Regan, 2004).

The phospholipase D (PLD) subfamily is responsible for modulation and regulation of several signal transduction cascades, influencing vesicular transport, cell proliferation, cytoskeletal reorganization, cell motility and several secretory events. This enzyme's action generates phosphatidic acid (PA), which modulates several protein and enzyme functions. Excessive production of PA leads to hydrolysis of this acid, resulting in inordinate concentrations of the second messengers DAG (enhancing Ca^{2+} release from the ER) and lysophosphatidic acid (LPA). Excessive concentrations of LPA deregulate its functioning in adjusting signalling pathways, membrane trafficking, secretion and mitogenesis (Philles and O'Regan, 2004).

The caspases, when excessively activated, are responsible for destructive cleaving of the Ca^{2+}-ATPases in the cytoplasmic membrane, leading to a reduced capacity to extrude the already high intracellular Ca^{2+} levels (Gasic and Nicotera, 2003). Caspase enzymes also play a major role in the apoptotic cascade, where it is the final link responsible for

catalysis of several functional structures in and around the mitochondrion (see section 2.3.3) (Nicholls and Budd, 2000).

Lastly, the endonuclease enzyme group might also be implicated in pathological apoptosis, which results in membrane blebbing, the relocation and compactation of organelles and the condensation of the chromatin material. The endonuclease enzyme group is involved in DNA splitting, which may create damage when overly functional (Nicotera et al., 1993; Kuo and Zhu, 2000). Other nuclear enzymes, like topoisomerase II, are also hyperactivated by excessive Ca^{2+} influx, which then cleave the DNA without performing its normal religatory function (Nicotera et al., 1992).

2.3.2) Role of ROS

ROS are defined as reactive forms of oxygen with the capacity to oxidize or reduce molecular targets. These compounds are physiologically important for subcellular signal transduction and probably in cellular defense against foreign body invasion. Under physiological conditions, enough anti-oxidants are present to render excessive ROS inactive. When this balance is disturbed, as happens during Ca^{2+} overload related insults, the structural and functional integrity of the cell is compromized both directly and indirectly by ROS-induced alterations in the structure and function of the DNA and several proteins and lipids. Some of the most influential ROS (Cui et al., 2004) will be discussed in this section.

Singlet oxygen is synthesized through the enzymatic activation of oxygen. It is a potent radical, which targets polyunsaturated fatty acids (PUFAs) and the DNA, having mutagenic, genotoxic and carcinogenic effects. The well-known vasodilator, nitrogen oxide (NO), combines with superoxide to produce peroxynitrite, which is a powerful oxidizing agent. It has potent inactivating effects on several proteins and has the ability to decompose and generate other ROS types. The electron-transport chain in the mitochondria's oxidative metabolism produces hydroxyperidol, hydroxyl, hydrogen peroxide and superoxide, which are all ROS or are so potentially. Superoxide, although

inactive and not permeable to membranes, undergoes a dismutation reaction to form hydrogen peroxide which is, although not a ROS, permeable to membranes. It tends to react with transition metals to form the hydroxyl ion, which is the most aggressive member of the ROS family. The hydroxyl ion causes damage on three levels: (1) Nucleic acids, where bases and sugars are modified, bases are cross-linked, DNA and proteins are cross-linked, strands are broken and adducts are formed. (2) Lipids, where PUFAs are the prime ROS target. These reactions influence the membrane's electrical potential, permeability and fluidity. Additionally, AA is formed, increasing the concentration of local oxidants. (3) Proteins of various sorts are also a prime target for ROS (Cui et al., 2004). Ca^{2+} overload of the mitochondrial matrix results in excessive activation of phospholipases in the mitochondria and altered permeability of the mitochondrial membrane. These changes generate increased levels of ROS, even in the absence of oxidative phosphorilation (Rajendra et al., 2004).

2.3.3) Role of the mitochondria

The mitochondria play a crucial role in Ca^{2+} overload-induced cell death due to its central role in ATP generation through the process of oxidative phosphorilation. As mentioned previously (see section 2), ATP concentration levels in the cell are essential to its survival after an insult, as well as towards determining the consequential mechanism (either necrosis or apoptosis) that mediates cell death when ATP levels decrease below a certain level. Disturbances in the electron transport chain reaction of oxidative phosphorilation have a wide range of detrimental consequences, resulting in the release of several messengers and deleterious effector proteins/enzymes. Besides not producing ATP anymore, abolishment of the oxidative phosphorilation process also reverses the ATP synthetase, which is the final protein in the electron transport chain, thus utilizing the already low levels of ATP (Nicholls and Budd, 2000).

Ca^{2+} overload-related cell death via mitochondria is proposed to be induced in part due to a mechanism known as permeability transition (PT). PT is characterized by a greatly enhanced permeability of the inner mitochondrial membrane to ions and molecules

smaller and equal to 1.5 kD. This leads to a complete loss of the mitochondrial membrane potential and cessation of ATP hydrolysis, followed by swelling and disintegration of the mitochondria. PT occurs due to the activation of a nonspecific channel in the mitochondrial membrane with a maximum conductance of 1-1.5 nS with long-lasting closed states between activated periods. The identity of the PT-pore (PTP) has been the subject of much research. The current candidates suspected of being involved in the formation of this apparently complex channel are the adenine nucleotide translocator (AdNT) and the outer membrane porin, although it seems as if these proteins probably only play a partial role in the formation of the PTP. The primary trigger for the activation of the PTP is a long-lasting excessive increase in the mitochondria's Ca^{2+} concentration (Kuo and Zhu, 2000; Friberg and Wieloch, 2002), as indicated by the effective reversal of PT by addition of EGTA. Activation of several ROS and phospholipases by this increased Ca^{2+} concentration is coupled to the eventual induction of PT (Friberg and Wieloch, 2002; Philles and O'Regan, 2004) Besides the primary role of Ca^{2+}, there are various secondary inducers of PT, as well as several endogenous inhibitory elements. Central to the secondary inducers is the protein called cyclophilin-D (CyP-D). This protein, located in the mitochondrial matrix, is thought to translocate to the intermembraneous space during events of Ca^{2+} overload, where it binds to and activates the PTP (Friberg and Wieloch, 2002). The level of increase in Ca^{2+} concentration required to induce PT varies considerably due to different ratios of endogenous modulators in the mitochondria of different cell types. For example, a much higher increase in Ca^{2+} concentration is required in cardiac myocyte mitochondria than in central neurons (Budd, 1998).

The significance of PT in neurons has been the subject of much debate and speculation. PT seems to appear transiently under certain unresolved conditions of non-lethal mitochondrial Ca^{2+} overload, where it serves to relieve the mitochondria from its excessive Ca^{2+}. More uncertainty surrounds the existence of persistant PT after pathological Ca^{2+} overload. Evidence suggests that PT is more likely to be of significance during reperfusion after an ischaemic insult, rather than during it (Friberg and Wieloch, 2002; Philles and O'Regan, 2004). Under hypoglycaemic conditions, the resulting slight

alkalosis due to the absence of lactate accumulation also seems to facilitate PTP opening and PT has also been observed following traumatic brain injury (Friberg and Wieloch, 2002).

Apoptosis is induced via mechanisms involving the mitochondria. Three gene types express protein families in mitochondria that are essential to the apoptotic process. The apoptotic protease activation factor (Apaf) and Bcl-2-like protein families both modulate the eventual activation of one or several enzymes of the caspase family. The caspases, all of which are not equally potent, are responsible for the eventual cell deterioration by cleavage of several proteins at Asp-X sites. Under physiological conditions, only a small fraction of the total caspase pool is activated, where the rest are present as inactive procaspases. This small active caspase presence is probably involved in the modelling of cell architecture (Nicholls and Budd, 2000).

An apoptotic pathway that has been elucidated is triggered upon the release of cytochrome C, a protein present in the mitochondrial inner membrane, into the intermembraneous space. Here it combines with procaspase-9 to form a complex with Apaf-1, called the apoptosome. Procaspase-9 is hereby activated, which subsequently activates caspase-3. This enzyme activates several DNAse enzymes and directly degrades several proteins that are directly involved in DNA and cytoskeletal repair processes. The release process of cytochrome C is not properly defined yet, but it is thought that it is mediated by either a controlled, specific opening of mitochondrial membrane pores, or an uncontrolled membrane disruption, which might be due to PT (Nicholls and Budd, 2000; Friberg and Wieloch, 2002).

Different members of the Bcl-2-like protein family, located in the inner mitochondrial membrane, are implicated in both the promotion and the prevention of apoptotic pathways (Kuo and Zhu, 2000; Nicholls and Budd, 2000; Friberg and Wieloch, 2002). Apoptosis promoting Bcl-2-like proteins are able to form heteromeric channels in the mitochondrial membrane which are wide enough to allow the release of cytochrome C. These proteins might also translocate through the inner mitochondrial membrane and

activate several caspases directly. The anti-apoptotic members of the Bcl-2-like proteins act by deactivating or preventing the activation of caspase enzymes. This happens by preventing the release of apoptosis inducing elements or by forming complexes with cytochrome C (Kuo and Zhu, 2000), the procaspases and the apoptosis induction Bcl-2-like proteins, or catalyzing the formation of heteromeric unreactive complexes by these proteins (Nicholls and Budd, 2000; Friberg and Wieloch, 2002).

2.3.4) Cytoplasmic membrane ion channels involved in the influx of Ca^{2+} leading to Ca^{2+} overload

The Ca^{2+} permeable ion channels of the cytoplasmic membrane are theoretically the primary pathway of Ca^{2+} entrance into the cell from the extracellular environment. For this obvious reason, these channels have been the focus of much research concerning Ca^{2+} overload and the prevention thereof. It should be noted, however, that these channels are not the only candidates for inducing an excessive elevation in intracellular Ca^{2+} concentration. Ca^{2+} may also rise excessively in the cytoplasm via inefficient Ca^{2+} extrusion mechanisms, the release of Ca^{2+} from intracellular stores as well as malfunction of cytoplasmic CBPs (Pringle, 2004).

2.3.4.1) The contribution of glutamate receptors

Since excessive synaptic glutamate concentrations are associated with Ca^{2+} overload, the iGluRs and mGluRs have been the focus of many studies investigating the initial path of glutamate excitotoxicity through the cytoplasmic membrane. The major route by which the excessive Ca^{2+} influx during Ca^{2+} overload occurs is thought to be the NMDAR channel, with other channels seemingly playing quantitatively less important roles (Budd, 1998). However, all of the GluRs have been implicated in glutamate excitotoxicity in some or other way (Rajendra et al., 2004). The exact quantitative contribution of the different channel types and hence the exact mechanism of the initiation of Ca^{2+} overload varies considerably depending on the cell type and developmental criteria as well as the character of the insult (Budd, 1998).

Considering the possible role of the mGluRs, it is important to consider each subtype's specific signal transduction mechanism. mGluRs are divided into three structurally distinct classes, each with a separate signal transduction mechanism. Class I is linked to the PLC signal transduction system, which produces increased intracellular DAG and IP_3 levels. These channels are primarily localized on the postsynaptic membrane and regulate neuronal excitability through modulation of ion channel activity. IP_3 leads to increased release of Ca^{2+} from the IP_3 sensitive stores, while DAG activates the PKC system which may lead to an aggravated neurotoxic insult (Budd, 1998; Gasparini et al., 2002). Also, the possibility has been mentioned that class I coupling to PLC might be linked to phosphorilation reactions that release neurotoxic free fatty acids from the membrane during ischaemia (Philles and O'Regan, 2004). Activation of classes II and III are negatively coupled to adenylyl cyclase, which may result in inhibition of cAMP. These receptors are located primarily on the presynaptic membrane, where they probably contribute to glutamate neurotransmitter release (Budd, 1998; Gasparini et al., 2002). Activation of the mGluRs with the agonist, aminocyclopentane-1,3-dicarboxylic acid (ACPD), shows that these receptors probably have no major part to play in Ca^{2+} overload neurotoxicity (Budd, 1998). The more recently developed class I antagonist, BAY36-7620, is much more selective and potent and demonstrated promising therapeutical results in an animal excitotoxicity model (Gasparini et al., 2002), while the class I agonist, (S)-3,5-dihydroxyphenylglycine (DHPG) resulted in protection against NMDA-induced excitotoxicity (Blaabjerg et al., 2003). Thus, although still controversial, it seems as if class I mGluRs might play a quantitatively important role in excitotoxicity.

The functions of the two non-NMDA iGluRs apparently do not have a major influence on Ca^{2+} overload, with some exceptions. These channels are mostly permeable to monovalent cations and only minimally transport Ca^{2+}. An exception is the AMPAR channels, which have been implicated in being responsible for excessive influx of Ca^{2+} in the type II hippocampus neurons, the cerrebellar Purkinje neurons as well as the medial septal neurons. This feature is due to a variation in the structure of the GluR2-subunit of the AMPAR channels expressed in these neuronal populations resulting in a higher

permeability to Ca^{2+} (Budd, 1998; Arundine and Tymianski, 2003). Both non-NMDA iGluRs have also been implicated in Ca^{2+} overload induction in oligodendrocytes (Alberdi et al., 2002). A further definite contribution of these non-NMDAR iGluR channels is of an indirect nature. At the normal resting membrane potential of -70mV, the NMDAR channels are blocked by Mg^{2+} in the pore. The depolarization needed to relieve this blockade is partially induced by the Na^{+} influx via the AMPA and kainate receptor channels that are activated by synaptic glutamate (Kornhuber and Weller, 1997; Budd, 1998).

The NMDAR channels are uniquely suited to be the culprit in Ca^{2+} overload: the bigger current transport ability, the non-desensitization property, Ca^{2+} as the prime current carrier and the synaptic membrane localization of the receptors are crucial in establishing NMDAR channels' identity as a primary pathway of excessive Ca^{2+} influx leading to Ca^{2+} overload (Budd, 1998).

The induction of excessive activation of the NMDAR channels is linked to the exposure levels of the receptors to the agonists, mainly glutamate, since glycin's basal concentration tends to be high enough for continuous activation, as well as, very importantly, depolarization, in order to abolish the voltage-sensitive Mg^{2+} block (Kornhuber and Weller, 1997). This depolarization can be induced by a wide range of mechanisms, in which most major membrane channels and transporters may contribute. As for the excessive glutamate, it might be released in excessive quantities pre-synaptically, or the glial glutamate uptake (by the glutamate transporter) and degradation mechanisms might be dysfunctional (Li et al., 2001).

The Ca^{2+} entering through these channels seem to be the essential factor determining ultimate cell death, since addition of EGTA potently suppresses cell death induced by the NMDAR channels. It has not been determined up to this stage whether a certain threshold of Ca^{2+} influx is needed in terms of concentration or in terms of the time the cell is exposed to the excessive Ca^{2+} (Li et al., 2001). Most likely, a combination of these factors is decisive as to the extent of cell death.

Although the receptor-coupled intracellular events following Ca^{2+} overload through the NMDAR channels is not properly understood yet, Li and his colleagues (2001) found that a rise in intracellular Ca^{2+} concentration conducted through the L-type VACCs does not induce cell death, compared to the same rise in Ca^{2+} concentration via NMDAR channels, which is lethal to the same cells. A possible explanation might be the constitution of the downstream NMDAR channel receptor-coupled machinery and/or the fact that NMDAR channels are located on the post-synaptic membrane compared to the L-type VACC's main expression on the cell body (Rothman and Olney, 1995; Li et al., 2001). The major contribution of NMDAR channels in Ca^{2+} overload is vividly demonstrated by the extreme sensitivity of hippocampus neurons to Ca^{2+} overload inducing insults like ischaemia. The hippocampus has an extraordinarily dense NMDAR channel expressional pattern (Moriyoshi et al., 1991).

This controversial phenomenon is called source specificity, describing a paradigm that gained in popularity due to several experiments observing equal rises in intracellular Ca^{2+} concentration through the VACCs and the NMDARs, with the influx through the NMDARs inducing excitotoxic cell death, but not through the VACCs (Aarts and Tymianski, 2003; Arundine and Tymianski, 2003; Hardingham and Bading, 2003). The theoreticists still holding true to the initial concept of excessive intracellular Ca^{2+} increase being the decisive factor, regardless of the influx route, argue that the inappropriate use of Ca^{2+} indicators in the mentioned experimental findings is the cause of the misguided source specificity hypothesis. Both paradigms are probably correct and the inconsistent findings regarding this matter might be due to conclusions based on experiments using different cell types and different models of excitotoxicity induction (Hardingham and Bading, 2003).

The mechanism for source specificity is speculated to be linked to tight functional and/or physical coupling between the NMDAR channel and the excitotoxic process. It is proposed that this coupling involves enhanced mitochondrial uptake of Ca^{2+} that entered via the NMDAR, for which experimental confirmation was obtained (Hardingham and

Bading, 2003). Furthermore, the critical region in the microdomain surrounding the NMDAR channel where high local Ca^{2+} concentration is established after NMDAR channel activation, contains several local enzymes, which might be activated by the local rise in Ca^{2+} concentration (Krieger and Duchen, 2002; Aarts and Tymianski, 2003; Arundine and Tymianski, 2003).

The coupling between the NMDAR channel and its effects during excitotoxicity is probably mediated by the C-termini of the NMDAR-subunits (Arundine and Tymianski, 2003; Hardingham and Bading, 2003). This large cytoplasmic structure is linked to cytoplasmic proteins such as the cytoskeletal, cell adhesion, adaptor and scaffolding proteins, as well as other components involved in the signal transduction pathway (Hardingham and Bading, 2003). These C-termini linked proteins facilitate Ca^{2+} uptake into the mitochondria. Neuronal nitric oxide synthase (nNOS), which is coupled to the NMDAR channel via the post-synaptic density-95 scaffolding protein (PSD-95), catalyze the production of nitric oxide (NO), which is directly involved in this enhanced mitochondrial Ca^{2+} uptake and probably acts synergistically towards depolarizing the mitochondrial membrane. This view was supported by the reduction in cell death observed in models where PSD-95 expression was suppressed, although the Ca^{2+} influx levels remained the same (Krieger and Duchen, 2002).

2.3.4.2) The contribution of voltage-activated Ca^{2+} channels

VACCs are primarily activated by depolarization. Besides the ability of VACCs to allow influx of huge amounts of Ca^{2+} upon depolarization (Boxer and Bigge, 1997), VACC function might also be directly modulated by excitotoxic messengers, resulting in increased currents (Ekinci et al., 2003). Additionally, tight physiological coupling might exist between the VACCs and Ca^{2+} release and uptake proteins of the ER (Philles and O'Regan, 2004).

Several antagonists and agonists have been identified for most subtypes and the extensive use of these ligands in experimental models for Ca^{2+} overload has led to contradicting conclusions regarding the contribution of the VACCs to excessive Ca^{2+} influx leading to Ca^{2+} overload cell death (Kobayashi and Mori, 1998; Pringle, 2004). One possible solution to these complications is to divide the contributions of these channels: divisions like VACC subtype, expressional density, subcellular localization, cell type, insult type as well as whether the measure is made *in vivo* or *in vitro* and the model used may lead to greater unity of results (Kobayashi and Mori, 1998). Nevertheless, VACCs is, along with the NMDARs, the main conduit for extracellular Ca^{2+} into the cell and, therefore, still is, and should be regularly investigated for its role in Ca^{2+} overload.

2.4) Pharmacological interventions against Ca^{2+} overload

Protection against Ca^{2+} overload-induced neuronal cell death by channel specific blockers gives many clues as to the involved channels' causal effect in Ca^{2+} overload. After the clinical successes achieved with the use of VACC antagonists against cardiovascular disease, the possibility of extending this utility to protect against neuronal Ca^{2+} overload has attracted many scientists. Generally, the clinical efficacy has been disappointing, with some exceptions (Kobayashi and Mori, 1998). The isolated *conus magus* peptide, ω-conotoxin MVIIA, also called SNX111, as well as the dihydropyridine AE0047 show great promise in protecting against stroke (Boxer and Brigge, 1997).

The mixed successes and contradictory evidence obtained experimentally is probably partially due to the variety in possible protective mechanisms combined with the vastly different experimental setups. Protection might be manifested through the improvement of cerebral blood circulation, thus a vascular effect. On the other hand, direct blockade of neuronal Ca^{2+} channels may lead to protection against Ca^{2+} overload. This pathway can be utilized by inhibition of neurotransmitter release (thus a presynaptic effect) or by inhibiting Ca^{2+} influx into postsynaptic neurons (Kobayashi and Mori, 1998).

The disappointing results obtained with VACC antagonists lured researchers to focus on the therapeutic possibilities of intervening with other Ca^{2+} overload pathways and effects by using GluR antagonists, radical scavengers, Na^{+} overload inhibitors and NOS inhibitors (Kobayashi and Mori, 1998).

2.4.1) Blockade of the L-type VACC as a possible protective measure

Modulation of L-type VACC function holds obvious promise for therapeutic use because of the channels' slow inactivation and large current properties, which could make a significant quantitative contribution towards an excessive rise in intracellular Ca^{2+} concentration. Systemic hypotension induced by many of these compounds, as well as the mixed efficacy obtained *in vivo* and *in vitro*, hamper intensive clinical investigation of these compounds (Boxer and Bigge, 1997). L-type VACCs are blocked by three distinct ligand-groups: the dihydropyridines (e.g. nifedipine), the benzothiazepines (e.g. diltiazem) and the phenylalkylamines (e.g. verapamil) (Kochegarov et al., 2003). Although there are multiple similarities in the binding properties between these groups, binding studies concluded that these compounds enhance each other's binding and thus cannot be competing for the same binding site (Hille, 2001).

2.4.1.1) Diltiazem

Diltiazem is a prototype of the benzothiazepine group and consists of two benzene structures bound to the prime thiazepine structure by a nitrogen and a sulphur atom. It binds from the extracellular side to the L-type Ca^{2+} channel with a Kd value of 314 ± 25 nM. Its proposed binding site is situated on the S6 transmembrane segment of domains III and IV, near or inside the pore region (Kochegarov et al., 2003).

Its blocking mechanism is use/frequency-dependent, where binding is enhanced by accelerated activation frequencies and depolarized holding potentials in the patch-clamp setup (Kanaya et al., 1983). Diltiazem's inhibition of the Ca^{2+} current resembles

attenuation of the recovery from channel inactivation and it is proposed that the channel is allosterically modulated upon binding with the antagonist into the same or similar state as that of inactivation (Kochegarov et al., 2003).

Brooks and Kauppinen (1993) determined the levels of phosphocreatine to assess cell damage *in vitro* during aglycaemic hypoxia. Of the three L-type VACC antagonists administered, only diltiazem (25 μM) displayed protection. Surprisingly, NMDAR channel antagonists showed no protection in this study, indicating that the VACCs are mainly responsible for the neurodegeneration. Clentiazem, an analogue of diltiazem, is known to dilate the cerebral artery. This compound was effective in protecting against ischaemia in animal models (Kobayashi and Mori, 1998).

2.4.1.2) Nifedipine

Nifedipine consists of a dihydropyridine and a benzene group and also binds to the L-type VACC from the extracellular side. It is proposed to bind to the S5 segment of domain III and also in/near the pore region of the channel (Kochegarov et al., 2003) with an ED_{50} value of between 20 nM and 50 μM (Hille, 2001). As is the case with diltiazem, nifedipine binds in a use/frequency-dependent manner (Kochegarov et al., 2003).

The ischaemia-induced as well as the post-ischaemic rise in intracellular Ca^{2+} concentration in CA1 of the hippocampus is attenuated by nifedipine. Interestingly, the post-ischaemic protection is not equaled by the NMDAR antagonist MK-801, which suggests that lethal post-ischaemic elevation in Ca^{2+} concentration is mediated by L-type like channels, rather than by NMDAR channels. The nifedipine concentration necessary for this effect was rather low (10^{-8} M) compared to the normal *in vitro* standard (0.1-10 μM) due to nifedipine's, as well as verapamil's (see later) voltage-sensitivity. The blocking effect is, therefore, more pronounced at depolarized potentials, which is the case during ischaemia (Kubo et al., 2001).

2.4.1.3) Other L-type VACC antagonists

Among the dihydropyridines, nimodipine has been extensively investigated. Part of the reason for the attention has been its high selectivity for L-type channels in the cerebral artery. Nimodipine was effective in protecting against ischaemia-induced cell death in animal models, but ineffective in clinical trials for stroke (Kobayashi and Mori, 1998). No difference was found between hypoxic and hypoglycaemic hippocampal brain slices that have been treated with nimodipine and control slices (Small et al., 1997). It is officially approved as treatment against subarachnoid hemorrhage (Boxer and Bigge, 1997; Kobayashi and Mori, 1998) though, and it has been used successfully in some cases of traumatic brain injury (Kobayashi and Mori, 1998). Nicardipine and isradipine were efficient as neuroprotectors in animal models for ischaemia, but clinical effects were marginal. Lemdipine and the dihydropyridines known as F-0401 and S-312-d also exhibited protective effects in ischaemic animal models or ischaemia-induced hippocampal slices (Kobayashi and Mori, 1998).

Mimicking Alzheimer's disease *in vitro* by administration of the Aβ protein, microglial cell death was significantly diminished by simultaneous addition of diltiazem, nifedipine and verapamil, which decreased the excessive intracellular Ca^{2+} concentration by approximately 50% (Silei et al., 1999). It is thought that mitogen-activated protein (MAP) kinase, an enzyme that is activated by Aβ proteins, phosphorilates the L-type VACC, which leads to increased currents. Blockade of these channels decreased these currents and prevented tau phosphorilation, a neurotoxic effect typically observed during Alzheimer's disease. This observation demonstrates the central contribution of L-type VACCs in Alzheimer's disease pathogenesis (Ekinci et al., 2003)

Verapamil, a phenylalkylamine derivative, has the same effect as nifedipine in lowering the rise in intracellular Ca^{2+} concentration in the CA1 region of the hippocampus, as induced by ischaemia (Kubo et al., 2001). The verapamil analogue, emopamil, is like clentiazem also known for its dilatory effect on the cerebral arteries and also protected against ischaemia in animal models (Kobayashi and Mori, 1998).

In many of the studies where L-type antagonists have been found to be effective protectors against neuronal injury, the effect is likely due to vascular effects rather than to direct binding to L-type channels on the neuronal membrane as demonstrated by the frequent absence of the protection when using brain slices. Confirming these observations, neuronal L-type Ca^{2+} channels in the hippocampus are mainly expressed on the cell bodies of pyramidal neurons and are not among the VACCs involved in synaptic transmission where, theoretically, channel block might be therapeutically more relevant (Small et al., 1997; Kobayashi and Mori, 1998; Pringle, 2004).

2.4.2) Blockade of the N-type VACC as a possible protective measure

Investigations of N-type VACC antagonists hinged upon ω-conotoxin MVIIA (SNX-111), a 25 amino acid peptide blocker, after reports that these conopeptides blocked neurotransmitter release (Small et al., 1997; Kobayashi and Mori, 1998).

This N-type Ca^{2+} channel antagonist demonstrated excellent protective action against neurodegeneration in several models of global and focal ischaemia (Boxer and Bigge, 1997; Small et al., 1997; Kobayashi and Mori, 1998). Conclusively, it was found to ameliorate the increase in intracellular Ca^{2+} concentration in the CA1 and CA2 regions of the hippocampus following ischaemia (Kubo et al., 2001). These promising findings were almost without exception for *in vivo* studies, and interestingly, could not be repeated *in vitro* (Boxer and Bigge, 1997; Small et al., 1997). One group (Small et al., 1997) mentioned that, when all N-type channels are blocked, the degree of protection (43%) resembles the degree of the contribution of N-type channels to synaptic transmission (40%). The finding that ω-conotoxin MVIIA was effective even if administered 24 hours after the ischaemic insult is of great therapeutic significance, since it shows that the pathophysiological pathway leading to cell death after an ischaemic insult can be reversed after the insult (Kobayashi and Mori, 1998).

ω-Conotoxin MVIIA is a weak blocker of excitatory amino acid release. Yet, it is effective as a neuroprotector in contrast to the related peptide SNX-230, which is a good excitatory amino acid release blocker (Boxer and Bigge, 1997; Kobayashi and Mori, 1998). This demonstrates the complex process involved in neurodegeneration, and the fact that the current glutamate excitotoxicity and NMDAR channel source specificity theories have their shortcomings (Kobayashi and Mori, 1998).

Besides ω-conotoxin MVIIA, its related peptide ω-conotoxin GIVA also has protective properties against ischaemic Ca^{2+} overload (Small et al., 1997), yet, ω-conotoxin MVIIA has no known equal in terms of protective efficacy (Boxer and Bigge, 1997).

2.4.3) Blockade of the P and Q-type VACC as a possible protective measure

The P and Q-type Ca^{2+} channels are very attractive therapeutic targets, since they have been shown to be directly involved in synaptic transmission *in vitro*. The potent *in vivo* toxicity of these compounds, however, is hampering efforts to elucidate the exact efficacy (Small et al., 1997).

ω-Agatoxin-IVA shows protection against a hypoxic/hypoglycaemic insult in hippocampal slices of the rat. ω-Agatoxin-IVA's selectivity for P-type VACCs are well known, but the concentrations necessary to induce a therapeutic effect blocks Q-type Ca^{2+} channels as well. It might, therefore, be the case that the crucial effect is solely mediated through the Q-type channel (Small et al., 1997; Kobayashi and Mori, 1998). It is worth mentioning that doubt existed over the existence of separate P and Q-type channels. In support of the channels being separate, ω-agatoxin-IVA has different IC_{50} values for the P and Q-type Ca^{2+} channels (Small et al., 1997).

ω-Conotoxin-MVIIC is effective in protecting hippocampus slices against hypoxic neurodegeneration although it has no obvious effects *in vivo*. The reason for this ineffectiveness might be ω-conotoxin -MVIIC's tendency to block glutamate release, which, being toxic, might mask its positive effects *in vivo*. ω-Conotoxin's effect is

mediated through the block of N-type as well as P and Q-type VACCs (Kobayashi and Mori, 1998). Comparing the percentage protection of 100 nM ω-conotoxin -MVIIC versus the percentage protection of 200 nM ω-agatoxin -IVA, where both concentrations lead to the respective channels being maximally blocked, it is remarkable that the protection estimates correlate with the relative degree of contribution that the respective channels have on synaptic transmission (Small et al., 1997).

Two alternative compounds that have been investigated are the natural product, eudesmol and the alkaloid, deurisoline, of which both are thought to block P-type channels. Eudesmol blocks Ca^{2+}-dependent glutamate release in rat synaptosomes and reduces brain edema and infarct size in the rat middle cerebral artery occlusion model. Daurisoline blocks P-type channels in Purkinje neurons. Its *in vivo* efficacy as a neuroprotective agent during ischaemia is diminished by its side-effect of suppressing respiration (Kobayashi and Mori, 1998).

2.4.4) Blockade by non-selective VACC antagonists as a possible protective measure

Flunarizine is a potent, non-selective VACC antagonist, which also has a Na^+ channel blocking effect. Although it is known to improve cerebral circulation, this property is not related to its recorded neuroprotective action based upon similar results in ischaemic animal models and hippocampal brain slices. However, a double-blind clinical trial establishing its effect on patients who suffered from acute ischaemic stroke showed no positive results. Several analogues like cinarizine and lifarizine, also had protective effects on animal models of ischaemia (Kobayashi and Mori, 1998).

The diltiazem analogue, T-477, as well as two other compounds known as NS-649 and NNC 09-0026 are non-selective antagonists of VACCs and were shown to be protective in different types of ischaemia-related animal models. The compound SB 201823 blocks HVA Ca^{2+} channels and lessens the impact of focal ischaemia, even if administered 30 minutes after the insult. Both NS-683 and CNS-1237 decrease the infarct volume in

animal models, NS-683 via blockade of the N and L-type channels and CNS-1237 by inhibiting current through both the VACCs and Na^+ channels (Kobayashi and Mori, 1998). To summarize, it seems as if broad-spectrum Ca^{2+} channel blockers are more effective in inhibiting the adverse effects leading to or caused by to Ca^{2+} overload than specific VACC blockers. Broad-spectrum blockers probably exert their effects through various pathways, which increase its efficacy (Small et al., 1997; Kobayashi and Mori, 1998). According to Small et al. (1997) the relative contribution of the different Ca^{2+} channel subtypes towards neuronal death due to hypoxic and hypoglycaemic insults is Q>N>>P>L (Small et al., 1997).

2.4.5) Blockade of NMDAR channels as a possible protective measure

The use of NMDAR channels as targets for interventions against Ca^{2+} overload related pathologies has been hampered by the psychotomimetic side effects induced after administration of the prototypic uncompetitive NMDAR antagonist, MK-801 (Kornhuber and Weller, 1997). The main challenge in finding a therapeutically suitable NMDAR channel antagonist lies in separating the inhibition of pathological function of the channel from inhibition of normal physiological function (Parsons et al., 1999; Frankiewics et al., 2000). The incapabability of most antagonists to inhibit pathological function selectively leads to a series of side-effects, of which the psychotomimetic side-effects are well-known. Currently, it seems as if the solution might be with open-state, use-dependent, so-called uncompetitive NMDAR channel antagonists similar to MK-801, but only those which, unlike MK-801's high affinity, display low to moderate binding affinity. Evidence shows that the crucial pharmacodynamic elements determining therapeutic efficiency are probably the antagonist's voltage-dependency as well as on-off kinetics - both properties are related to the binding affinity (Frankiewics et al., 2000).

2.4.5.1) MK-801's properties as a protective agent

MK-801 serves as the prototypic uncompetitive antagonist of NMDAR channels in relation to which other NMDAR channel antagonists are characterized and compared

(Frankiewics et al., 2000). The limited cases of therapeutic successes of MK-801 administration are primarily mediated by its high affinity NMDAR channel block, but more than the single mechanism might be relevant since it has been shown that MK-801 also serves as an antagonist of fast-activated Na^+ channels (Palmer, 2001) and probably has L-type VACC antagonistic properties as well, as demonstrated, amongst other indications, by the displacement of MK-801 binding by diltiazem (Schurr et al., 1995a; Robert et al., 2002).

2.4.5.2) Memantine's properties as a protective agent

The low-affinity uncompetitive NMDAR antagonist, memantine, which was introduced in 1964 as an antiviral agent, is a prototypical derivative of the amino-adamantane group of compounds. It has been shown to be NMDAR-selective by both electrophysiological and ligand binding studies (Kornhuber and Weller, 1997). Regarding its binding site, memantine displaces MK-801 in human and rat cortex as well as in the CA1 region of the hippocampus with an average K_i (dissociation constant, measure of affinity) of 1 μM. Despite its moderate affinity, memantine is quite selective for the specific binding site on the NMDAR, since it does not displace any NMDAR channel ligands from the glutamate, glycin or sigma sites. Some doubt existed on the possibility of the polyamine site being the binding site of memantine, but no difference in memantine's potency was detected in the presence or absence of the polyamine site agonist, spermine. In the absence of spermine the site was accessed by a therapeutically irrelevant high memantine concentration. Nevertheless, spermine has a 100 times higher affinity for the polyamine site than memantine, which is indicative of the polyamine site's therapeutic insignificance as a possible binding site for memantine (Parsons et al., 1999).

Some speculation surrounded the possible therapeutic significance of other non-NMDAR neural channels as mediators of memantine's effect. The nicotinic receptor is relevant *in vivo* for the therapeutic effect of the memantine derivative, amantadine (Parsons et al., 1999; Palmer, 2001). Studies on memantine's own affinity for nicotinic receptors concluded that memantine has, compared to amantadine, weak binding affinity which

probably is of no therapeutic relevance. High memantine concentrations (> 100 μM) delay neural action potential firing patterns. This effect is mediated by inhibiting the activation of voltage-activated Na^+ channels. Furthermore, the L and N-type Ca^{2+} channels in hippocampus neurons as well as the P-type channels in cerebellar Purkinje neurons are partially blocked by memantine with an IC_{50} of >180 μM. Because of the high concentrations necessary for this effect, both the Na^+ and the Ca^{2+} channel blockage are of unlikely therapeutic relevance (Parsons et al., 1999).

Two amino-adamantane binding sites have been identified in the NMDAR channel pore (Sobolevsky and Koshelev, 1998; Parsons et al., 1999). The one deep and one shallow binding site are partially negatively charged and are located in the depth of the membrane electric field. The ligand can bind directly from the extracellular side to the second site, or it can bind initially to the first site, after which it "jumps" to the second site, both mechanisms sooner or later leave the first site open for binding, thus, two molecules can bind simultaneously to a single channel (Sobolevsky and Koshelev, 1998). Mutations to the N-site of transmembrane segment M2 of the NR1-subunit lessen the potency of memantine binding 20 times, while double mutations in this pore-forming region lessen the potency by 30-100 times (Parsons et al., 1999).

2.4.6) Differences between the binding properties of high affinity and low affinity NMDAR channel antagonists

Various mechanistic differences exist between the binding characteristics of low affinity NMDAR antagonists (like memantine) and high affinity NMDAR antagonists (like MK-801). These differences gave rise to the formulation of several models to explain the difference in therapeutic efficiency of these compounds. In future, new models might develop as new mechanistic differences between these antagonists are discovered. Current models are based on some of the following differences, as described by Palmer (2001):

1. Binding affinity – low affinity antagonists' effective binding affinity is in the μM range, compared to a nM range for high affinity antagonists.
2. On/off rate kinetics – low affinity antagonists' binding kinetics are considerably more rapid, especially the off rate.
3. Ca^{2+} entry – blockade of NMDAR channel Ca^{2+} entry by low affinity compounds is more rapid, but limited. High affinity blockers completely block Ca^{2+} entry.
4. Antagonist entrapment – low affinity antagonists are trapped partially in the channel between impulses in contrast to high affinity compounds, which are completely and more permanently trapped.
5. Region selectivity – low affinity compounds have higher affinity for receptors in the hindbrain region, while high affinity compounds preferrentially bind to receptors in the forebrain structures.
6. Subtype selectivity – low affinity blockers display slightly more inhibition of channels that contain the NR2C and NR2D-subunits.
7. Dose separation – there is a wider separation between therapeutic concentrations and concentrations causing serious side-effects with low affinity antagonists. For high affinity compounds, no difference exists between these concentrations.

2.4.6.1) Theories explaining the difference in therapeutic effectivity

As mentioned before, the ideal therapeutic compound does not interfere with normal physiological NMDAR channel function, while blocking pathological function. According to the first theory proposed here, uncompetitive NMDAR antagonists fulfill these criteria as soon as their affinity is above the 220 nM K_i range. Apparantly, the affinity correlates with on/off rates and voltage-dependency, with low affinity compounds having fast on/off rates and high voltage-dependency. The affinity of the ideal compound thus has to be low enough for the blocker to unbind during physiological activation, which is associated with strong depolarization and synaptic glutamate concentrations of approximately 1 mM (compared to ±1 μM at rest). These conditions only last for 1-2 ms (although LTP-induction may last longer) before the increased glutamate is rapidly cleared and the membrane potential returns to normal. During this

strong depolarization, the ideal compound should, like the Mg^{2+} ion, leave the channel and bind again upon repolarization. On the contrary, the affinity of the ideal compound has to be high enough to block pathological events such as hypoxia or ischaemia, with a moderate rise in glutamate concentration being less than 100 μM and a moderate but much longer-lasting depolarization of minutes to hours (Kornhuber and Weller, 1997; Parsons et al., 1999).

MK-801, a high affinity uncompetitive antagonist with low voltage-dependency and slow unblocking kinetics thus is not the ideal therapeutic blocker. This compound, once bound, is typically unable to leave the NMDAR channel during both pathological events and physiological function. In contrast, the endogenous channel blocker, the Mg^{2+} ion, has a voltage-sensitivity that is too pronounced, resulting in the block being uplifted during both pathological and physiological activity. The ideal blocker, memantine, disposes over the desirable binding properties which are approximately between that of Mg^{2+} and MK-801 (Kornhuber and Weller, 1997; Parsons et al., 1999). To further demonstrate this theory, the offset kinetics of memantine would still be too slow to leave the channel in time for physiological activation if the membrane is held at the resting potential. During depolarization, though, there is an increase in the weight of the faster recovery time constant and thus in offset rate, which results in the blocker leaving the channel in time (Parsons et al., 1999).

The concentrations of the adamantanes used in the therapeutic setup are such that it is likely that it interacts with other neuronal receptors as well. Amantadine, for example, needs to be administered for Parkinson's disease at 10 to 20 fold higher concentrations than memantine and is, therefore, probably less specific. This possible multi-system influence might be therapeutically beneficial, as mentioned for Ca^{2+} channel blockers as well, since amantadine is therapeutically more effective than memantine (Kornhuber and Weller, 1997).

Another valid theory holds that the amino-adamantanes are partially trapped in the NMDAR channel. Owing to their very specific kinetic properties, these compounds have

a lesser tendency to stay bound, which form the crucial part of their therapeutic profile. After the amino-adamantanes are administered, 15-20% of the NMDAR channels are constantly unblocked and thus available as a Ca^{2+} passage. The channels are thus constantly kept partially active by the amino-adamantanes. In contrast, high affinity antagonists stay properly bound and do not allow any activity (Blanpied et al., 1997).

The last theory included here concerns the difference in the unselective blockers' selectivity. It is based on the observation that the two NMDAR antagonists, ifenprodil and eliprodil, which are NR1/NR2B specific, have better therapeutic profiles in some animal models than memantine (Boxer and Bigge, 1997; Parsons et al., 1999). This observation indicates the possible therapeutic relevance of subtype selectivity. Memantine, while not binding commonly in the forebrain, has a high affinity for the cerebellar region. This tendency might be explained by the higher expression of channels containing the NR2C-subunit in the cerebellum to which memantine binds 3 times more potently than to NR1/NR2A channels. MK-801 on the contrary, prefers channels containing the NR2A and NR2B-subunits. This difference in selectivity might be the key to explaining the difference in the therapeutic profile of these antagonists (Parsons et al., 1999).

The inferior efficiency of MK-801 as a therapeutic agent versus memantine's success was well demonstrated in a study by Frankiewics et al. (2000). They found that LTP is blocked by a high memantine concentration in the CA1 region of hippocampal slices (IC_{50} = 11.6 μM). After induction of hypoxia/hypoglycaemia, the therapeutically relevant concentration had a relatively low EC_{50} value of approximately 1 μM and a therapeutic index value (IC_{50} LTP over EC_{50} hypoxia/hypoglycaemia) of 0.82. In contrast, MK-801 displayed a much higher EC_{50} value (0.53 μM) for therapeutic action in comparison with the concentration needed for the inhibition of LTP (IC_{50} = 0.13 μM). This is rather surprising, since it would be expected from MK-801's low voltage-dependency and slow kinetics that the values would be more or less the same. During behavioural experiments it was found, though, that low MK-801 doses (0.05-0.1 mg/day) block synaptic plasticity, while the concentration needed to protect against ischaemia was 1-10 mg/day. A possible

explanation for this phenomenon is that the proportion of NMDAR channels that are to be blocked in order to protect during ischaemia is much greater than the proportion involved in synaptic plasticity, thus, the latter is more easily blocked by a lower concentration (Frankiewics et al., 2000). To further emphasize high affinity antagonists' possible negative effects, phencyclidine (PCP) (a high affinity NMDAR antagonist, similar to MK-801) administration is employed as the most realistic model available for schizophrenic psychosis is (Kornhuber and Weller, 1997).

2.4.6.2) Therapeutic effects of memantine

Therapeutic doses in male rats are 5 mg/kg if administered acutely and 20 mg/kg/day by subchronic infusion. These doses result in therapeutically effective doses in the brain. Typical side-effects will probably appear if the dose is not kept below or equal to 20 mg/kg. It is generally accepted that the primary if not single site of therapeutically relevant antagonistic action is the NMDAR channel (Parsons et al., 1999).

Since memantine increases the duration of LTP *in vivo*, it has been hypothesized that animals with inherently poor performance at learning tasks might benefit from memantine administration. This hypothesis was proved when learning-impaired rats showed improved performance in the Morris maze after memantine treatment. A possible explanation for this positive effect is that, under certain conditions, direct tonic activation of the NMDAR channels cause, instead of LTP, an increase in so-called synaptic noise, which leads to the impairment of memory capability. The success of memantine with these learning-impaired animals led to experiments assessing its effect on memory of brain lesioned animals. After a clear initial impairment of 9 days, the memantine treated animals improved until there was no apparent difference in learning task performance between these animals and non-lesioned animals. MK-801 administration, on the other hand, enhanced the detrimentary effects of the lesions. These results led to the conclusion that, besides memantine having a protective effect, it also improves memory performance at the same doses (Parsons et al., 1999). The direct involvement of NMDAR channels in learning, memory and synaptic plasticity, as well as the brain lesions observed in post-

mortem brains can intuitively be linked to Alzheimer's disease. NMDAR antagonism by memantine might facilitate the learning process and might, therefore, lead to improvement of Alzheimer's disease patients (Parsons et al., 1999).

Memantine has proved effective in several animal models with exciting implications for Alzheimer's disease treatment. A certain structure in the brain, the cholinergic nucleas of Meynert (NBM), is known to degenerate to a great extent in patients with Alzheimer's disease. After direct NMDA injection, a steep decline in the acetylcholine synthesizing enzyme, choline acetyltransferase, was detected in the cholinergic neurons that compose the NBM. The same deficiency is common in the brains of post-mortem Alzheimer's disease victims. Memantine protected against this tendency at an ED_{50} of 2.8 mg/kg without any side-effects. Memantine was protective during quinolinic acid administration and malonate-induced striatal lesions, both implicating effectiveness in neurodegenerative diseases, especially with the latter model, where deficits in mitochondrial function is involved. To simulate realistic pathological conditions more closely, quinolinic acid was administered directly into the brain by an Alzet osmotic minipump. A second pump was used to inject either saline (control) or memantine. After two weeks the memantine administered animals, in contrast to the saline animals, were able to acquire the involved learning tasks normally (Parsons et al., 1999).

Several structured clinical trials were carried out on the effects of memantine on patients with Alzheimer's disease-related dementias. Widespread relief of symptoms and positive improvements were found throughout and results like improvement in cognitive function (attention and memory), motor function, social behaviour, emotionality, motivation and drive as well as a decline in symptoms such as fatigue and insomnia were common (Palmer, 2001).

Memantine, like amantadine, has been used as treatment against Parkinson's disease - induced spasticity for more than twenty years in Europe (Le and Lipton, 2001; Palmer, 2001). Budipine, another recognized anti-Parkinsonian agent, has demonstrated, in

support of the use of amino-adamantanes, that it also has low-affinity NMDAR antagonistic properties (Kornhuber and Weller, 1997).

Memantine has been effective in several animal models for Parkinson's disease (Palmer, 2001) and in some even more effective than its counterpart, amantadine, although studies comparing protective action against neuroleptic induced catalepsy (a prominent symptom of Parkinson's disease) showed less effectivity for memantine (Parsons et al., 1999). Clinical studies demonstrated memantine's effectiveness repeatedly, as patients receiving approximately 20 mg/day, experienced improvement of symptoms such as rigidity, bradykinesia, tremor, gait and postural reflexes (Palmer, 2001). Although memantine and amantadine have never been compared directly in clinical studies, it is generally accepted that amantadine is still the better choice. Combined therapy with one of these amino-adamantanes and L-DOPA seem to be the approach for the future since it has synergistic therapeutic effects (Parsons et al., 1999).

Considering its therapeutic mechanism, it seems as if adamantane administration results in the inhibition of a hyperactive glutamatergic neurotransmitter system in order to rebalance the interaction between the glutamatergic and the dopaminergic neurotransmitter systems in the basal ganglia (Kornhuber and Weller, 1997; Palmer et al., 1999).

Several *in vivo* animal studies demonstrated memantine's protective effect against cerebral ischaemia, more so in focal ischaemia than in global ischaemia (Parsons et al., 1999; Le and Lipton, 2001). The necessary doses used in many of these studies were above the level at which memantine has serious behavioural side effects. With most of these models, though, the ischaemic insult was quite severe and it has been demonstrated that at lower doses, memantine reduces neuronal damage in ischaemic animal models. Combined treatment with the VACC blocker, flunarizine, delivered a greatly enhanced outcome. Surprisingly, memantine has no effect against traumatic spinal cord injury. MK-801 displacement studies on spinal cord tissue have shown that memantine has a 2

times less affinity for NMDARs in the spinal cord which might explain its ineffectiveness (Parsons et al., 1999).

Evaluating memantine's possible therapeutic relevance as a NMDAR blocker in the treatment of AIDS-related dementia, it was found that exposure of neuronal cultures to gp120, an HIV envelope protein, leads to the activation of PLA_2, which leads to the release of arachidonic acid. Arachidonic acid inhibits glutamate uptake by the astrocytes and/or up-regulates NMDAR channels, possibly resulting in Ca^{2+} overload (Parsons et al., 1999). Memantine protects against the neuronal damage induced by HIV-1 proteins (Le and Lipton, 2001) and reduces damage in the CA1 region of the hippocampus caused by the HIV-induced β-amyloid (Miguel-Hidalgo et al., 2002).

Memantine also displayed mixed effectiveness in animal models for epilepsy, with a clear synergistic effect with NBQX (Parsons et al., 1999). Memantine is at several different stages of development with regards to possible therapeutic action against a wide range of other neural and especially dementia-related pathologies such as chronic pain, Huntington's disease, glaucoma, hepatic encelopathy, multiple sclerosis, tinnitus, tardive dyskinesia and spasticity (Parsons et al., 1999; Le and Lipton, 2001; Palmer, 2001).

2.4.6.3) Therapeutic effects of MK-801

Due to its binding characteristics (see sections 2.4.6 & 2.4.6.1), MK-801 is clearly of much less therapeutic use than memantine. Yet many studies investigated MK-801 as a possibility for treatment of several Ca^{2+} overload-associated diseases. Prior administration of MK-801 to the induction of ischaemia in brain slices resulted in effective neuroprotection of the CA1 region, but not the CA3 region and the dentate gyrus of the hippocampus (Kubo et al., 2001). In animal models, though, there exists considerable doubt as to MK-801's protective efficiency against ischaemia because of many conflicting results (Palmer, 2001) and theoretical considerations.

MK-801 was clinically evaluated for protection against refractory epilepsy, with some minor improvements that were overshadowed by detrimental side-effects. Although MK-801 never reached the clinical evaluation phase with Parkinson's disease, it showed initial protection in the MPTP parkinsonian animal model for monkeys. However, these effects were negated by increased toxicity after seven days (Palmer, 2001).

2.4.6.4) Pentacyclo undecylamines and its derivatives as possible protective agents

The synthesis and chemistry of novel hydrocarbon cage structures became a regular subject of research since the introduction of the amino-adamantane, amantadine, as an antiviral agent in the 1960's and even more so when it was unexpectedly discovered that the adamantanes have protective qualities against neurodegenerative diseases such as Parkinson's and Alzheimer's disease (Oliver et al., 1991, Parsons et al., 1999)

Such a compound, 8-benzylamino-8,11-oxapentacyclo[5.4.0.0^{2,6}.0^{3,10}.0^{5,9}]-undecane (NGP1-01), was according to Van der Schyf et al. (1986), first synthesized by Sasaki et al. in the early seventies. Van der Schyf et al. (1986) observed Ca^{2+} channel antagonistic properties for NGP1-01, which was a first for molecules consisting of a cage structure. Upon further investigation, it was found that NGP1-01's blocking characteristics are non-stereoselective. In myocytes, it resembles the binding profile of the 1,4-dihydropyridines, and is thus L-type VACC selective. In contrast to the dihydropyridines, though, NGP1-01 shows weaker antagonism with more selectivity at lower membrane potentials (-30 to -35 mV). Yet it was proposed that NGP1-01 mediate its effect by the same or at least a similar binding site than that of the 1,4-dihydropyridines (Malan et al., 1998). Activation or opening of the Ca^{2+} channel is required for NGP1-01 block as indicated by the fact that binding accelerates the channel's activation rate. Ca^{2+} channel block by NGP1-01 is strongly frequency-dependent, resembling that of the dihydropyridines, verapamil and D-600. The dihydropyridines, though, display a strong voltage-dependence in addition to the frequency-dependence, with enhanced blockade at depolarized potentials. NGP1-01's frequency-dependent block is more similar to that of diltiazem, which should make it

more effective in tissues with frequently repetitive activation patterns (Van der Walt et al., 1988).

It was the structural similarity to known NMDAR-ligands like memantine which prompted the interest in NGP1-01's potential as a neuroprotective compound. As a first approach to elucidate the structure of NGP1-01, it was fitted onto the PCP binding site by computer chemical modelling software. Similar interaction of NGP1-01 with the PCP binding site than the template compounds PCP, MK-801 and memantine was assumed after a favourable root mean square (RMS) fit was obtained using the modelling software. This was done by obtaining the minimum energy conformation assumed to be the most likely conformation of the templates (Malan et al, 2000; Geldenhuys et al., 2003). Using the Hyperchem modelling software, a favourable RMS-fit was then obtained for NGP1-01 onto this structure, confirming the structural similarity with PCP, MK-801 and memantine (Geldenhuys et al., 2003).

An initial dose-range study on the effects of NGP1-01 on animals revealed signs of weak CNS stimulation, increased locomotor activity and signs of stereotype behaviour, regularly a sign of dopamine receptor stimulation, including head flicking and uncontrolled licking. The onset of these effects was approximately 30 minutes post-administration and it lasted as long as 5 hours post-dose. Deaths occurred only 24 hours after administration. These behavioural changes show a striking similarity to that of amantadine (Oliver et al., 1991) and thus confirm the conclusions made about the structural similarities using the computer modelling.

This *in vivo* effectual and model-based structural similarity between NGP1-01 and memantine and amantadine, as well as the observed L-type Ca^{2+} channel antagonistic properties of NGP1-01 prompted the suggestion that NGP1-01 might have neuroprotective properties against pathological states related to Ca^{2+} overload. These properties of NGP1-01 persuaded Geldenhuys et al. (2003) to hypothesize that this putative neuroprotective action might be accomplished by a so-called dual mechanism, mediated by simultaneous antagonism of the NMDAR channel (contributed by NGP1-

01's adamantane similarity) and the L-type VACC (as observed with previous studies) (Geldenhuys et al., 2003).

The stereochemistry of compounds may play a determining role in the compounds receptor binding activity. For example, Kwon and Triggle (as quoted by Malan et al., (1998)) mentioned the opposite action of the (S) and (R)-enantiomers of a 1,4-dihydropyridines, Bay K 8644 and H160/51, that decreases and enhances current through the L-type Ca^{2+} channel respectively. Similar investigations on NGP1-01's (+) and (-)-enantiomer actions, revealed no difference in its activity profiles for Ca^{2+} channels, though (Malan et al., 1998). However, minor structural alterations to NGP1-01 that affect its physicochemical and electronic properties can bring about major changes in its activity profile (Malan et al., 2000). It was postulated by Van der Schyf et al. (1986) that the pentacycloundecane skeleton may serve as the bulk contributor to NGP1-01's activity. In order to investigate the effect of structural alterations on the activity profile and structure-activity relationships of NGP1-01, Malan et al. (2000) modified this compound by altering the aromatic amine side chain by introducing a series of nitrobenzylamines, methoxybenzylamines, methylpyridines and phenylhydrazines.

2.4.6.4.1) Anti-parkinsonian activity of NGP1-01 and its derivatives

With the observations of NGP1-01's antagonistic effect on reserpine-induced catatonia, its reduction of oxotremorine-induced tremor and salivation in rats (Oliver et al., 1991), as well as the Geldenhuys et al. (2003) dual mechanism hypothesis as rationale, NGP1-01 and its derivatives were assessed for protective activity in the rat MPTP parkinsonian model.

Administration of MPTP results in generation of the neurotoxic oxidated product MPP^+. This compound is transported by the dopamine transporter, and accumulates inside the nigrostriatal dopaminergic neurons. Here it has an adverse effect on electron transport in the mitochondrial complex I, which results in decreased ATP synthesis and eventually cell death. The measurable parameters in this model are a decrease in striatal dopamine

content and a decrease in the number of nigrostriatal dopaminergic neurons. These effects closely mimic the cellular image of idiopathic Parkinson's disease (Geldenhuys et al., 2003).

Amongst NGP1-01 and its derivatives tested by Geldenhuys et al. (2003), only the phenylethyl derivative proved to attenuate the proposed dopamine depletion mediated by MPTP. The amino derivative showed a drastic decrease in striatal dopamine content compared to MPTP treated animals only. The aminobenzylamino, nitrobenzylamino and hydroxybenzylamino derivatives displayed a somewhat better profile than the amino derivative. Surprisingly, the two known NMDAR antagonists failed to display any protective activity as well. From the measured parameters, memantine and MK-801 displayed tendencies in the same direction as many of the evaluated pentacyclo-undecylamines. It is thus possible, as mentioned in other investigations, that the MPTP parkinsonian model is not ideal for the mechanistic screening involved in this particular study. The possibility of neuroprotection by NGP1-01 and its derivatives could thus not be dismissed by this investigation and it was recommended that it be further elucidated by means of other models and methods (Geldenhuys et al., 2003).

To further investigate the possible mechanism involved in the putative neuroprotective activity of the pentacyclo-undecylamines, Geldenhuys and his colleages recently assessed these compounds for their effect on dopamine release and uptake inhibition as well as for inhibition of monoamine oxidase (MAO) B. They observed that these compounds inhibit dopamine uptake rather than stimulating release and have no relevant effect on the MAO-B system. The IC_{50} values of inhibition were comparable to that of amantadine, with the most effective compound, the phenylethylamine derivative, having an IC_{50} of 23 μM. When the polycyclic cage amines were substituted by aromatic substituents, no selectivity between uptake inhibition and release stimulation was found. Selectivity for uptake inhibition was enhanced by increasing the size of the cage moiety. The distance between the aromatic moiety and the cage structure also appears to be of interest, since this distance is the greatest in the phenylethylamine derivative. Structure-activity relationships for the pentacyclo-undecylamines thus seem to be more influenced by

geometric and steric elements than by the compounds' electronic properties (Geldenhuys et al., 2004).

3) APPROACHES TO THE ASSESSMENT OF CELL VIABILITY

Viability of acutely isolated cells or cell cultures can be assessed by manual counting by means of a microscope or automated procedures, both of which eventually estimate the number of dead cells versus the number of cells that are alive. Microscope counting procedures is labour intensive and less objective than the automatic procedures, since the experimenters' personal judgement is critical. However, a possible advantage of manual counting procedures over automatic procedures is that it can use morphological changes as an important criterium. Alternatively or in addition to this criterium, as is the case with automatic procedures, manual counting procedures use colorimetric changes in the cell to assess cell viability. These changes are brought about by a specific indicator which, when added to the cellular medium, alters the cell preparate's colour due to reactions with the composing cells' biochemical constituency or changes in the integrity of the plasma membranes. When deciding on a suitable technique for a study, it is important to consider the compatibility of the presumed mechanism inducing cell death and the effect that the particular assay measures (Mickuviene et al., 2004), as well as possible practical constraints that are characteristic of these assays. Some of the frequently employed techniques for viability assessment will henceforth be discussed.

3.1) Lactate dehydrogenase (LDH)-release assay

The LDH-release assay is one of the most frequently used assays for viability (Abe and Matsuki, 2000). It is based on the fact that LDH is released from the mitochondria upon cellular injury or death (Abe and Matsuki, 2000; Lobner, 2000; Uliasz and Hewett, 2000), causing the mitochondrial membrane to disintegrate. The resultant conversion of lactate to pyruvate, mediated by LDH catalyses, is coupled to the oxidative conversion of NAD to NADH. The actual assay kit is a tetrazolium dye or salt, which is reduced by

NADH into a deep blue farmazan dye (Abe and Matsuki, 2000), which can be read spectrophotometrically at 490 nm (Promega Corporation, 1999). It has been proved that the release of LDH is directly proportional to the number of dead or injured neurons. Unfortunately, the values given by this assay may be artificially increased by factors other than LDH that oxidise NAD, for example the peroxynitrate decomposition catalyst, Fe(III)TTPS (Uliasz and Hewett, 2000). It is recommended that at least 5 000 cells are used per well (Promega Corporation, 1999), which is a problem for acutely isolated cell preparations where the cell number is less.

3.2) MTT assay

The most used viability assay, together with the LDH-release assay, is the 3-(4,5-dimethylthiazol-2-yl)-2,5-diphenyltetrazolium bromide (MTT) assay. MTT is supposedly reduced by succinate dehydrogenase in the mitochondria of functional cells (Abe and Matsuki, 2000). The product of the redox reaction is a dark blue farmazan dye. Procedurally, the cell medium is initially incubated with the MTT dye for a few hours, after which cell lysis is induced and the farmazan coloured product assesed spectrophotometrically at 570 nm (Promega Corporation, 1999). The disadvantages of the MTT assay are comparable to that of the LDH assay.

3.3) Fluorescent screening

Fluorescent detection of biological phenomena is based on the changes in fluorescent iluminescence when a probe binds with a certain target material. The resulting fluorescence can be detected by various detection systems like fluorescent microscopes, fluorescence plate scanners and flow cytometers. The viability/excitotoxicity fluorescence assay kit contains two probes. Calcein AM is a measure of intracellular esterase activity. It enters and is retained within the cytoplasmic membrane of viable cells, where, upon interaction with intracellular esterase enzymes, it produces a bright green fluorescence, which can be observed at the excitation/emission spectra of 495/515 nm. Ethidium homodimer (EthD-1) assesses dead/damaged cells based on cytoplasmic

membrane integrity. It does not pass intact membranes, but when it binds to nucleic acids after passing through damaged cytoplasmic membranes, its fluorescent wavelength increases by 40 times, which results in a bright red fluorescence observed at a 495/635 nm excitation/emission spectra. Fluorescent methods' validity has been proved in many laboratories and is very sensitive. A further advantage is its versatility in terms of assessment apparatus and the fact that both dead and live cells can be independently assessed (Molecular Probes, Inc., 2001).

3.4) Trypan blue exclusion assay

The trypan blue exclusion assay is a commonly used method which stains non-viable cells, giving them a dark blue appearance (Uliasz and Hewett, 2000). Its mechanism is also based on membrane integrity, and it has been shown to be effective in several studies where cell death was induced by glutamate excitotoxicity (Dubinsky et el., 1995; Nishikawa et al., 2000; Taguchi et al., 2003), as well as in DRG cell death (Reichling et al., 1997). This assay's advantage over the LDH and MTT assays is the fact that it is not sensitive to reductive agents in the cellular environment. Another advantage that the trypan blue assay shares with the LDH and fluorescent assays is that dead cell assays are more accurate when assessing mixed cultures (containing both astrocytes and neurons), as the astrocytes are not affected by glutamate excitotoxicity and thus do not form a part of the measure. A possible disadvantage of trypan blue is that it is generally used for microscope counting and, therefore, labour-intensive and prone to experimenter bias (Uliasz and Hewett, 2000).

4) DORSAL ROOT GANGLIA

4.1) Structure and function of dorsal root ganglia

The term ganglia is used for structures where cell bodies of neurons are assembled. It is usually found outside the CNS (Reber and Reber, 2001). The dorsal root ganglia are found on both sides of the spinal segment (Fig. 5). These ganglia contain cell bodies of sensory neurons, of which the axons provide sensory information to the spinal cord via the dorsal root.

Afferent sensory neurons and efferent motor neurons come together between the CNS and the peripheral nervous system to form a thicker neural track. This thicker track is called the spinal nerve. Each spinal nerve divides into two separate tracks close to the spinal cord. The ventral branch or ventral root contains the efferent motor neurons and joins the spinal cord from the ventral side. The dorsal branch leads to the dorsal root ganglion, of which the axons, as described previously, join the spinal cord via the dorsal root (Martini, 1998). The ganglia are surrounded by connective tissue capsules, which are continuous with the capsule surrounding the dorsal roots called the epi and perineurium (Slomianka, 2003).

The individual neuronal cell bodies contained within the ganglia are surrounded by flat satellite cells. Each cell body has a single T-shaped process. The arms of this process represent a single axon which act as the connection between the periphery and the spinal cord while the stem of the T-shaped process is connected to the cytoplasm. It is thus evident that DRGs play an important role in the transfer of sensory information toward higher brain centres (Slomianka, 2003). A primary focus of research involving DRGs is its role in pain conduction. It has been shown that glutamate and calcium play a central role in the conduction of pain through these ganglia towards higher centres (Millan, 1999; Chaplan, 2000). The stem of the T-shaped process serves as the channel for the transfer of the cell body's trophic function (Slomianka, 2003) and its function as a modulatory centre for sensory information, since the cell bodies within the ganglia have the capability to communicate with each other (Harding et al., 1999).

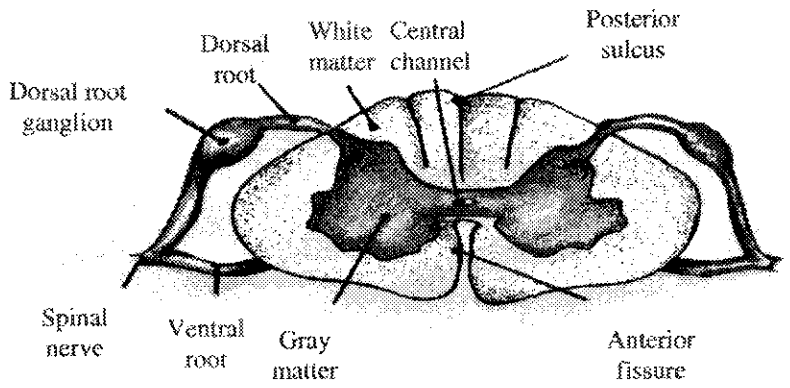

Figure 5. Cross section through the spinal cord to demonstrate the anatomy of the dorsal root ganglia and adjacent structures (Edited from Martini, 1998)

4.2) The expression of different types of VACCs in DRGs

HVA and LVA VACCs are expressed in DRGs. In a study by Yusaf et al. (2001) the presence of Ca^{2+} channel subunits in DRGs of the rat was investigated using *in situ* hybridization techniques. This study has shown the presence of the encoding mRNA of α_{1A}, α_{1B}, α_{1C}, α_{1D}, α_{1E}, α_{1I} and α_{1S}-subunits in DRG neurons of various sizes. According to them, the α_{1F}-subunit mRNA is present at very low levels, while the α_{1G}-subunit is only minimally expressed. The same study also found that $\alpha_2\delta_1$, $\alpha_2\delta_2$ and $\alpha_2\delta_3$-subunits are commonly expressed in DRG's. $\alpha_2\delta_1$ and $\alpha_2\delta_2$-subunits are more commonly found in smaller, C-type sensory neurons, while $\alpha_2\delta_3$-subunits are more common in greater diameter Aβ-type neurons (Yusaf et al., 2001). C-type neurons are unmyelinated and have a slow conductance rate. A large part of the peripheral neurons are of this particular type. Most spinal neurons, though, can be classified under the myelinated and fast conductance A-type neurons, of which the Aβ-type is a subtype (Guyton and Hall, 2000).

The expression of the α_{1C}, α_{1D} and α_{1F}-subunits (α_{1F} with a low expression in DRG's) gives rise to a L-type current, while α_{1G} (not observed in DRG's), α_{1H} and α_{1I}-subunits show properties of the T-type current. α_{1A} gives rise to the P/Q-current, α_{1B} to the N-type and α_{1E} to the R-type current (Reuter, 1996; Yusaf et al., 2001). The α_{1S}-subunit was defined in the past as only expressed as part of the L-type channel in skeletal muscle (Lehmann-Horn and Jurkat-Rott, 1999). However, this subunit's mRNA has been found at a relatively high distribution in rat DRG, where it probably forms part of the L-type Ca^{2+} channel (Yusaf et al., 2001).

4.3) The expression of NMDAR channels in DRGs

Several studies and a wide range of analytical techniques were used to confirm the expression of all the NMDAR channel subunits on DRG membranes. The NR1-subunit was observed on all DRG neurons, with a high co-expression of NR2B-subunits (Carlton, 2001; Marvizon et al., 2002; Li et al., 2004) in up to 90% of the observed channels (Marvizon et al., 2002). This expressional pattern is especially applicable to the cell body membrane, where a functionally homogenous NMDAR population was observed (Li et al., 2004). The NR2C-subunit was also detected (Marvizon et al., 2002), but at much lower levels than either the most prevalent NR2B or the selectively expressed NR2D-subunits (Marvizon et al., 2002; Li et al., 2004). Although the NR2A-subunit was not detected with several methods, immunofluorescent techniques positively identified this scarcely expressed subunit (Marvizon et al., 2002). Although NMDAR channels are thus widely expressed in all DRG neurons, the other iGluR subtypes are only expressed in small diameter DRG neurons (Carlton, 2001).

NMDAR channels displayed very similar electrophysiological properties in DRGs compared to central neurons. DRG NMDAR channels displayed inward Ca^{2+} permeation upon activation by glutamate and glycin. Activation of the channel was strongly voltage-dependent due to a Mg^{2+} blockade (Lovinger and Weight, 1988; Li et al., 2004). With Lovinger and Weight's (1988) voltage-clamp investigations, 40% cells displayed inward

Ca^{2+} current upon 100 μM glutamate application. From this sample, 70% required simultaneous depolarization to activate, while the rest displayed an increase in glutamate-induced current amplitude when depolarized. Upon ketamine administration, the channels showed use-dependent block and the NR2B-subunit selective antagonist, ifenprodil, had an almost complete inhibitory effect on the NMDAR current (Li et al., 2004). According to MK-801 displacement studies, memantine's affinity for NMDARs in the spinal cord is two times less than in the brain (Parsons et al. 1999).

5) REFERENCES

Aarts MM and Tymianski M. Novel treatment of excitotoxicity: targeted disruption of intracellular signalling from glutamate receptors. Biochem. Pharmacol., 2003; 66(6): 877-86.

Abe K and Matsuki N. Measurement of cellular 3-(4,5-dimethylthiazol-2-yl)-2,5-diphenyltetrazolium bromide (MTT) reduction activity and lactate dehydrogenase release using MTT. Neurosci. Res., 2000; 38: 325-329.

Alberdi E, Sanchez-Gomez MV, Marino A, Matute C. Ca^{2+} influx through AMPA or kainite receptors alone is sufficient to initiate excitotoxicity in cultured oligodendrocytes. Neurobiol. Dis., 2002; 9: 234-243.

Anderson PAV and Greenberg RM. Phylogeny of ion channels: clues to structure and function. Comp. Biochem. Physiol., 2001; 129: 17-28.

Arundine M and Tymianski M. Molecular mechanisms of calcium-dependent neurodegeneration in excitotoxicity. Cell Calcium, 2003; 34: 325-337.

Ashcroft FM. Ion channels and disease. Academic Press: London, 2000: 106, 108, 163-164, 169-170, 178-182, 301-302.

Augustine GJ. How does calcium trigger neurotransmitter release? Curr. Opin. Neurobiol., 2001; 11: 320-326.

Baldassa S, Zippel R, Sturani E. Depolarization-induced signaling to Ras, Rap1 and MAPKs in cortical neurons. Mol. Brain Res., 2003; 119: 111-122.

Bean BP. Multiple types of calcium channels in heart muscle and neurons: Modulation by drugs and neurotransmitters. Ann. N. Y. Acad. Sci., 1989; 560: 334-345.

Blaabjerg M, Fang L, Zimmer J, Baskys A. Neuroprotection against NMDA excitotoxicity by group I metabotropic glutamate receptors is associated with reduction of NMDA stimulated currents. Exp. Neurol., 2003; 183: 573-580.

Blanpied TA, Boeckman FA, Aizenman E, Johnson JW. Trapping Channel Block of NMDA-Activated Responses By Amantadine and Memantine. J. Neurophysiol., 1997; 77: 309-323.

Bliss TVP. Young receptors make smart mice. Nature, 1999; 401: 24-27.

Bliss TVP and Collingridge GL. A synaptic model of memory: long-term potentiation in the hippocampus. Nature, 1993; 361: 31-39.

Boxer PA and Bigge CF. Mechanisms of neuronal cell injury/death and targets for drug intervention. DDT., 1997; 2(6): 219-228.

Brooks KJ and Kauppinen RA. Calcium-mediated damage following hypoxia in cerebral cortex ex vivo studied by NMR spectroscopy. Evidency for direct involvement of voltage-gated Ca^{2+}-channels. Neurochem. Int., 1993; 23(5): 441-450.

Brust PF, Simerson S, McCue AF, Deal CR, Schoonmaker S, Williams ME, Velicelebi G, Johnson EC, Harpold MM, Ellis SB. Human Neuronal Voltage-Dependent Calcium Channels: Studies on Subunit Structure and Role in Channel Assembly. Neuropharmacology, 1993; 32(11): 1089-1102.

Brustovetsky T, Purl K, Young A, Shimizu K, Dubinsky JM. Dearth of glutamate transporters contributes to striatal excitotoxicity. Exp. Neurol., 2004; Xx: xx.

Budd SL. Mechanisms of neuronal damage in brain hypoxia/ischemia: focus on the role of mitochondrial calcium accumulation. Pharmacol. Ther., 1998; 80(2): 203-229.

Carlton SM. Peripheral excitatory amino acids. Curr. Opin. Pharmacol., 2001; 1: 52-56.

Catterall WA. Functional Subunit Structure of Voltage-Gated Calcium Channels. Science, 1991; 253: 1499-1500.

Catterall WA, Striessnig J, Snutch TP, Perez-Reyes E. IUPHUR Ion Channel Compendium, 2000; [Web:] http://www.iuphar-db.org/iuphar-ic/sodium.html [Date of access: 2 Sept. 2004].

Chaplan SR. Neuropathic pain: role of voltage-dependent calcium channels. Region. Anaesth. Pain Med., 2000; 25(3): 283-285.

Chung C-H and Kuyucak S. Recent advances in ion channel research. Biochim. Biophys. Acta, 2002;

Coggeshall RE and Carlton SM. Receptor localization in the mammalian dorsal horn and primary afferent neurons. Brain Res. Brain Res. Rev., 1997; 24: 28-66.

Corry B, Allen TW, Kuyucak S, Chung S-H. A model of calcium channels. Biochim. Biophys. Acta, 2000; 1509: 1-6.

Cui K, Luo X, Keyi X, Ven Murthy MR. Role of oxidative stress in neurodegeneration: recent developments in asay methods for oxidative stress and nutraceutical antioxidants. Prog. Neuro-Psychopharmacol. Biol. Psychiatry, 2004; Xx: xx

Cull-Candy S, Brickley S, Farrant M. NMDA receptor subunits: diversity, development and disease. Curr. Opin. Neurobiol., 2001; 11: 327-335.

Dubinsky JM, Kristal BS, Elizondo-Fournier M. On the probabalistic nature of excitotoxic neuronal death in hippocampal neurons. Neuropharmacology, 1995; 34(7): 701-711.

Ekinci FJ, Ortiz D, Shea TB. Okadaic acid mediates tau phosphorylation via sustained activation of the L-voltage-sensitive calcium channel. Brain Res. Mol. Brain Res., 2003; 117: 145-151.

Ferger D and Krieglstein J. Determination of intracellular Ca^{2+} concentration can be a useful tool to predict neuronal damage and neuroprotective properties of drugs. Brain Res., 1996; 732: 87-94.

Frankiewics T, Pilc A, Parsons CG. Differential effects of NMDA-receptor antagonists on long-term potentiation and hypoxic/hypoglycaemic excitotoxicity in hippocampal slices. Neuropharmacology, 2000; 39: 631-642.

Friberg H and Wieloch T. Mitochondrial permeability transition in acute neurodegeneration. Biochimie, 2002; 84: 241-250.

Gasic GP and Nicotera P. To die or to sleep, perhaps to dream. Toxicol. Lett., 2003; 139: 221-227.

Gasparini F, Kuhn R, Pin J-P. Allosteric modulators of group I metabotropic glutamate receptors: novel subtype-selective ligands and therapeutic perspectives. Curr. Opin. Pharmacol., 2002; 2: 43-49.

Geldenhuys WJ, Malan SF, Murugesan T, Van Der Schyf CJ, Bloomquist JR. Synthesis and biological evaluation of pentacyclo[5.4.0.0^{2,6}.0^{3,10}.0^{5,9}]undecane derivatives as potential therapeutic agents in Parkinson's disease. Bioorg. Med. Chem., 2004; 12: 1-8.

Geldenhuys WJ, Terre'Blanche G, Van Der Schyf CJ, Malan SF. Screening of novel pentacyclo-undecylamines for neuroprotective activity. Eur. J. Pharmacol., 2003; 458: 73-79.

Guyton AC and Hall HE. Textbook of medical physiology, tenth ed. W.D. Saunders Company: Philadelphia, Pa., 2000: 532-533p.

Harding LM, Beadle DJ, Bermudez I. Voltage-dependent calcium channel subtypes controlling somatic substance P release in the peripheral nervous system. Prog. Neuro-Psychopharmacol. Biol. Psychiatry, 1999; 23: 1103-1112.

Hardingham GE and Bading H. The Yin and Yang of NMDA receptor signalling. Trends Neurosci., 2003; 26(2): 81-89.

Hille B. 2001. Voltage-gated calcium channels.

Hille B. 1992. Ionic channels of excitable membranes. 2nd ed. Sunderland, Mass. : Sinauer Associates. 607 p.

Hodgkin AL and Huxley AF. A quantitative description of membrane current and its application to conduction and excitation in nerve. J. Physiol., 1952; 117: 500-544.

Hölscher. 2001. Neuronal mechanisms of memory formation. Cambridge University Press: Cambridge, 2001: 1-4.

Hosey MM, Chien AJ, Puri TS. Structure and regulation of L-type calcium channels; A current assessment of the properties and roles of channels subunits. Trends Cardiovasc. Med., 1996; 6(8): 265-273.

Hynd MR, Scott HL, Dodd PR. Glutamate-mediated excitotoxicity and neurodegeneration in Alzheimer's disease. Neurochem. Int., 2004; 45: 583-595.

Ioudina M, Uemura E, Greenlee HW. Glucose insufficiency alters neuronal viability and invreases susceptibility to glutamate toxicity. Brain Res., 2004; xxx: xxx

Jing G, Grammatopoulos T, Ferguson P, Schelman W, Weyhenmeyer J. Inhibitory effects of angiotensin on NMDA-induced cytotoxicity in primary neuronal cultures. Brain Res. Bull., 2004; 62: 397-403.

Jonas P. Glutamate Receptors in the Central Nervous System. Ann. N. Y. Acad. Sci., 1993; 707: 126-135.

Kanaya S, Arlock P, Katzung BG, Hondeghem LM. Diltiazem and Verapamin preferentially block inactivated cardiac calcium channels. J. Mol. Cell. Cardiol., 1983; 15: 145-148.

Ke Z-J and Gibson GE. Selective response of various brain cell types during neurodegeneration induced by mild impairment of oxidative metabolism. Neurochem. Int., 2004; 45: 361-369.

Kiedrowski L. The difference between mechanisms of kainate and glutamate excitotoxicity *in vitro*: Osmotic lesion versus mitochondrial depolarization. Restor. Neurol. Neurosci., 1998; 12: 71-79.

Kobayashi T, Strobeck M, Schwartz A, Mori Y. Inhibitory effects of a new neuroprotective diltiazem analogue, T-477, on cloned brain Ca^{2+} channels expressed in Xenopus oocytes. Eur. J. Pharmacol., 1997; 332: 313-320.

Kobayashi T, Mori Y. Ca^{2+} channel antagonists and neuroprotection from cerebral ischemia. Eur. J. Pharmacol., 1998 363: 1-15.

Kochegarov AA. Pharmacological modulators of voltage-gated calcium channels and their therapeutic application. Cell Calcium, 2003; 33: 145-162.

Kornhuber J and Weller M. Psychotogenicity and N-methyl-D-aspartate Receptor Antagonism: Implications for Neuroprotective Pharmacotherapy. Biol. Psychiatry, 1997; 41: 135-144.

Krieger C and Duchen MR. Mitochondria, Ca^{2+} and neurodegenerative disease. Eur. J. Pharmacol., 2002; 447: 177-188.

Kubo T, Yokoi T, Hagiwara Y, Fukumori R, Goshima Y, Misu Y. Characteristics of protective effects of NMDA antagonist and calcium channel antagonist on ischemic calcium accumulation in rat hippocampal CA1 region. Brain Res. Bull., 2001; 54(4): 413-419.

Kume T, Nishikawa H, Taguchi R, Hashino A, Katsuki H, Kaneko S, Minami M, Satoh M, Akaike A. Antagonism of NMDA receptors by σ-receptor ligands attenuates chemical ischemia-induced neuronal death *in vitro*. Eur. J. Pharmacol., 2002; 455: 91-100.

Kuo TH and Zhu L. Ca^{2+} homeostasis and apoptosis. Electr. J. Pathol. Histol., 2000; 6(1): 06.

Le DA and Lipton SA. Potential and current use of N-methyl-D-aspartate (NMDA) receptor antagonists in diseases of aging. Drugs Aging, 2001; 18(10): 717-724.

Lehmann-Horn F and Jurkat-Rott K. Voltage-gated ion channels and hereditary disease. Physiol. Rev., 1999; 79(4): 1317-1361.

Li J, Kato K, Ikeda J, Morita I, Murota S-I. A narrow window for rescuing cells by the inhibition of calcium influx and the importance of influx route in rat cortical neuronal cell death induced by glutamate. Neurosci. Lett., 2001; 304: 29-32.

Li J, McRoberts JA, Nie J, Ennes HS, Mayer EA. Electrophysiological characterization of N-methyl-D-aspartate receptors in rat dorsal root ganglia neurons. Pain, 2004; 109(3): 443-452.

Lobner D. Comparison of the LDH and MTT assays for quantifying cell death: validity for neuronal apoptosis? J. Neurosci. Methods, 2000; 96: 147-152.

Lovinger DM and Weight FF. Glutamate induces a depolarization of adult rat dorsal root ganglion neurons that is mediated predominantly by NMDA receptors. Neurosci. Lett., 1988; 94: 314-320.

Malan SF, Dockendorf G, Van Der Walt JJ, Van Rooyen JM, Van Der Schyf CJ. Enantiomeric resolurion of the calcium channel antagonist 8-benzylamino-8,11-oxapentacyclo[5.4.0.0^{2},6.$0^{3,10}$.$0^{5,9}$]undecane (NGP 1-01). Pharmazie, 1998; 53: 859-862.

Malan SF, Dyason K, Wagenaar B, Van Der Walt JJ, Van Der Schyf CJ. The structure and ion channel activity of 6-benzylamino-3-hydroxyhexacyclo[6.5.0.03,7.04,12.05,10.09,13]-tridecane. Arch. Pharm., 2003; 336(2): 127-133.

Malan SF, Van Der Walt JJ, Van Der Schyf CJ. Structure-Activity Relationships of Polycyclic Aromatic Amines with Calcium Channel Blocking Activity. Arch. Pharmacol. Pharmaceut. Med. Chem., 2000; 333: 10-16.

Marks JD, Bindokas VP, Zhang X-M. Maturation of vulnerability to excitotoxicity: intracellular mechanisms in cultured postnatal hippocampal neurons. Brain Res. Dev. Brain Res., 2000; 124: 101-116.

Martini FH. Fundamentals of anatomy & physiology, fourth ed. Prentice Hall: New Jersey, 1998: 417.

Marvizon JC, McRoberts JA, Ennes HS, Song B, Wang X, Jinton L, Corneliussen B, Mayer EA. Two N-methyl-D-aspartate receptors in rat dorsal root ganglia with different subunit composition and localization. J. Comp. Neurobiol., 2002; 446: 325-341.

Masu M, Nakajima Y, Moriyoshi K, Ishii T, Akazawa C, Nakanashi S. Molecular characterization of NMDA and Metabotropic Glutamate receptors. Ann. N. Y. Acad. Sci., 1993; 707: 153-164.

Meir A, Ginsburg S, Butkevich A, Kachalsky SG, Kaiserman I, Ahdut R, Demirgoren S, Rahamimoff R. Ion channels in presynaptic nerve terminals and control of transmitter release. Physiol. Rev., 1999; 79(3): 1019-1064, Jul.

Mickuviene I, Kirveliene V, Juodka B. Experimental survey of non-clonogenic viability assays for adherent cells *in vitro*. Toxicol. In Vitro, 2004; xxx: xxx

Miguel-Hidalgo JJ, Alvarez XA, Cacabelos R, Quack G. Neuroprotection by memantine against neurodegeneration induced by β-amyloid (1-40). Brain Res., 2002; 958: 210-221.

Millan MJ. The induction of pain: an integrative review. Prog. Neurobiol., 1999; 57(1): 1-164.

Mishina M, Mori H, Araki K, Kushiya E, Meguro H, Kutsuwada T, Kashibabuchi N, Ikeda K, Nagasawa J, Yamazaki M, Masaki H, Yamakura T, Morita T, Sakimura K. Molecular and functional diversity of the NMDA receptor channel. Ann. N. Y. Acad. Sci., 1993; 707: 136-152.

Molecular Probes, Inc. LIVE/DEAD® Viability/Cytotoxicity Kit (L-3224). 2001; [Web:] http://www.probes.com/media/pis/mp03224.pdf [Date of access: 2 Sept. 2004].

Mori H and Mishina M. Structure and Function af the NMDA Receptor Channel. Neuropharmacology, 1995; 34(10): 1219-1237.

Moriyoshi K, Masu M, Ishii T, Shigemoto R, Mizuno N, Nakanashi S. Molecular cloning and characterization of the rat NMDA receptor. Nature, 1991; 354: 31-37.

Moser EI, Krobert KA, Moser M-B, Morris RGM. Impaired spatial learning after saturation of long-term potentiation. Nature. 1998; 281: 2038-2042.

Nencioni ALA, Lebrun I, Dorce VAC. Dantrolene protects hippocampal cells from damage induced by TsTX, and α-scorpion toxin from Tityus serrulatus. Toxicon, 2004; 44: 179-183.

Nicholls DG and Budd SL. Mitochondria and neuronal survival. Physiol. Rev., 2000; 80(1): 315-360.

Nicotera P, Bellomo G, Orrenius S. Calcium-mediated mechanisms in chemically induced cell death. Ann. Rev. Pharmacol. Toxicol., 1992; 32: 449-470.

Nishikawa H, Hashino A, Kume T, Katsuki H, Kaneko S, Akaike A. Involvement of direct inhibition of NMDA receptors in the effects of σ-receptor ligands an glutamate neurotoxicity *in vitro*. Eur. J. Pharmacol., 2000; 404: 41-48.

Nishizawa Y. Glutamate release and neuronal damage ischemia. Life Sci., 2001; 69: 369-381.

Oliver DW, Dekker TG, Snyckers FO. Pentacyclo[5.4.0.$0^{2,6}$.$0^{3,10}$.$0^{5,9}$]undecylamines. Synthesis and pharmacology. J. Med. Chem., 1991; 26: 375-379.

Olney JW. Excitotoxicity, apoptosis and neuropsychiatric disorders. Curr. Opin. Pharmacol., 2003; 3: 101-109.

Palmer GC. Neuroprotection by NMDA receptor antagonists in a variety of neuropathologies. Curr. Drug Targets, 2001; 2: 241-271.

Parsons CG, Danysz W, Quack G. Memantine is a clinically well tolerated N-methyl-D-aspartate (NMDA) receptor antagonist – a review of preclinical data. Neuropharmacology, 1999; 38: 735-767.

Phillies JW and O'Regan MH. A potentially critical role of phospholipases in central nervous system ischemic, traumatic, and neurodegenerative disorders. Brain Res. Brain Res. Rev., 2004; 44: 13-47.

Pringle AK. In, out, shake it all about: elevation of $[Ca^{2+}]_i$ during acute cerebral ischaemia. Cell Calcium, 2004; 36: 235-248.

Promega Corporation. CellTiter 96® Non-Radioactive Cell Proliferation Assay. 1999; [Web:] http://www.shpromega.cn/tb112.pdf [Date of access: 2 Sept. 2004].

Rajendra W, Armugam A, Jeyaseelam K. Neuroprotection and peptide toxins. Brain Res. Brain Res. Rev., 2004; 45: 125-141.

Reber AS and Reber E. The Penguin dictionary of psychology. third ed. Penguin: London, 2001: 293.

Reichling DB, Barrat L, Levine JD. Heat-induced cobalt entry: an assay for heat transduction in cultured rat dorsal root ganglion neurons. Neuroscience, 1997; 77(2): 291-294.

Reuter H. Diversity and function of presynaptic calcium channels in the brain. Curr. Opin. Neurobiol., 1996; 6: 331-337.

Riedel G, Platt B, Micheau J. Glutamate receptor function in learning and memory. Behav. Brain Res., 2003; 140: 1-47.

Robert F, Bert L, Stoppini L. Blockade of NMDA-receptors or calcium-channels attenuates the ischaemia-evoked efflux of glutamate and phosphoethanolamine and depression of neuronal activity in rat organotypic hippocampal slice cultures. C.R. Biologies, 2002; 325: 495-504.

Rodriguez MJ, Bernal F, Andres N, Malpesa Y, Mahy N. Excitatory amino acids and neurodegeneration: a hypothetical role of calcium precipitation. Int. J. Dev. Neurosci., 2000; 18: 299-307.

Rothman SM, Olney JW. Excitotoxicity and the NMDA receptor – still lethal after eight years. Trends Neurosci., 1995; 18: 57-58.

Schurr A, Payne RS, Rigor BM. Protection by MK-801 against hypoxia-, excitotoxin-, and depolarization-induced neuronal damage *in vitro*. Neurochem. Int., 1995a; 26(5): 519-525.

Schurr A, Payne RS, Rigor BM. Synergism between diltiazem and MK-801 but not APV in protecting hippocampal slices against hypoxic damage. Brain Res., 1995b; 684: 233-236.

Sidach SS and Mintz IM. Kurtoxin, a gating modifier of neuronal high- and low-threshold Ca channels. J. Neurosci., 2002; 22(6): 2023-2034, Mar. 15.

Silei V, Fabrizi C, Venturini G, Salmona M, Bugiani O, Tagliavini F, Lauro GM. Activation of microglial cells by PrP and β-amyloid fragments raises intracellular calcium through L-type voltage sensitive calcium channels. Brain Res., 1999; 818: 168-170.

Slomianka L. Blue Histology – Nervous Tissue. 2003; [Web:] http://www.lab.anhb.uwa.edu.au/mb140/CorePages/Nervous/Nervous.htm#GANGLIA [Date of access: 2 Sept. 2004].

Small DL, Monette R, Buchan AM, Morley P. Identification of calcium channels involved in neuronal injury in rat hippocampal slices subjected to oxygen and glucose deprivation. Brain Res., 1997; 753: 209-218.

Snutch TP, Sutton KG, Zamponi GW. Voltage-dependent calcium channels – beyond dihydropyridine antagonists. Curr. Opin. Pharmacol., 2001; 1: 11-16.

Sobolevsky A and Koshelev S. Two Blocking Sites of Amino-Adamantane Derivatives in Open N-Methyl-D-Aspartate Channels. Biophys. J., 1998; 74: 1305-1319.

Spafford JD and Zamponi GW. Functional interactions between presynaptic calcium channels and the neurotransmitter release machinery. Curr. Opin. Neurobiol., 2003; 13: 308-314.

Taguchi R, Nishikawa H, Kume T, Terauchi T, Kaneko S, Katsuki H, Yonaga M, Sugimoto H, Akaike A. Serofendic acid prevents acute glutamate neurotoxicity in cultured cortical neurons. Eur. J. Pharmacol., 2003; 477: 195-203.

Tang Y-P, Shimizu E, Dube GR, Rampon C, Kerchner GA, Zhuo M, Liu G, Tsien JZ. Genetic enhancement of learning and memory in mice. Nature, 1999; 402: 63-69.

Triggle DJ. The pharmacology of ion channels: with particular reference to voltage-gated Ca^{2+}-channels. Eur. J Pharmacol., 1999; 375: 311-325.

Uliasz TF, Hewett SJ. A microtiter blue absorbance assay for the quantitative determination of excitotoxic neuronal injury in cell culture. J. Neurosci. Methods, 2000; 100: 157-163.

Urch CE, Rahman W, Dickenson AH. Electrophysiological studies on the role of the NMDA receptor in nociception in the developing rat spinal cord. Brain Res. Dev. Brain Res., 2001; 126: 81-89.

Van Der Schyf CJ, Squier GJ, Coetzee WA. Characterization of NGP 1-01, an aromatic polycyclic amine, as a calcium antagonist. Pharmacol. Res., 1986; 18(5): 407-417.

Van Der Walt JJ, Van Der Schyf CJ, Van Rooyen JM, De Jager J, Van Aarde MN. Calcium current blockade in cardiac myocytes by NGP 1-01, an aromatic polycyclic amine. S. A. J. Science, 1988; 84: 448-449.

Vergun O, Han YY, Reynolds IJ. Glucose deprivation produces a prolonged increase in sensitivity to glutamate in cultured rat cortical neurons. Exp. Neurol., 2003; 183: 682-694.

West AE, Chen WG, Dalva MB, Dolmetsch RE, Kornhauser JM, Shaywitz AJ, Takasu MA, Tao X, Greenberg ME. Calcium regulation of neuronal gene expression. Paper Nat. Acad. Sci., 2001; 98(20):11024-11031.

Yakamura T and Shimoji K. Subunit- and site-specific pharmacology of the NMDA receptor channel. Prog. Neurobiol., 1999; 59: 279-298.

Yusaf SP, Goodman J, Pinnock RD, Dixon AK, Lee K. Expression of voltage-gated calcium channel subunits in rat dorsal root ganglion neurons. Neurosci. Lett., 2001; 311(2): 137-141.

Zhang J-F, Ellinor PT, Aldrich RW, Tsien RW. Molecular determinants of voltage-dependant inactivation in calcium channels. Nature, 1994; 372: 97-100.

3

JOURNAL ARTICLE

Evaluation of isolated dorsal root ganglion cells as a model to study neural calcium overload

Esaias Engelbertus Jordaan[a,*]

Catharina Maria Theresia Fourie[a]

Karin Dyason[a]

[a] ***School for Physiology, Nutrition and Consumer Science of the North-West University, Potchefstroom, Republic of South Africa.***

Text pages: 21
Figures: 4
Tables: 1

Corresponding author. Tel.: (018) 299 2433
Fax: (018) 299 2433
E-mail address: flgeej@puknet.puk.ac.za

ABSTRACT

The event of neural Ca^{2+} overload associated with ischaemia, hypoglycaemia, hypoxia and neurodegenerative diseases such as Alzheimer's disease, Parkinson's disease and AIDS-related dementia has several deleterious effects resulting in cell death. In vitro models for investigating the mechanisms involved in Ca^{2+} overload include brain slice preparations, neuronal cultures as well as acutely isolated neurons, mostly from the hippocampus and cortical brain areas. Additional models for investigating Ca^{2+} overload may bring about new knowledge to areas of the phenomenon that are still unresolved. In this study several theoretical Ca^{2+} overload-related interventions were combined, aimed at inducing cell death in acutely isolated rat dorsal root ganglia (DRGs). Cell death was indicated by the trypan blue exclusion assay and recorded after 18 hours exposure to the interventions by counting live and dead neurons under a light microscope. The goal was to evaluate the possible application of DRGs as a model for Ca^{2+} overload outside the brain. It is concluded that the observed induced cell death was indeed primarily due to Ca^{2+} overload, most probably via the voltage-activated Ca^{2+} channels (VACCs).

Key words: Ca^{2+} overload; glutamate excitotoxicity; model; dorsal root ganglia; viability; trypan blue; voltage-activated Ca^{2+} channels; NMDAR channels

1) INTRODUCTION

The cellular event culminating in the excessive flux of Ca^{2+} into the cytoplasm, known as Ca^{2+} overload, commonly occurs during events ultimately leading to cell death. These overload-inducing events include various pathological states such as ischaemia, hypoxia and hypoglycaemia, which have been observed in a variety of excitable cells . Ca^{2+} overload is also related to several neurodegenerative diseases such al Alzheimer's and Parkinson's disease (Riedel et al., 2003). Scientists are in pursuit of elucidating the mechanisms involved in Ca^{2+} overload in different tissues and due to different types of cellular interventions.

The event responsible for inducing Ca^{2+} overload and the resulting cell death is usually linked to sustained depolarization (Fig. 1 - references shown in figure) mediated by various membrane-coupled and intracellular mechanisms, usually leading towards a decrease in cellular ATP levels. The depolarization might also be induced directly by an event, as is the case for example during pathological disturbances in local ion concentrations. Depolarization activates a cascade of reactions as illustrated in Fig. 1. Various membrane-bound channels are activated, causing ion-movement over the membrane resulting in even more depolarization. Since the initiating factor is still present the membrane's ability to re-establish the resting membrane potential is negated. The ions that have the greatest potential to induce cell death are especially Na^+ and Cl^- to a lesser extent, through osmotic swelling, and then of course the Ca^{2+} conduits, relevant for the induction of Ca^{2+} overload. These include the VACCs and the semi voltage-activated, glutamate activated N-methyl-D-aspartate receptor (NMDAR) channels facilitating excessive influx of Ca^{2+} into the cytoplasm. The NMDAR channels' involvement in Ca^{2+} overload has been specifically linked to glutamate excitotoxicity initiated by excessive synaptic glutamate concentrations. Reversal of the Na^+/Ca^{2+} exchanger, caused by an excessive intracellular Na^+ concentration and excessive Ca^{2+} release from intracellular stores may also contribute to the Ca^{2+} overload (Fig. 1).

The excessive rise in intracellular Ca^{2+} might lead to the activation of several Ca^{2+} - dependent intracellular enzymes. Erratic activation of these enzymes triggers a cascade of deleterious effects. Additionally, the mitochondria buffer the rise in cytosolic Ca^{2+}, which might lead to abolishment of the mitochondrial membrane potential, eventually resulting in mitochondrial degeneration and exhaustion of ATP levels. These factors ultimately cause cellular damage through the action of Ca^{2+}-dependent enzymes directly, generation of excessive reactive oxygen species (ROS) and

activation of several apoptosis initiating messengers. All these elements interactivate each other and aggravate the other's damaging influence. Several crucial cell structures are eventually damaged, including macromolecules, membranes, the cytoskeleton, mitochondria and nuclei, resulting in cell death (Fig. 1).

In vitro models for investigating glutamate excitotoxicity and Ca^{2+} overload are valuable, not only for elucidating the yet unresolved underlying subcellular mechanisms, but also for basic research in the development of protective measures. Most models for Ca^{2+} overload involve preparations from brain tissue, frequently from the hippocampus, since this area is notoriously vulnerable to excitotoxic interventions and has a dense NMDAR channel expression (Moriyoshi et al., 1991). Slice preparations from this area are a popular approach (Frankiewics et al., 2000), but neuronal cultures (Marks et al., 2000; Taguchi et al., 2003) and freshly isolated neurones of the hippocampus and other areas (e.g. cortical neurones (Li et al., 2001)) are also commonly used. Ca^{2+} overload is induced by exposing the cells to a combination of interventions such as a high concentration of glutamate (Li et al., 2001) or another glutamate receptor agonist (Jing et al., 2004), thus inducing glutamate excitotoxicity. An excessive extracellular Ca^{2+} concentration (Li et al., 2001) is also commonly used to enhance the electrochemical gradient of Ca^{2+}, thus creating increased Ca^{2+} influx and eventually overload. In addition, cells are frequently depolarized (Kiedrowski, 1998) and/or incubated in an environment devoid of adequate oxygen (Small et al., 1997), glucose (Kume et al., 2002) or Mg^{2+} (Kiedrowski, 1998). Glucose deprivation apparently reduces ATP levels, having various damaging effects upon cellular functioning and also adding further to depolarization. This effect is primarily mediated by the influence of hypoglycaemia on glycolysis and also indirectly, through lowered pyruvate levels, on oxidative phosphorilation (Vergun et al., 2003; Ioudina et al., 2004). The absence of Mg^{2+} in the cell's environment activates NMDAR channels, potentially leading to excessive Ca^{2+} influx due to the ion's blocking effect that is negated under these circumstances (Ashcroft, 2000).

In this study, the use of freshly isolated DRG neurons as a model for investigating Ca^{2+} overload has been evaluated. Attempts were made to induce cell death by exposing cells to interventions that should result in Ca^{2+} overload mainly through activation of NMDAR channels and VACCs. The expression of VACCs on the rat DRG cytoplasmic membrane has been confirmed by in situ hybridization studies performed by Yusaf et al. (2001). Several studies and a wide range of analytical techniques were used to

confirm the expression of all the NMDAR channel subunits on the cell bodies of DRG membranes (Marvizon et al., 2002; Li et al., 2004).

Once cell death was induced, the evaluation was extended by the introduction of several well-known antagonists of the mentioned channels. If Ca^{2+} overload can be studied successfully in DRGs it can be used as an additional model for investigations regarding the character of the lethal mechanisms involved in, as well as measures for protection against, Ca^{2+} overload.

2) MATERIALS AND METHOD

DRGs were removed from the vertebral column of Sprague Dawley rats (± 250g) in cold (± 4 °C) phosphate-buffered salt medium (PBS) (Highveld Biological). Ganglia were treated enzymatically, initially with collagenase-D (Roche) for 45 min, followed by 1:250 trypsin (Gibco) for 30 minutes. Both treatments were performed in a shaking water bath at 37 °C. DRGs were separated from non-neurons by centrifuge (2 250 r/min for 10 min) in a Percoll gradient (Sigma), whereafter the pellet was suspended in Dulbecco's modified eagle's medium (DMEM) (Highveld Biological) on a fetal calf serum (Highveld Biological) -coated Petri dish (90 min at 37°C). The DMEM cell solution was centrifuged (1400 r/min for 5 min) and the pellet resuspended in DMEM, whereafter it was divided into experimental samples.

To induce glutamate excitotoxicity and Ca^{2+} overload, the cells were suspended and incubated in a glucose and Mg^{2+}-free DMEM solution with increased concentrations of glutamate (10 mM – BDH), glycin (10 mM - Merck), $CaCl_2$ (5.4 mM) and KCl (100 mM). Alterations to the composition of this main intervention were made in interventions 2-6 (Table I), in order to elucidate the mechanism/s involved in the observed cell death. Protection against cell death was investigated by addition of 300 µM concentrations of nifedipine (Bayer), diltiazem (MP Biomedicals Inc.), memantine (Sigma) and MK-801 (ICN Biomedicals Inc.) to the main intervention. Control (in standard DMEM) and experimental samples were incubated at 37 °C. Assessment of cell death in the various mediums was done at room temperature immediately after addition to the intervention (thus at 0 hours), followed by a second assessment of each sample after an 18 hour incubation period. Changes in the viability were expressed as %viability after 18 hours / %viability at 0 hours.

Trypan blue (Sigma) was freshly diluted (0,4%) in PBS before each set of assessments. The various samples were centrifuged (5 min) and washed with PBS. After removal of the PBS, trypan blue was added for 5 min and the medium was centrifuged for another 5 minutes. Trypan blue was cautiously removed and PBS added. The cell solution was suspended on a gridded counting bath and left for 10 min for the cells to settle. At least 200 cells (Nishikawa et al., 2000; Kume et al., 2002; Taguchi et al., 2003) were counted with every sample using a light microscope (Olympus IMT-2 - 400 x magnification). Cells with a clear cytoplasmic appearance (Fig. 2A) were assumed to be viable. Dead cells' cytoplasm ranged in appearance from a light to a dark, almost black, shade of blue (Fig. 2B).

Four easily discernable cell categories were excluded from the recordings: (1) cells that formed clusters, thus complicating the discernability of individual cells. (2) Cells with clear cytoplasm but with obviously disintegrated cytoplasmic membranes, and (3) cells with a grey tint to the cytoplasm (thus not blue or clear) were also excluded. Finally (4) cells with a diameter of less than 20 µm were ignored during the counting procedure, since their identity was in doubt.

Frequency tables and log linear analyses were performed by means of the software package Statistica Version 6. Graph construction and further statistical analyses were performed by means of Microcal Origin version 5.0 software. P-values ≤ 0.05 were considered as significant.

3) RESULTS

A 2-way frequency table was compiled with the intervention and live/dead cells as factorial inputs. Phi-coefficients from this table indicated that initial recordings (at 0 hours) within each cell isolation did not differ significantly from each other, with a maximum coefficient value of 0.23 and an average value of 0.085. A 3-way log linear analysis was also performed on the 0 hour recordings, using the same factors as in the 2-way frequency table in addition to the element of different cell isolations. According to the Chi-square value (at 18 degrees of freedom), only the variation between different cell isolations is statistically significant ($p \leq 0.05$). This significant difference implicates decreased accuracy of the averages calculated from repeat interventions and diminishes the validity of directly comparing recordings from different cell isolations. The influence of this significant difference on the average values of repeats can be minimized by expressing each intervention's viability as a percentage of the control

value recorded from the same cell isolation as that used for the specific intervention. Using such "paired" cell isolations is also important for comparing values between different interventions, to suppress the influence of the difference between cell isolations. Practical constraints resulted in this important requirement not being satisfied with all the recordings that were to be compared. All the cell isolations were exposed to the main intervention though, to which most of the altered interventions are compared directly.

To overcome the constraints identified by the statistical analyses, averages of the altered interventions (interventions 2-6, Table I) were expressed as percentages of paired control averages. Averages of the main intervention (Table I) recordings from these same cell isolations were also expressed as percentages of the control averages of the same paired cell isolations. Subsequently, the calculated main and altered intervention averages were jointly represented with stacked column graphs (Fig. 3 & 4).

Cell death was induced by interventions (Table I) which contained elements thought to be individually capable of inducing cell death by excessive Ca^{2+} influx via the NMDAR channels and the VACCs. Initially, the capability to induce cell death was assessed by exposure of samples to intervention 2 (Table I). Recordings were made after exposure periods of 4 and 18 hours (results not shown).

Intervention 2 resulted in the viability being statistically significantly less than control after both intervals. Relative to the control recordings, the average viability after 18 hours (52 ± 6.32%; n = 11) was less than the average after 4 hours (77 ± 8.42%; n = 6). Cell death could not be induced consistently during the 4 hour interval, since 3 of the 6 recordings resulted in values corresponding to control values. Since cell death was consistently observed after 18 hours incubation, further assessments were recorded exclusively after 18 hours.

The main intervention demonstrated 51 ± 3.51% viability relative to the average of the control recordings in paired cell isolations (Fig. 3). Viability was subsequently recorded following exposure to the altered interventions (interventions 2-6; Table I) parallel to main intervention recordings to establish the cause of the observed cell death in the latter. The difference in viability percentage between the altered interventions and the paired main intervention (represented by white bars in Fig. 3) is an indication of the

altered element/s in the altered intervention's contribution towards cell death induced by the main intervention.

All six interventions induced increased cell death compared to the control (Fig. 3). The viability percentage of the main intervention and intervention 2 (70 ± 12.44%; n = 5) differed statistically significantly from the paired control recordings. Interventions 3 (87 ± 6.36%; n = 5), 4 (95 ± 2.35%; n = 5), 5 (80 ± 8.86%; n = 6) and 6 (72 ± 4.59%; n = 6) had high viability percentages, which did not differ significantly from each other or from the control, but indeed from the main intervention.

The difference between the viability of the main intervention and intervention 2 demonstrates the effect that the absence of glucose and Mg^{2+} has on the viability. A slight increase in viability (8%) is evident for intervention 2 indicating that the absence of glucose and Mg^{2+} caused increased cell death.

Differences in cell viability between the main intervention and intervention 3 and between interventions 2 and 4 demonstrate the effect of KCl-induced depolarization. The difference in the percentage viability between interventions 3 and 4, indicated that the absence of glucose and Mg^{2+} did not increase cell death when there was no KCl-induced depolarization. Interventions 3 and 4 were done on different cell isolations, making these comparisons less reliable.

Both interventions without KCl-induced depolarization displayed significantly more viability than the main intervention. These differences of 55% and 41% for interventions 3 and 4 respectively, did not differ significantly from each other.

Results comparing the main intervention with interventions 5 and 6 relate to the involvement of Ca^{2+} ions in the induction of cell death observed after exposure to the main intervention. The Ca^{2+}-free (intervention 5) and EGTA-containing (intervention 6) recordings demonstrated consistent protection against the observed cell death of the main intervention. Intervention 5 demonstrated 49% more viability, with a 41% higher value after exposure to intervention 6.

Further investigation regarding the contribution of Ca^{2+} overload in the observed cell death involved the cytoplasmic membrane ion channels supposedly responsible for Ca^{2+} influx associated with Ca^{2+} overload. Several acknowledged antagonists of these channels, some of which are used clinically against Ca^{2+} overload, were added to the

main intervention (Fig. 4). To ensure comparability between these interventions, a standard concentration of 300 µM was used for all the antagonists. This concentration was decided upon following pilot experiments where a concentration range of 100 µM – 300 µM was screened.

Nifedipine and diltiazem, both antagonists of the L-type VACC, demonstrated different results. Diltiazem induced an insignificant decrease in viability (8%) at 51± 6.15% and is thus assumed to have no protective properties in this model. In the presence of nifedipine, on the contrary, 76 ± 11.74% of the DRGs were still alive after 18 hours, while only 52 ± 5.37% were viable after main intervention exposure. Nifedipine thus demonstrated a 24% increase in viability. Although its effect does not differ statistically significantly from the main intervention, it might be of physiological significance, since it is a notably bigger difference than that of the rest of the non-statistically significantly different values observed during this evaluation.

To determine the role of NMDAR channels in cell death induced by the main intervention, the effects of the NMDAR channel antagonists, memantine and MK-801, were assessed. Memantine and MK-801 displayed a 57 ± 10.46% and 56 ± 6.53% percentage viability, with paired main intervention percentages of 45 ± 10.04% and 43 ± 10.04% respectively. Memantine thus demonstrated 12% and MK-801 13% protection. These effects are not statistically significant.

If excessive influx of Ca^{2+} via the L-type VACCs and the NMDAR channels is a main pathway for Ca^{2+} overload, it is expected that a combination of antagonists for these channels should provide a greater degree of protection than an antagonist for only one type of channel. Since it was reported in the literature that MK-801 and diltiazem demonstrated synergism in protecting hippocampal slices against hypoxic damage (Schurr et al., 1995b), the combined effect of these two antagonists (both at 300 µM) was assessed. Individually, diltiazem displayed no protection and MK-801 only minimal protection (Fig. 4). The combination of these antagonists displayed a 66 ± 17.32% viability. Although this value is high, the paired main intervention average was close to it (57 ± 7.05%), thus demonstrating protection of 9%. Although nifedipine had a significant effect on its own, surprisingly, its combination with memantine demonstrated a 10% decrease in viability (53 ± 11.61%).

4) DISCUSSION

Manual viability assessments have the disadvantage of researcher subjectivity, which is thought to lower the reliability substantially. Since the results recorded here displayed no statistically significant difference between 0 hour recordings within a specific cell isolation it is concluded that the experimental procedure used in this study, including the counting procedure, is reliable. Nevertheless, this method should be regarded as a rather unsophisticated method compared to for example patch-clamp studies and should therefore only be considered as a screening assay. Subtle differences between recordings should thus not be regarded as significant and statistical significance should rather serve as the criterium for indicating real tendencies..

Dubinsky (1995) proposed that cell death can be both rapidly and slowly triggered. Rapidly triggered cell death is likely to occur after exposure to high concentrations of Ca^{2+}-permeable channels agonists and is probably related to eventual osmotic lysis of the membrane. Slowly triggered mechanisms are likely to be induced after exposure to lower concentrations of these agonists for longer periods and this route implies the involvement of Ca^{2+}-dependent mechanisms. Assessments of Ca^{2+} mediated cell death, are usually done over longer periods of 18 to 24 hour. Cell death over such an extended period probably takes a sigmoidal course with various platos during which less cells die, with steep inclines of increased cell death in between, corresponding to periods during which a deleterious cascade reaches its endpoint, thus inducing death in several cells simultaneously (Dubinsky, 1995). Based on the composition of intervention 2, rapid cell death was expected. However, only the 18 hour intervention demonstrated consistent inductions of cell death, which might indicate the involvement of slowly induced Ca^{2+}-dependent mechanisms despite exposure to high concentrations of NMDAR channel agonists. Due to the inconsistent cell death observed after the 4 hour exposure period, the possibility of osmotic lysis cannot be discarded as contributive to the observed cell death. These inconsistent results should be confirmed with more experiments before a conclusion can be made, however.

To further elucidate the pathway responsible for cell death over the 18 hour period, cell samples were exposed to the altered interventions, as illustrated in Fig. 3. The increase in viability (8%) observed with intervention 2 can be attributed to the presence of Mg^{2+} and/or glucose. Hypoglycaemia is known to inhibit cellular energy metabolism, ultimately resulting in depolarization of the cytoplasmic membrane via

exhaustion of transport mechanisms in the membrane (Vergun et al., 2003; Ioudina et al., 2004). Mg^{2+} acts as a voltage-dependent blocking particle inside the pore of the NMDAR channel. NMDAR channels inherit their voltage-dependent activation properties from the fact that this block can only be abolished by depolarization (Ashcroft, 2000).

It is thus expected that a Mg^{2+}-free environment should result in sustained NMDAR channel activation and thus excessive influx of Ca^{2+} provided that the channels' agonists, glutamate and glycin, are present. Both these agonists were indeed added to the intervention medium in high concentrations (Table I). With the main intervention and intervention 2, the high concentration of KCl induces depolarization (Baldassa et al., 2003). Under depolarized conditions, Mg^{2+} is unlikely to block NMDAR channels. The presence of glucose and not Mg^{2+} in intervention 2 probably contributes to the observed 8% increase in viability. From the results with interventions 3 and 4 it is evident that the induction of depolarization via KCl and not necessarily the absence of glucose (and Mg^{2+}) is a determining factor for cell death. When comparing interventions 3 and 4 it was expected that the increase in viability would be more pronounced with intervention 4 due to the presence of Mg^{2+} and glucose, which was not the case. An unsophisticated method such as the one involved requires larger values before definite conclusions could be drawn. These apparent contrasting results observed with the glucose and Mg^{2+}-altered interventions may thus be due to the insensitivity of the method. Intervention 2 also displayed a relatively large standard error value (12.44). Furthermore, interventions 3 and 4 were done on different cell isolations, making comparisons between these recordings less reliable. Therefore, the observed effect cannot be considered as a real tendency at this point in time. It therefore appears that the absence of glucose and Mg^{2+} do not contribute significantly towards the induction of the observed cell death in this model. If the effect demonstrated by intervention 2 is real, it might speculatively be explained by glucose absence requiring KCl depolarization to induce its effect, thus only inducing increased cell death when the membrane is already depolarized.

Although the extent of depolarization induced by KCl is unknown, it presumably causes influx of ions through various voltage-activated channels. Large quantities of Na^+, Cl^- and Ca^{2+} probably enter the cell, whilst the flux of K^+ out of the cell to repolarize the membrane is abolished due to its high extracellular concentration. The influx of Na^+ is known to be the main contributor towards osmotic deregulation, leading to excessive water influx and eventually lysis of the cell membrane due to swelling (Rodriguez et al.,

2000). Since the aim of this study was to study Ca^{2+} overload in DRGs, the possible role of Na^+ was not specifically assessed further and the focus was subsequently on the VACCs and NMDAR channels. Disorders associated with Ca^{2+} overload have been linked to hyperactivtion of NMDAR channels to such an extent that the contribution of Ca^{2+} permeable channels other than NMDAR channels is still a matter of debate (Hardingham and Bading, 2003). Apart from its role in Ca^{2+} overload, excessive activation of NMDAR channels are expected to add to Na^+-dependent osmotic lysis, since these channels are, although to a lesser extent than is the case with Ca^{2+}, permeable to Na^+ (Riedel et al., 2003)

The contribution of Ca^{2+} was investigated directly by exposure of the DRGs to interventions 5 and 6. If Ca^{2+} overload contributed significantly towards the observed cell death, it is expected that the addition of EGTA and/or the withdrawal of extracellular Ca^{2+} from the intervention medium should display significantly less cell death, as observed by Li et al. (2001). Comparison of the main intervention with interventions 5 and 6 demonstrates that the absence of extracellular Ca^{2+} indeed provides significant protection against cell death.

The possible contribution of the NMDAR channels and L-type VACCs was further explored by the introduction of well-known channel antagonists (Fig. 4). Nifedipine and diltiazem bind to different sites on the L-type VACC. Both antagonists have shown some measure of protection against Ca^{2+} overload-related events. Kubo et al. (2001) for example, demonstrated decreased Ca^{2+} accumulation in ischaemic hippocampal slices after nifedipine administration. Brooks and Kauppinen (1993) observed decreased levels of phosphocreatine, which was used to assess in vitro cell damage during aglycaemic hypoxia, after administration of diltiazem.

Considerable protection against cell death is observed with nifedipine only. Nifedipine and diltiazem bind use/frequency and voltage-dependently onto L-type VACCs, binding with increased affinity upon depolarization (Kochegarov et al., 2003). Usually, in vitro experiments with nifedipine and diltiazem are conducted at much lower antagonist concentrations. It is likely that 300 µM antagonist concentrations have non-specific effects. It is known, for example, that diltiazem also binds onto cardiac fast-activated Na^+ channels at micromolar concentrations (Tanonaka et al., 1999). Tanonaka et al. (1999) further demonstrated that a high nifedipine concentration do not influence the Na^+ channels. According to the different effects observed with diltiazem and nifedipine, the L-type VACCs seemingly do not contribute significantly towards cell death.

Although nifedipine is known to be very specific for the L-type VACC (Mori et al., 1993), its protective effect might be explained speculatively by possible binding onto other, non-L-type VACCs at the relevant high concentration.

MK-801 is a prototypic uncompetitive antagonist of NMDAR channels in relation to which other NMDAR channel antagonists are characterized and compared (Frankiewics et al., 2000). It displays high affinity and stays bound to the channel, even under more extreme depolarizing episodes typical of physiological functioning. Clinically, one of the best tolerated antagonists is the amino-adamantane, memantine. It has moderate affinity for the channel and thus allows physiological functioning while blocking chronic, subtle depolarization. Both MK-801 and memantine have demonstrated protection in a wide range of in vitro models of Ca^{2+} overload-related events (Palmer, 2001).

Based on observations that the NMDAR antagonists, MK-801 and memantine, display insignificant protection in the DRG model and that the role of Mg^{2+} is apparently of minor significance, it is speculated that NMDAR channels do not contribute significantly towards the observed cell death. Although several studies confirmed the presence of NMDAR channel subunits on the cell bodies of DRG membranes (Marvizon et al., 2002; Li et al., 2004), However, the whole-cell NMDAR currents measured by Lovinger and Weight (1988) in DRGs were small compared to the currents measured in hippocampal neurons. The insignificant effect of NMDAR channels may therefore be explained by these channels having a sparse expressional density on the DRG membrane. The minor protective effects demonstrated by the NMDAR channel antagonists could be due to effects different from their NMDAR channel blocking properties. Memantine is known to possess anti-oxidative (Sonkusare et al., 2004) and partial VACC blocking (Parsons et al., 1999) properties and MK-801 has been reported to block fast-activated Na^{+} channels (Schurr et al., 1995a) and L-type VACCs (Robert et al., 2002).

When interpreting these results involving channel antagonists, it should be mentioned that the binding properties of different compounds in different areas of the brain differ considerably (Sonkusare et al., 2004). This maze of variability has not been thoroughly elucidated yet. An example of this variability is memantine's two-times lower affinity for NMDAR channels in the spinal cord compared to that generally applicable for brain neurons (Parsons et al. 1999).

To enhance the investigation of the involvement of Ca^{2+} overload in the current model, the regular experimental practice of adding combinations of VACC and NMDAR channel antagonists (Schurr et al., 1995b; Kubo et al., 2001) to the interventions was introduced. The reported synergistic protection by the combination of MK-801 and diltiazem against hypoxic damage in hippocampal slices (Schurr et al., 1995b) was not evident in this DRG model. The 9% increase in viability is probably due to the effect of MK-801. Both MK-801 and diltiazem are known to inhibit current through the fast-activated Na^{+} channel (Schurr et al., 1995a; Tanonaka et al., 1999). If these channels thus played a significant role in the induction of cell death, this combined antagonist intervention would have displayed considerable protection.

The reason for the decreased viability by the combination of nifedipine and memantine compared to nifedipine alone is unclear. Both the protective effect displayed by nifedipine individually and the effect of decreased viability demonstrated by nifedipine combined with memantine might be overrated though, since the variation between the constituting recordings was relatively large.

In conclusion, due to the composition of the main intervention, cell death was expected via the mechanism of Ca^{2+} overload. Based on the observed importance of Ca^{2+} influx, Ca^{2+} overload seemingly did contribute significantly towards the cell death observed in this model. Furthermore, the results indicate dependency between the KCl-induced depolarization and the effect of Ca^{2+}, since the one factor apparently did not induce significant cell death without the other. The KCl-induced depolarization probably activates the VACCs and the NMDAR channels. However, since the effects of the NMDAR channel antagonists are apparently insignificant it is proposed that these channels do not contribute significantly towards the cell death observed in this model. The L-type VACC antagonists do not protect significantly against cell death either, but these channels only constitute a 6 to 52% fraction of the total VACC current, as observed electrophysiologically in DRGs (Rola et al., 2001). The bulk of the deleterious Ca^{2+} influx might thus be conducted via the non-L-type VACCs. Although Ca^{2+} seemingly adds significantly to the observed cell death, removal of Ca^{2+} from the intervention does not equal complete protection. Other mechanisms like osmotic lysis and abolishment of the energy metabolism probably also add to the observed cell death.

It is recommended that investigations regarding the pathway involved in the proposed Ca^{2+} overload be enhanced by addition of antagonists of non-L-type VACC subtypes

as well as specific antagonists of the Na^+ channel and the Na^+/Ca^{2+}-exchanger. The effects of antagonists of other ion channels such as K^+ channels and the glutamate receptors AMPA and kainate, might also be revealing. Alternatively, the extracellular concentrations of Na^+ and Cl^- could be manipulated to assess the contribution of these ions. The effect of glutamate excitotoxicity should be more thoroughly explored by altering the glutamate and glycin concentrations in the intervention solutions. The effect of energy metabolism might also be further examined by addition of ATPase inhibitors. It is recommended that repetitions of recordings be increased to decrease the influence of variability observed with some interventions. Once the exact pathway of the proposed Ca^{2+} overload is elucidated beyond reasonable doubt, the model could be of value as a screening assay for studying neural Ca^{2+} overload outside the brain.

5) ACKNOWLEDGEMENTS

Prof. Faans Steyn of the Statistical Consultation Services at the North-West University for statistical analysis and statistical input. The North-West University for the use of facilities and financial support.

6) REFERENCES

Ashcroft FM. Ion channels and disease. Academic Press: London, 2000: 302.

Baldassa S, Zippel R, Sturani E. Depolarization-induced signaling to Ras, Rap1 and MAPKs in cortical neurons. Mol. Brain Res., 2003; 119: 111-122.

Brooks KJ and Kauppinen RA. Calcium-mediated damage following hypoxia in cerebral cortex ex vivo studied by NMR spectroscopy. Evidency for direct involvement of voltage-gated Ca^{2+}-channels. Neurochem. Int., 1993; 23(5): 441-450.

Dubinsky JM, Kristal BS, Elizondo-Fournier M. On the probabalistic nature of excitotoxic neuronal death in hippocampal neurons. Neuropharmacology, 1995; 34(7): 701-711.

Frankiewics T, Pilc A, Parsons CG. Differential effects of NMDA-receptor antagonists on long-term potentiation and hypoxic/hypoglycaemic excitotoxicity in hippocampal slices. Neuropharmacology, 2000; 39: 631-642.

Hardingham GE and Bading H. The Yin and Yang of NMDA receptor signalling. Trends Neurosci., 2003; 26(2): 81-89.

Hynd MR, Scott HL, Dodd PR. Glutamate-mediated excitotoxicity and neurodegeneration in Alzheimer's disease. Neurochem. Int., 2004; 45: 583-595.

Ioudina M, Uemura E, Greenlee HW. Glucose insufficiency alters neuronal viability and invreases susceptibility to glutamate toxicity. Brain Res., 2004; xxx: xxx

Jing G, Grammatopoulos T, Ferguson P, Schelman W, Weyhenmeyer J. Inhibitory effects of angiotensin on NMDA-induced cytotoxicity in primary neuronal cultures. Brain Res. Bull., 2004; 62: 397-403.

Kiedrowski L. The difference between mechanisms of kainate and glutamate excitotoxicity in vitro: Osmotic lesion versus mitochondrial depolarization. Restor. Neurol. Neurosci., 1998; 12: 71-79.

Kobayashi T, Mori Y. Ca^{2+} channel antagonists and neuroprotection from cerebral ischemia. Eur. J. Pharmacol., 1998 363: 1-15.

Kochegarov AA. Pharmacological modulators of voltage-gated calcium channels and their therapeutic application. Cell Calcium, 2003; 33: 145-162.

Kubo T, Yokoi T, Hagiwara Y, Fukumori R, Goshima Y, Misu Y. Characteristics of protective effects of NMDA antagonist and calcium channel antagonist on ischemic calcium accumulation in rat hippocampal CA1 region. Brain Res. Bull., 2001; 54(4): 413-419.

Kume T, Nishikawa H, Taguchi R, Hashino A, Katsuki H, Kaneko S, Minami M, Satoh M, Akaike A. Antagonism of NMDA receptors by σ-receptor ligands attenuates chemical ischemia-induced neuronal death in vitro. Eur. J. Pharmacol., 2002; 455: 91-100.

Li J, Kato K, Ikeda J, Morita I, Murota S-I. A narrow window for rescuing cells by the inhibition of calcium influx and the importance of influx route in rat cortical neuronal cell death induced by glutamate. Neurosci. Lett., 2001; 304: 29-32.

Li J, McRoberts JA, Nie J, Ennes HS, Mayer EA. Electrophysiological characterization of N-methyl-D-aspartate receptors in rat dorsal root ganglia neurons. Pain, 2004; 109(3): 443-452.

Lovinger DM and Weight FF. Glutamate induces a depolarization of adult rat dorsal root ganglion neurons that is mediated predominantly by NMDA receptors. Neurosci. Lett., 1988; 94: 314-320.

Marks JD, Bindokas VP, Zhang X-M. Maturation of vulnerability to excitotoxicity: intracellular mechanisms in cultured postnatal hippocampal neurons. Brain Res. Dev. Brain Res., 2000; 124: 101-116.

Marvizon JC, McRoberts JA, Ennes HS, Song B, Wang X, Jinton L, Corneliussen B, Mayer EA. Two N-methyl-D-aspartate receptors in rat dorsal root ganglia with different subunit composition and localization. J. Comp. Neurobiol., 2002; 446: 325-341.

Mori Y, Niidome T, Fujita Y, Mynlieff M, Dirksen RT, Beam KG, Iwabe N, Miyata T, Furutama D, Furuichi T, Mikoshiba K. Molecular diversity of voltage-dependent calcium channel. Ann. N. Y. Acad. Sci., 1993; 560: 87-108.

Moriyoshi K, Masu M, Ishii T, Shigemoto R, Mizuno N, Nakanashi S. Molecular cloning and characterization of the rat NMDA receptor. Nature, 1991; 354: 31-37.

Nencioni ALA, Lebrun I, Dorce VAC. Dantrolene protects hippocampal cells from damage induced by TsTX, and α-scorpion toxin from Tityus serrulatus. Toxicon, 2004; 44: 179-183.

Nishikawa H, Hashino A, Kume T, Katsuki H, Kaneko S, Akaike A. Involvement of direct inhibition of NMDA receptors in the effects of σ-receptor ligands an glutamate neurotoxicity in vitro. Eur. J. Pharmacol., 2000; 404: 41-48.

Palmer GC. Neuroprotection by NMDA receptor antagonists in a variety of neuropathologies. Curr. Drug Targets, 2001; 2: 241-271.

Parsons CG, Danysz W, Quack G. Memantine is a clinically well tolerated N-methyl-D-aspartate (NMDA) receptor antagonist – a review of preclinical data. Neuropharmacology, 1999; 38: 735-767.

Phillies JW and O'Regan MH. A potentially critical role of phospholipases in central nervous system ischemic, traumatic, and neurodegenerative disorders. Brain Res. Brain Res. Rev., 2004; 44: 13-47.

Pringle AK. In, out, shake it all about: elevation of $[Ca^{2+}]_i$ during acute cerebral ischaemia. Cell Calcium, 2004; 36: 235-248.

Rajendra W, Armugam A, Jeyaseelam K. Neuroprotection and peptide toxins. Brain Res. Brain Res. Rev., 2004; 45: 125-141.

Riedel G, Platt B, Micheau J. Glutamate receptor function in learning and memory. Behav. Brain Res., 2003; 140: 1-47.

Robert F, Bert L, Stoppini L. Blockade of NMDA-receptors or calcium-channels attenuates the ischaemia-evoked efflux of glutamate and phosphoethanolamine and depression of neuronal activity in rat organotypic hippocampal slice cultures. C.R. Biologies, 2002; 325: 495-504.

Rodriguez MJ, Bernal F, Andres N, Malpesa Y, Mahy N. Excitatory amino acids and neurodegeneration: a hypothetical role of calcium precipitation. Int. J. Dev. Neurosci., 2000; 18: 299-307.

Rola R, Szulczyk PJ, Witkowski G. Voltage-dependent Ca^{2+} currents in rat cardiac dorsal root ganglion neurons. Brain Res., 2003; 961: 171-178.

Schurr A, Payne RS, Rigor BM. Protection by MK-801 against hypoxia-, excitotoxin-, and depolarization-induced neuronal damage in vitro. Neurochem. Int., 1995a; 26(5): 519-525.

Schurr A, Payne RS, Rigor BM. Synergism between diltiazem and MK-801 but not APV in protecting hippocampal slices against hypoxic damage. Brain Res., 1995b; 684: 233-236.

Small DL, Monette R, Buchan AM, Morley P. Identification of calcium channels involved in neuronal injury in rat hippocampal slices subjected to oxygen and glucose deprivation. Brain Res., 1997; 753: 209-218.

Sonkusare SK, Kaul CL, Ramarao P. Dementia of Alzheimer's disease and other neurodegenerative disorders – memantine, a new hope. Pharmacol. Res., 2004; Xxx: xxx

Taguchi R, Nishikawa H, Kume T, Terauchi T, Kaneko S, Katsuki H, Yonaga M, Sugimoto H, Akaike A. Serofendic acid prevents acute glutamate neurotoxicity in cultured cortical neurons. Eur. J. Pharmacol., 2003; 477: 195-203.

Tanonaka K, Kajiwara H, Kameda H, Takasaki A, Takeo S. Relationship between myocardial cation content and injury in reperfused rat hearts treated with cation channel blockers. Eur. J. Pharmacol., 1999; 37-48.

Vergun O, Han YY, Reynolds IJ. Glucose deprivation produces a prolonged increase in sensitivity to glutamate in cultured rat cortical neurons. Exp. Neurol., 2003; 183: 682-694.

Yusaf SP, Goodman J, Pinnock RD, Dixon AK, Lee K. Expression of voltage-gated calcium channel subunits in rat dorsal root ganglion neurons. Neurosci. Lett., 2001; 311(2): 137-141.

FIGURES

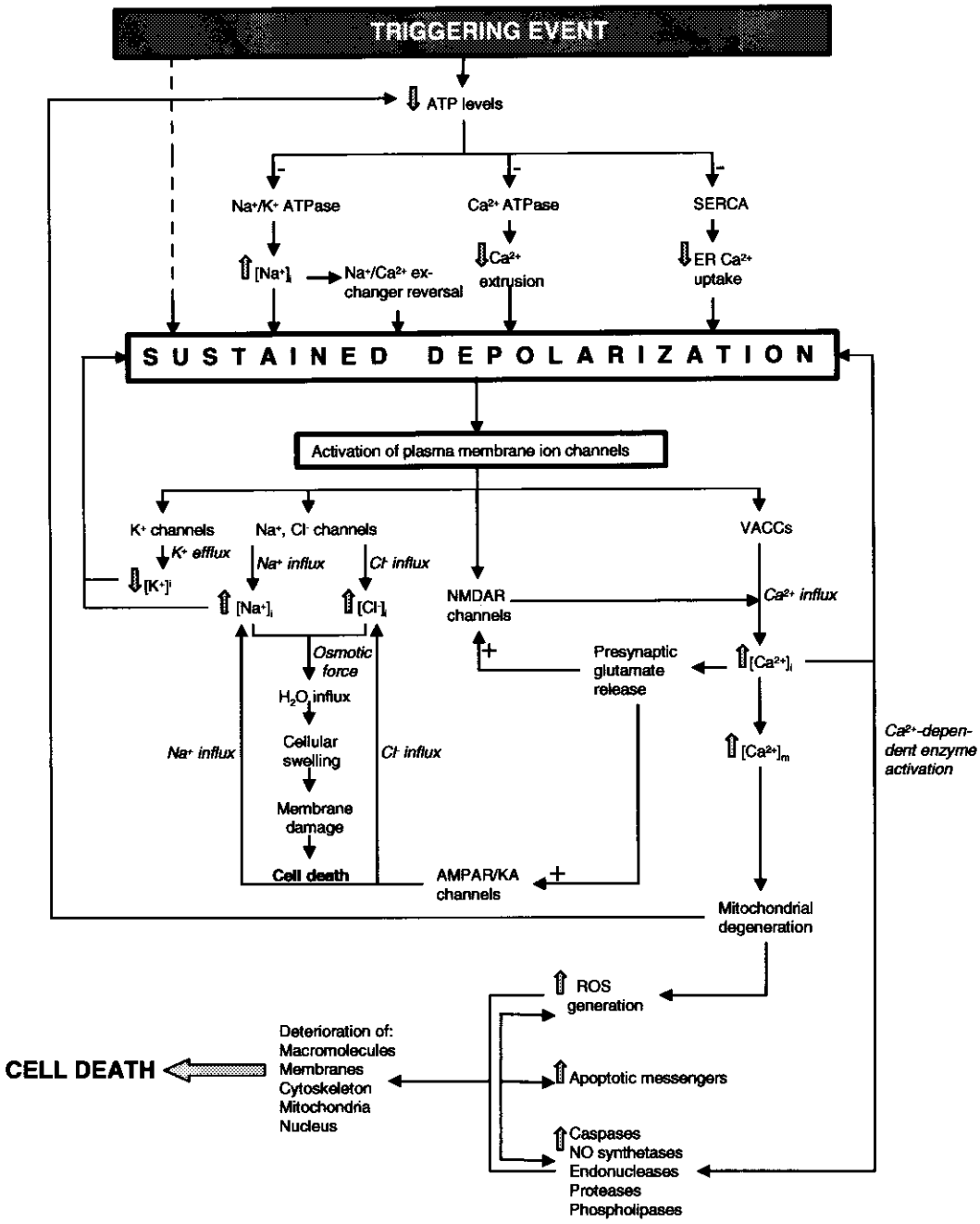

Fig. 1.

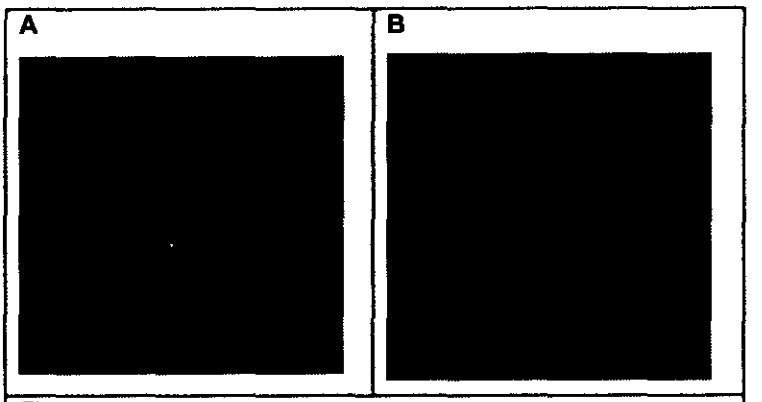

Fig. 2.

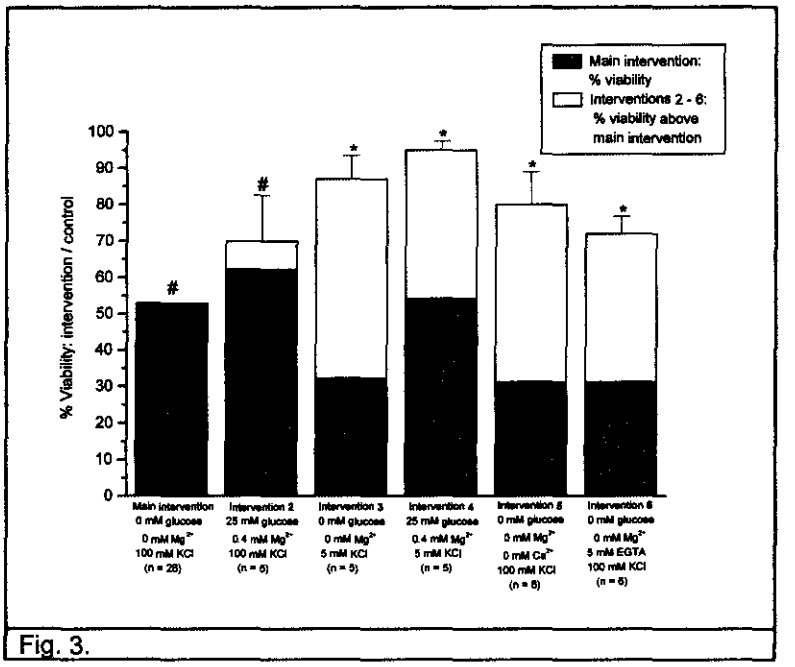

Fig. 3.

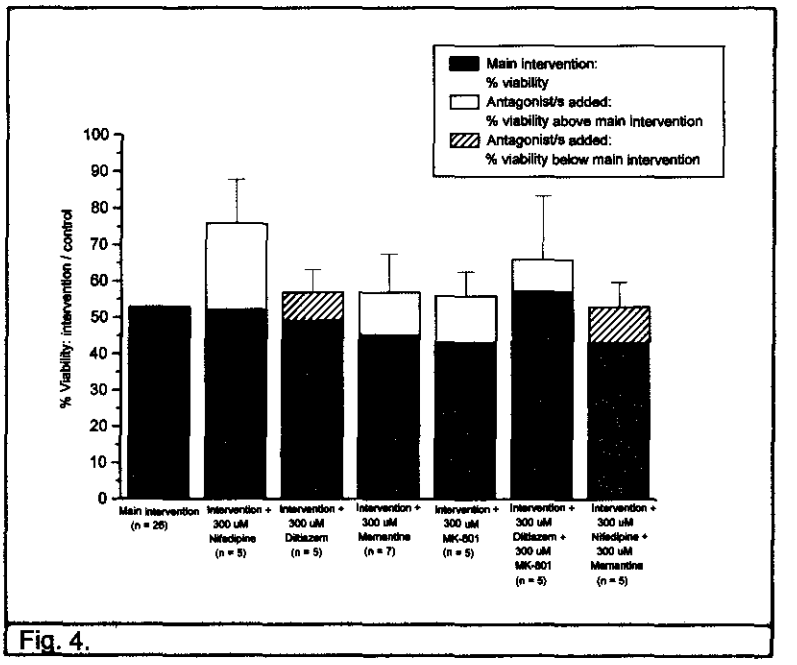

Fig. 4.

TABLES

Table I. Exposition of the control and intervention solutions

	Control	Main inter-vention	Inter-vention 2	Inter-vention 3	Inter-vention 4	Inter-vention 5	Inter-vention 6
Glutamate (mM)	0	10	10	10	10	10	10
Glycin (mM)	0.5	10	10	10	10	10	10
$MgCl_2$ (mM)	0.4	0	0.4	0.4	0	0	0
Glucose (mM)	25	0	25	25	0	0	0
KCl (mM)	5	100	100	5	5	100	100
$CaCl_2$(mM)	1.4	5.4	5.4	5.4	5.4	0	0
EGTA (mM)	0	0	0	0	0	0	5

LEGEND

Fig. 1. Proposed neurodegenerative pathway following an assault upon the cell's energy metabolism (compiled from Rodriguez et al., 2000; Hynd et al., 2004; Nencioni et al., 2004; Philles and O'Regan, 2004; Pringle, 2004; Rajendra et al., 2004)

Abbreviations: **SERCA** – sarco/endoplasmic reticulum Ca2+ ATPase; **ER** – endoplasmic reticulum; **[ion]I** – intracellular ion concentration; **[ion]m** – mitochondrial ion concentration; **VACCs** – voltage-activated calcium channels; **NMDAR** – N-methyl-D-aspartate receptor; **AMPAR** - S-α-amino-3-hidroxy-5-methyl-4-isoxazolepropionic acid receptor; **KA** - kainate receptor; **ROS** – reactive oxygen species; **NO** – nitric oxide; **+ sign** – activation; ***- sign*** – inhibition

Fig. 2. Picture of a live DRG (A) and a trypan blue stained, dead DRG (B) as viewed under a light microscope.

Fig. 3. Graphic representation comparing the effects of recordings from paired cell isolations between the main intervention and the altered interventions. Averages are expressed in relation to paired cell preparation control values (see text for details).
*$p \leq 0.05$ compared to paired main intervention recordings.
#$p \leq 0.05$ compared to paired control recordings

Fig. 4. Graphic representation comparing the effects of recordings from paired cell isolations between the main intervention and the antagonist-added interventions. Averages are expressed in relation to paired cell preparation control values (see text for details).

4

SUMMARY, CONCLUSIONS & RECOMMENDATIONS

CHAPTER 4

SUMMARY, CONCLUSIONS AND RECOMMENDATIONS

DRGs were evaluated as an experimental model for the investigation of the clinically important phenomenon of neural Ca^{2+} overload. An overview of the literature was compiled, discussing the background of aspects relevant to Ca^{2+} overload in general and specifically the development of a cellular model of Ca^{2+} overload.

Firstly, the cytoplasmic membrane channels thought to be primarily involved in the induction of Ca^{2+} overload were discussed in depth, including aspects such as classification, channel structure, kinetics and function. The phenomenon of Ca^{2+} overload, the cellular mechanisms involved and their relation to eventual cell death and the induction thereof *in vitro* were subsequently considered. Cellular mechanisms as well as potential therapeutic measures were central to this discussion. Methods for assessing cell viability *in vitro* and aspects concerning DRGs were finally discussed.

After the development and execution of the experimental protocol, the DRG model was evaluated. The hypothesis revolved around this evaluation and stated that this model is an appropriate tool for investigating Ca^{2+} overload and the protection against it.

Acutely isolated DRGs from Sprague Dawley rats were exposed to different interventions over an 18 hour period. The main intervention contained elements which are associated with the induction of Ca^{2+} overload in neurons. This intervention consisted of high glutamate, glycin, $CaCl_2$ and KCl concentrations, while $MgCl_2$ and glucose were absent. The composition of the main intervention was altered in an attempt to elucidate the mechanism/s mediating the observed cell death after exposure to it.

In the development of the experimental protocol, practical constraints did not always comply with theoretical ideals. Such an issue was revealed by a log-linear analysis

which demonstrated that recordings made immediately after exposure to the intervention varied significantly between different cell isolations. This was not expected, since the different interventions did not have enough time to induce effects at the 0 hour recording stage and the exact same isolation procedure was used for each cell isolation. The number of available cells differed remarkably with each isolation, though, which indicated some measure of variability in the isolation procedure. This variability implicated that valid comparisons could not be made unless the recordings of the intervention to be compared were made on the same set of cell isolations. Since the main intervention was induced in every isolation and was the main factor against which the other interventions in this study were compared, this requirement was largely attainable. In some instances, comparisons between other interventions were necessary, for instance between interventions 3 and 4, to evaluate the influence of the absence of glucose and Mg^{2+} without KCl-induced depolarization. Since these recordings were not executed on the same cell isolations, making conclusions based on the comparison between these interventions are less accurate in an already rather insensitive method. Because of restrictions in terms of the quantity of cells available from a single isolation, with future experiments it would be necessary to do some extra repeats of some interventions to satisfy this requirement.

The basic experimental procedure included an initial recording (after 0 hours) of the percentage viability immediately after the intervention medium was added to the DRG sample. With each recording, approximately 200 cells were counted under a light microscope. This amount of cells was accepted as adequate in several published studies using comparable manual methods of viability assessment (Nishikawa et al., 2000; Kume et al., 2002; Taguchi et al., 2003). Cells were considered dead when their cytoplasm appeared from a light, ranging to a dark, seemingly black shade of blue. Viable or live cells had a clear cytoplasm. Another sample from the same isolation containing the identical intervention solution than the recorded sample, was incubated at 37 °C for 18 hours, whereafter the recording procedure was repeated. The percentage viable cells observed with each recording was calculated, whereafter the percentage over the 18 hour period in relation to the 0 hour recording was calculated by applying the formula *(% viability 18 hours / % viability 0 hours)* x *100.* The interventions were repeatedly induced ($n \geq 5$) in order to obtain realistic average values. These values are influenced, though, by the mentioned difference between

different cell isolations, thus making the representation of data by average recordings less accurate. This problem was largely overcome by representing data relationally as a percentage of the same isolation control percentage. Each 18 hour / 0 hour percentage in a series of repeats for a particular intervention was subjected to the calculation *(18 hour % / 0 hour % of intervention) / (18 hour % / 0 hour % of control) x 100*. This formula was applied to the altered and the main intervention recordings from the same isolations. The averages of these relational percentages of the main and altered interventions were then jointly represented on the same bar on a stacked column graph. The effects of the altered interventions and thus the specific elements altered from/added to the main intervention could be easily compared to the main intervention. In this manner, only same day interventions were directly compared, while relational calculations for averages eliminated the influence of the difference between preparations to a large extent.

The trypan blue exclusion assay is a well-known and recognized method for discerning between live and dead cells (Uliasz and Hewett, 2000). Its staining mechanism is based on membrane integrity, staining cells with disintegrated membranes. The trypan blue exclusion assay has been shown to be effective in several studies including those on DRGs (Reichling et al., 1997) and where cell death was induced by Ca^{2+} overload (Dubinsky et el., 1995; Nishikawa et al., 2000; Taguchi et al., 2003). Several other staining assays, based on more complex staining interactions than with trypan blue, are frequently used. The LDH and MTT assays assess certain biochemical interactions within live cells (Uliasz and Hewett, 2000), while the fluorescent screening viability assay combines membrane integrity criteria for dead cells and biochemical interactions for live cells (Molecular Probes, Inc., 2001). Unfortunately, the dead cell count assayed by the LDH and MTT assays may be artificially increased by reductive elements in the cellular environment (Uliasz and Hewett, 2000). Trypan blue is not influenced by this kind of interaction. In comparison to these comparable assays, the trypan blue assay is inexpensive and simple to apply. A possible problem with viability assessments solely based upon membrane disintegration, though, is that the assay may be applied to dead cells before the membrane disintegrates, resulting in cells being recorded as alive whilst being dead. Cell death along paths of Ca^{2+} overload do indeed include membrane disintegration as one of the final results (Nicotera et al., 1992; Nencioni et al., 2004),

but a variety of other assaults onto the cell's viable state is activated, which might result in the cell being dead before the membrane disintegrates. This phenomenon might result in the underrating of the percentage cell death due to Ca^{2+} overload. It could be that recordings during some interventions did induce more cell death than observed, but that it was not observable with the trypan blue, since membrane integrity was not yet compromised after 18 hours.

Another issue concerning the choice of assessment method is the manual method of counting cells individually by means of a light microscope. This method implies possibilities for subjectivity from the researcher concerning the decision of whether a cell is dead or alive. It is therefore preferable that all the recordings are done by the same researcher. Manual recordings also allow the opportunity for human error in the counting procedure, thus increasing the necessity for more repeats. Since the frequency table constructed concerning the initial recordings (0 hours) indicated no significant differences between 0 hour recordings within a cell isolation, it is assumed that researcher subjectivity did not have a significant influence in this study. An advantage of counting the cells manually is that the DRG samples frequently contain non-neural tissue material. This material is frequently stained along with the dead DRGs. If examined under a light microscope, this material can be excluded from the assessment. On the same issue, doubt existed concerning the inclusion of various cells in the assessment. As more thoroughly mentioned in the method section of the article, these cells were excluded, which would probably not have been possible with automatic procedures.

As mentioned before, staining assays are regularly done automatically by means of a spectrophotometer, measuring the applied light's density after passing through the sample-containing assay wells. This method is frequently used in combination with MTT and LDH assays. Spectrophotometric recording is also possible, although less effective than with the abovementioned assays, using trypan blue (Uliasz and Hewett, 2000). Automatic procedures surmount the problems encountered with manual recordings and have the added advantage of being fast since a number of recordings can be made in a matter of seconds. The restricting factor inherent to the relevant model as towards the possibility of automatic viability assesment, is that the applied method of DRG isolation yields approximately 7 000 cells per isolation, with

variations as great as 5 000 cells more or less, dependent upon uncontrollable variables coupled to the isolation procedure. This yield is not adequate for making several spectrophotometric recordings with a single isolation, since the method requires a certain cell density on the bottom of each well to make a reliable recording, typically at least 5000 cells (Promega Corporation, 1999).

Considering the nature of the method on the whole, it should be viewed as a broad, exploratory method, useful to form a general opinion about or performing screening assays on the relevant interventions. For this reason small differences observed in the results should be interpreted with caution and statistical significance should be used as an indicator of real tendencies.

It was shown that both the KCl-induced depolarization and the presence of Ca^{2+} were important contributing factors to the induction of the cell death observed following exposure to the main intervention. Since these factors do not induce extensive cell death in the absence of the other, it is proposed that Ca^{2+} overload is triggered upon depolarization.

The exact pathway of the observed Ca^{2+} overload is unclear, although it apparently is not primarily induced via the NMDAR channels, since the presence or absence of Mg^{2+} does not appear to play a role and the NMDAR channel antagonists do not display significant protection. The VACCs are proposed to be responsible for the excessive influx of Ca^{2+}.

The evaluation of a model in which Ca^{2+} overload could be studied was the main aim of the study. Assessment of the effects of various protective or potentially protective compounds added to this evaluation in that any substantial protective effects should aid in the identification of the involved mechanism/s. Secondary to that, the evaluation of these compounds was aimed at evaluating the applicability of the model in the development of such compounds. Recognized or potential protective compounds were subsequently added to cell samples dispersed in the main intervention medium, whereafter a viability recording was made to assess the degree of protection by these compounds. Since the compounds discussed in Chapter 3 all demonstrated some degree of protection in previous *in vitro* studies of neural Ca^{2+}

overload, protection was expected in this model as well. The expected protective action was not visibly induced, however. Nifedipine, the only compound displaying considerable protection, did so relatively inconsistently. No effect was observed with the other L-type VACC antagonist, diltiazem. These different effects of two antagonists of the same channel might be explained along differing mechanisms of blocking action, since nifedipine and diltiazem bind onto different sites on the L-type VACC (Kochegarov et al., 2003). Drawing reliable conclusions based upon differences in these properties is not possible, based on the lack of adequate data, bearing in mind that the relevant method is rather unsophisticated. The 300 uM concentrations used are relatively high for an *in vitro* study, which might implicate non-specific effects at sites other than those that these compounds are known for. Since these high concentrations are not frequently used, though, studies exposing these non-specific effects are not readily available, which makes non-speculative conclusions regarding this matter difficult. Speculatively, though, nifedipine might display non-L-type VACC antagonism at these high concentrations.

Not mentioned in Chapter 3 was the addition of two related compounds with potential protective action against Ca^{2+} overload. NGP1-01 and SFM-5O (synthesized and donated by the Dept. of Pharm. Chem., North-West University) demonstrated L-type VACC blocking activity in myocytes (Van der Walt et al., 1988) and have considerable structural similarities to memantine (Geldenhuys et al., 2003). The ideal of simultaneous block of NMDAR channels and VACCS might thus be demonstrated by these compounds. Considering the absence of any real contribution by the individual L-type VACC and NMDAR channel antagonists, it was not surprising that neither NGP1-01 nor SFM-5O demonstrated any protective properties whatsoever.

Nevertheless, since it appears as if Ca^{2+} overload was involved in this model, the first part of the hypothesis which stated that Ca^{2+} overload can be induced in DRGs could conditionally be accepted. However, this conclusion cannot be made with full certainty. If VACC antagonists, or any other known protective measure against Ca^{2+} overload-induced cell death is shown to display protection against cell death in this model, the first part as well as the second part of the hypothesis would be accepted with more certainty.

1) RECOMMENDATIONS AND FUTURE PROSPECTS

The interventions containing 5 mM KCl, 0 mM Ca^{2+} and EGTA demonstrated significantly less cell death than the main intervention. From these observations the conclusion was made that cell death was induced via Ca^{2+}-dependent pathways, probably via the non-L-type VACCs, since the other possible pathways did not seem to contribute significantly. The proposed involvement of these pathways is therefore based upon elimination of the other pathways and was not examined further empirically. Therefore, it is recommended that the effects of antagonists of non-L-type VACCs be assessed. Evaluation of inhibitors of the Na^{+}/Ca^{2+} exchanger and of antagonists other voltage-activated channels, specifically the Na^{+} but also the K^{+} and Cl^{-} channels, could be revealing as well. The effect of energy metabolism might also be further investigated by the application of ATPase antagonists. Furthermore, other assay procedures that are less reliant on the disintegration of the cytoplasmic membrane, for example fluorescent viability assays, might be used. Since the technique is not sensitive, it is recommended that more repeats be done. Other, more sensitive methods like patch-clamping might be used on DRGs to further elucidate the ions and currents involved in the cell death observed during the relevant interventions.

2) REFERENCES

Dubinsky JM, Kristal BS, Elizondo-Fournier M. On the probabalistic nature of excitotoxic neuronal death in hippocampal neurons. Neuropharmacology, 1995; 34(7): 701-711.

Geldenhuys WJ, Malan SF, Murugesan T, Van Der Schyf CJ, Bloomquist JR. Synthesis and biological evaluation of pentacyclo[5.4.0.$0^{2,6}$.$0^{3,10}$.$0^{5,9}$]undecane derivatives as potential therapeutic agents in Parkinson's disease. Bioorg. Med. Chem., 2004; 12: 1-8.

Kochegarov AA. Pharmacological modulators of voltage-gated calcium channels and their therapeutic application. Cell Calcium, 2003; 33: 145-162.

Kume T, Nishikawa H, Taguchi R, Hashino A, Katsuki H, Kaneko S, Minami M, Satoh M, Akaike A. Antagonism of NMDA receptors by σ-receptor ligands attenuates chemical ischemia-induced neuronal death *in vitro*. Eur. J. Pharmacol., 2002; 455: 91-100.

Molecular Probes, Inc. LIVE/DEAD® Viability/Cytotoxicity Kit (L-3224). 2001; [Web:] http://www.probes.com/media/pis/mp03224.pdf [Date of access: 2 Sept. 2004].

Nencioni ALA, Lebrun I, Dorce VAC. Dantrolene protects hippocampal cells from damage induced by TsTX, and α-scorpion toxin from Tityus serrulatus. Toxicon, 2004; 44: 179-183.

Nicotera P, Bellomo G, Orrenius S. Calcium-mediated mechanisms in chemically induced cell death. Ann. Rev. Pharmacol. Toxicol., 1992; 32: 449-470.

Nishikawa H, Hashino A, Kume T, Katsuki H, Kaneko S, Akaike A. Involvement of direct inhibition of NMDA receptors in the effects of σ-receptor ligands an glutamate neurotoxicity *in vitro*. Eur. J. Pharmacol., 2000; 404: 41-48.

Promega Corporation. CellTiter 96® Non-Radioactive Cell Proliferation Assay. 1999; [Web:] http://www.shpromega.cn/tb112.pdf [Date of access: 2 Sept. 2004].

Reichling DB, Barrat L, Levine JD. Heat-induced cobalt entry: an assay for heat transduction in cultured rat dorsal root ganglion neurons. Neuroscience, 1997; 77(2): 291-294.

Taguchi R, Nishikawa H, Kume T, Terauchi T, Kaneko S, Katsuki H, Yonaga M, Sugimoto H, Akaike A. Serofendic acid prevents acute glutamate neurotoxicity in cultured cortical neurons. Eur. J. Pharmacol., 2003; 477: 195-203.

Uliasz TF, Hewett SJ. A microtiter blue absorbance assay for the quantitative determination of excitotoxic neuronal injury in cell culture. J. Neurosci. Methods, 2000; 100: 157-163.

Van Der Walt JJ, Van Der Schyf CJ, Van Rooyen JM, De Jager J, Van Aarde MN. Calcium current blockade in cardiac myocytes by NGP 1-01, an aromatic polycyclic amine. S. A. J. Science, 1988; 84: 448-449.

APPENDIX

APPENDIX A

Table I. Viability percentages expressed as *Viability% after 18 hours/ Viability% after 0 hours* of the main intervention (MI) and the different altered interventions (interventions 2-6).

Day	Control	MI	Intervention 2	Intervention 3	Intervention 4	Intervention 5	Intervention 6
6	71.1		15.5				
7	95.6		63				
8	79		31				
9	93.6		50.9				
10	89.9		49				
11	98		34.6				
12	105	59	60.7	84.3			
13	105	60.4	37.2	81.6			
14	89.4	40	90.9	68			
15	90.6	71	62.7	97.6			
16	68.5	26	68.5	68.6			
17	79	53.4					
18	97	53.4					
19	125	57					
20	94.8	31.8					
21	85.9	6.9				42.9	
22	82	38.6				69.9	
23	45.5	42.1				41.6	
24	75.8	43.3				83	
25	90.4	42.7				56.1	
26	75.5	48.4				70.3	
27	84.1	57.4					
28	89.7	63.1					
29	100	69.1					
30	87.8	50					
31	*	97.4					
32	95.9	40.4					
33	100	45.9					
34	94.5	36.7					
35	72.7	21			71.4		39.2
					74.1		49
36	78.8	31.1			69.4		62.3
					76.8		50
37	92.9	45.8			91.3		76
							74

Table II. Viability percentages expressed as *Viability% after 18 hours/ Viability% after 0 hours* of the main intervention (MI) alone and the MI with the added antagonists.

Day	Control	MI	MI + 300 uM Nifedipine	MI + 300 uM Diltiazem	MI + 300 uM Memantine	MI + 300 uM MK-801
17	79	53.4			56.2	59.2
18	97	53.4			60.4	58.9
19	125	57			110	67
20	94.8	31.8			34.6	45.7
21	85.9	6.9			20.9	38.5
27	84.1	57.4			64.7	
28	89.7	63.1	90.2	63.1		
29	100	69.1	89.1	43.1		
30	87.8	50		20.8		
31	*	97.4				
32	95.9	40.4	46.9	42.9		
33	100	45.9	90.6	64.5		
34	94.5	36.7	41.3		43.1	
35	72.7	21				
37	92.9	45.8	82.2			

Table III. Viability percentages expressed as *Viability% after 18 hours/ Viability% after 0 hours* of the main intervention (MI) alone and the MI with the combined antagonists as well as NGP1-01 and SFM-5O.

Day	Control	MI	MI + 300 uM Diltiazem + 300 uM MK-801	MI + 300 uM Nifedipine + 300 uM Memantine	MI + 300 uM NGP1-01	MI + 300 uM SFM-5O
22	82	38.6			76.2	68.6
23	45.5	42.1			27.8	67.2
24	75.8	43.3			56	24.3
25	90.4	42.7			52.8	59.6
26	75.5	48.4			41.4	43.4
27	84.1	57.4	93.2	63.5		
28	89.7	63.1	89.9	10.9		
29	100	69.1	28.1			
30	87.8	50				
31	*	97.4	90.7	80		
32	95.9	40.4	64.4	51.2		
33	100	45.9		55.2		
34	94.5	36.7	27.1	21.2		

Table IV. Viability percentages expressed as *Viability% after 18 hours/ Viability% after 0 hours* of cell samples after 4 hour and and 18 hour exposure periods.

Day	4 Hour Control	18 Hour Control	4 Hour intervention	18 Hour intervention
1	68.9		37.7	
2	86.2		55	
3	87		82	
4	80.9		72.5	
5	71.8		69.4	
6	91.5	71.1	60.3	15.5
7		95.6		63
8		79		31
9		93.6		50.9
10		89.9		49
11		98		34.6
12		105		60.7
13		105		37.2
14		89.4		90.9
15		90.6		62.7
16		68.5		68.5

APPENDIX B

Guide for Authors

SUBMISSION POLICY

Manuscripts should be addressed to one of the Editors-in-Chief. Submission of a paper to *Journal of Neuroscience Methods Research* is understood to imply that it has not previously been published (except in abstract form) and that it is not being considered for publication elsewhere. Manuscripts submitted under multiple authorship are reviewed on the assumption that all listed authors concur with the submission and that a copy of the final manuscript has been approved by all authors and tacitly or explicitly by the responsible authorities in the laboratories where the work was carried out. **Authors are invited to provide the Editors-in-Chief with the names (and addresses) of five potential reviewers** whom they feel are especially qualified in the subject area of the manuscript.

Submission Procedure

Hard Copy Submission

In the case of **hard copy** submission **three** copies of the manuscript, written in English, should be submitted to one of the Editors-in-Chief. The manuscripts should be typed, 1.5-spaced, with at least a 4 cm margin of uniform size, and accompanied by a list of 6-8 keywords and a summary of about 200 words on a separate page. Words to be printed in 'italics' should be underlined. The length of articles should be restricted to 10 printed pages; i.e., approximately 18 manuscript pages. Included also should be a set of the electronic files of the manuscript on floppy-disk, Zip-disk or CD-ROM. For preparation of electronic files, see the instructions herein below.

ORGANIZATION OF THE ARTICLE

As a rule, Full Length Reports and Review Articles should be **divided into sections** headed by a caption (Abstract, Introduction, Materials and Methods, Results, Discussion,

Acknowledgements, References, Tables, Figures and Legends). Acknowledgements for personal and technical assistance should follow the Discussion section. Financial support should be indicated in the Acknowledgements.

Title page. The title page should contain the following items: (i) complete title (preferably no chemical formulas or arbitrary abbreviations); (ii) full names of all authors; (iii) complete affiliations of all authors; (iv) the number of text pages of the whole manuscript (including figures and tables) and the number of figures and tables; (v) the name and complete address of the corresponding author (as well as telephone number, facsimile number and E-mail address.

Abstract. This should provide a concise description of the purpose of the report or review article and should not exceed 200 words. The abstract should include a maximum of 8 keywords, which reflect the entries the author(s) would like to see in an index.

Authors' full names, academic or professional affiliations, and **complete addresses** should be included on a separate title page. The name and address *plus telephone and fax numbers as well as e-mail address* of the author to whom proofs and correspondence are to be sent should be given.

Literature references.

References in the text should start with the name of the author(s), followed by the publication date in brackets, e.g. Jones (1970) has shown the importance of. . ., or . . . has been described (Jones, 1970; Brown and Jones, 1971; Chin et al., 1972). . .; using date order. All references cited in the text should be listed at the end of the paper on a separate page (also 1.5-spaced) arranged in alphabetical order of first author. All items in the list of references should be cited in the text and, conversely, all references cited in the text must be presented in the list. Literature references must be complete, including initials of the authors cited, title of paper referred to, abbreviated title, year, volume, and first and last page numbers of the article, in a periodical. The abbreviations of journal titles should conform to those adopted by List of Serial Title Word Abbreviations, CIEPS/ISDS, Paris, 1985, ISBN 2-904-938-02-8. (See example 2.) The form of literature references of books should be: author, initials, title of book, publisher and city, year, and page number referred to. (See example 1.) References to authors contributing to multi-author books or

to proceedings printed in book-form should be similar to those for books. (See example 3.)

Examples:-

Bures J, Buresová O, Huston JP. Techniques and Basic Experiments for the Study of Brain and Behavior, second ed. Elsevier: Amsterdam, 1983: 326.
Langston JW, Irwin I, Langston EB, Forno LS. The importance of the `4-5' double bond for neurotoxicity in primates of the pyridine derivative MPTP. Neurosci. Lett., 1984; 50: 289-94.
Sofroniew MV. Morphology of vasopressin and oxytocin neurones and their central and vascular projections. In Cross BZ, Leng G, editors. The Neurohypophysis: Structure, Function and Control, Progress in Brain Research. Elsevier: Amsterdam, 1983; 50: 101-14.

ILLUSTRATIONS

All illustrations must be submitted in triplicate and reach the editors in a **form and condition suitable for reproduction**. Authors should consult the Elsevier Science website for guidelines for preparing (electronic) artwork: http://authors.elsevier.com/artworkThe illustrations should bear the author's name and be numbered in Arabic numerals according to the sequence of their appearance in the text, where they are to be referred to as Fig. 1, Fig. 2, etc. Line drawings should be in Black ink on drawing or tracing paper or glossy sharp photographs of the same. Lettering should be clear and of adequate size to be legible after reduction. Professional labelling is preferable but, if this is not possible lettering should be in fine pencil. Photographs, including roentgenograms, electroencephalograms, and electron micrographs should be supplied as original **clear black-and-white prints** on glossy paper, rather than copies which reproduce detail badly, usually larger than the final size of reproduction, but not more than 20 by 25 cm. Micrographs should have a scale bar rather than a magnification factor in the legend.

Color reproduction. Reproduction in color will have to be approved by the Editor. The extra costs of color reproduction will be charged to the author(s).

Each illustration must have a legend. These should be typed with 1.5-spacing on a separate page and begin with the number of the illustration they refer to. If illustrations or other small parts of articles or books already published elsewhere are used in papers submitted to *The Journal of Neuroscience Methods,* the written permission of author and publisher concerned must be included in the manuscript. The original source must be indicated in the legend of the illustration in these cases.

Tables. Tables of numerical data should each be typed (also with 1.5-spacing) on a separate page, numbered sequence in Roman numerals (Tables I, II, etc.), provided with a heading, and referred to in the text as Table I, Table II, etc.

P.S. This *Guide for Authors* is available at
http://www.authors.elsevier.com/JournalDetail.html?PubID=506079
&Precis=DESC